2006

Application of short-term sediment dynamics and particle-bound phosphorus fractionation methods (SEDEX) to estimate the benthic nutrient loading potential in Upper Newport Estuary, California

Hilary Amanda Collis
Louisiana State University and Agricultural and Mechanical College

APPLICATION OF SHORT-TERM SEDIMENT DYNAMICS AND PARTICLE-BOUND PHOSPHORUS FRACTIONATION METHODS (SEDEX) TO ESTIMATE THE BENTHIC NUTRIENT LOADING POTENTIAL IN UPPER NEWPORT ESTUARY, CALIFORNIA

A Thesis

Submitted to the Graduate Faculty of the
Louisiana State University and
Agricultural and Mechanical College
in partial fulfillment of the
requirements for the degree of
Master of Science

in

The Department of Oceanography and Coastal Sciences

by
Hilary Amanda Collis
B.S., Pacific University, 2001
B.S., Pacific University, 2001
December, 2006

ACKNOWLEDGEMENTS

This project was funded by the Southern California Coastal Water Research Project (SCCWRP) I thank my major professor, Jaye Cable, for guidance and support over the past two years. I also want to thank committee members Sam Bentley and Robert Twilley for providing helpful comments that undoubtedly improved the quality of this thesis. Thanks to Martha Sutula with SCCWRP for allowing me to be an addition to the Upper Newport Bay project, also for providing guidance, help in the field, and fabulous accommodations when visiting California (many thanks to Juan and Benjamin as well). Thanks to Jamie Habben with the County of Orange/Watershed and Coastal Resources office for sharing time and data.

I was told to lean on other graduate students for support, and no one was a greater help on a daily basis than my office mate Chris Smith. Thanks for always asking the questions I would have preferred to avoid, and for swearing over and over again, that "there's no such thing as a stupid question." I'd also like to thank Bryan and Sarai Piazza, Michelle Satterwhite, Ashley Wilson, Kirsten Simonsen, Guerry Holm, Brad "Sweetgrass" Miller, and Emily Hyfield for always being there, whether I needed to get out, get over myself, get new ideas, or geek out. Thank you to Gregg Snedden for all the support, insight, love, and complete faith in my ability to complete this thesis.

And since everyone in life needs a cheerleading section, I would like to thank Kim, Tony, and Taryn Collis, the rest of my crazy family, Paige Wood, and my best friend Natalie Roberts, for their unconditional love and support and for never letting me give up on myself.

TABLE OF CONTENTS

LIST OF TABLES

LIST OF FIGURES

ABSTRACT

Estuaries act as sources, sinks, and biogeochemical transformation sites for natural and anthropogenically-derived nutrients. Sediment loading from watersheds provides an important source of particulate nutrients to estuaries often neglected when constructing nutrient budgets. Deposition and resuspension of these sediments are known to impact biogeochemical cycles in estuarine environments. Phosphorus (P) exists in many forms in aquatic environments, and increased P loading to coastal environments increases primary productivity potentially leading to eutrophication. Magnitude and variability of sediment deposition, resuspension, and sediment-bound P concentrations were evaluated in Upper Newport Bay (UNB), California. During 2004, seven push cores were collected from the intertidal and subtidal zones of three sites to evaluate recent sediment dynamics using ^{7}Be and sediment-bound P fractions. Two sequential phosphorus extraction methods were used to determine the distribution of potentially bioavailable forms of P (labile, iron-bound, and organic), and refractory forms of P (calcium-bound and detrital) in sediment. A seasonal trend appears with greatest deposition occurring during the wet season (spring) when watershed runoff increases (0.1 to 0.4 g/cm^2 d), and greatest sediment resuspension occurring during the dry season (summer) when minimal input from precipitation or stream runoff occurs. The average annual short-term sediment deposition rate calculated from the ^{7}Be inventories indicated that deposition is 24.7cm/yr in the upper estuary. However, the long-term sediment deposition rate of 0.15 cm/year indicates that less than 1% of the annual sediment deposited in UNB is permanently buried.

Sediment P concentrations revealed enrichment of P during the spring, corresponding to increased sediment input. During time periods when net sediment resuspension dominated over net deposition (e.g. summer), total-P concentrations decreased. This decrease was attributed to

increased biological uptake of water column P during summer blooms, which lead to the desorption of P from particles. Nonetheless, most of the sequentially extracted P (~66%) was contained in the refractory phase. Based on the long term deposition rate in UNB, the burial rate for the refractory P was approximately 0.97 μmol P/cm^2 yr. Sediment deposition and resuspension processes may act as important internal mechanisms for recycling phosphorus, particularly reactive P, and must be considered in estuarine biogeochemical cycles.

INTRODUCTION

Estuaries act as sources, sinks, and biogeochemical transformation sites for natural and anthropogenically-derived nutrients (Froelich et al. 1988; Lebo 1991; Zwolsman 1994; Giffin and Corbett 2003). These nutrients, when available in excess, can cause water quality problems such as eutrophication and harmful algal blooms. Sediment loading from the watershed provides an important source of particulate nutrients to estuaries, and the deposition and resuspension of these sediments are known to impact biogeochemical cycles in estuarine environments (Fanning et al. 1982; Clavaro et al. 1999). When nutrient budgets are calculated, influence from benthic particulates are often neglected. Depositional processes help to remove constituents from the water column (Fig. 1). Sediments and sediment-bound nutrients can be delivered to the seabed or sediment surface where they can be contained for short time spans to decades in the upper mixed sediment layer, or can be buried more permanently (Fig. 1). Conversely, when sediments are resuspended through tidal pumping, bioirrigation, or physical forcing, loosely-bound nutrients may transported out of the sediment to become available for biological production within the estuary water column or export to the coastal ocean (Booth et al. 2000; Giffin and Corbett 2003; Sutula et al. 2004). Giffin and Corbett (2003) found that advective fluxes of nutrients during resuspension events were as much as six times greater than during quiescent periods. Because of the dynamic nature of estuarine environments, deposition may not always serve as a long-term sink, thus making it important to examine estuarine sediment processes to better understand the fate of particle-bound nutrients and contaminants.

Phosphorus (P) is a macronutrient that exists in many forms in aquatic environments, and is considered an important element limiting marine primary productivity over geologically long timescales (Ruttenberg and Berner 2003). The primary mechanism for P delivery to the world's oceans is through the introduction of dissolved P from terrigenous sources (Froelich et al. 1982;

Chambers et al. 1995; Sutula et al. 2004). Delivery rates of particulate nutrients have greatly increased over the last century due to accelerated soil erosion and increases in anthropogenic nutrient sources from continents (Blake et al. 2002). Increased P loading to coastal environments increases primary productivity and can lead to eutrophication.

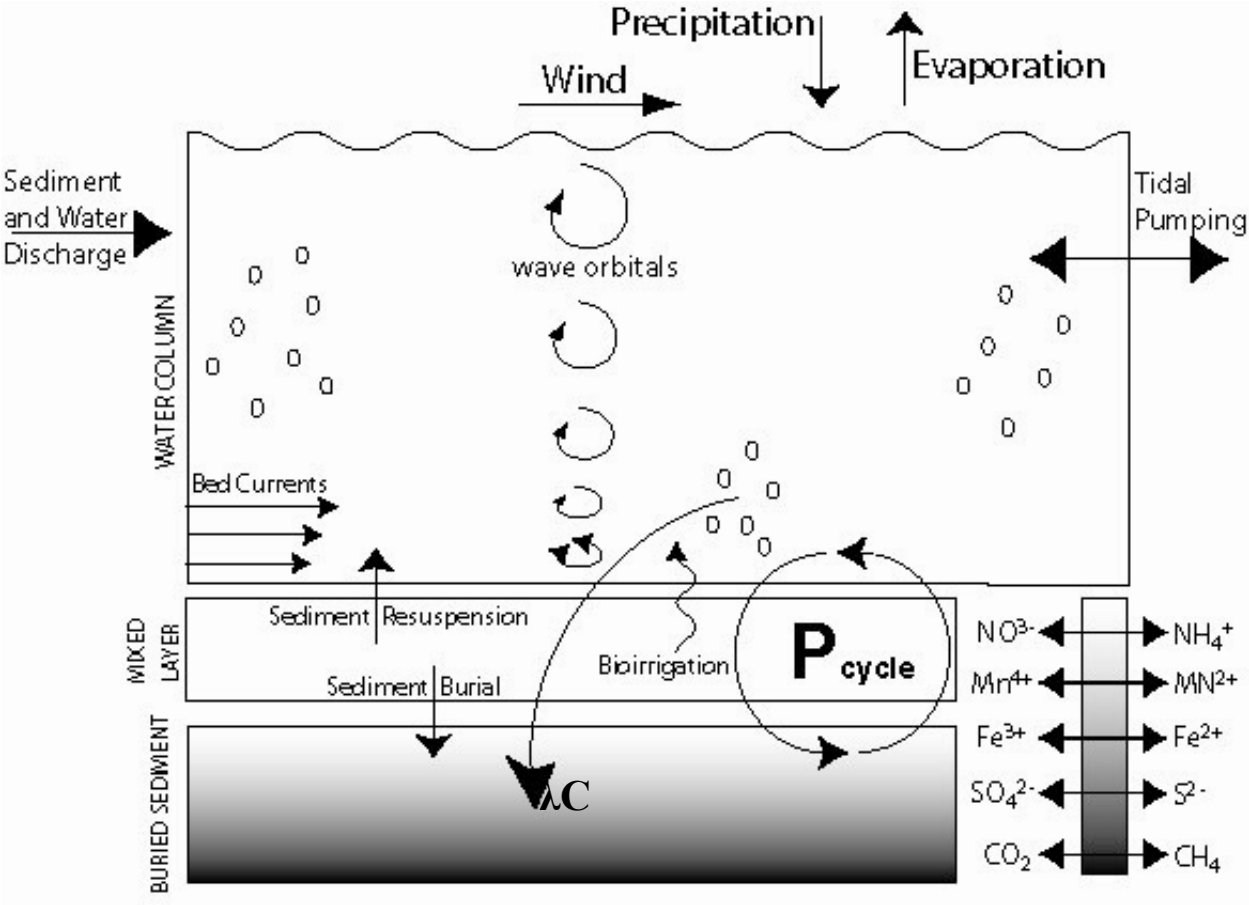

Figure 1. Conceptual model of sediment and phosphorus deposition and resuspending forces in estuaries. The upper box depicts the water column with sediment and nutrients settling out of solution. The middle box depicts the shallow sediments that were the focus of this study. The lower box represents permanently buried sediments that will not be acted upon by resuspending forces (bed currents, wave orbitals, etc.).

In general, P loading to the water column comes from two sources: external loading from point and non-point sources, and internal loading from sediment inventories (Zwolsman 1994; Coelho et al. 2004). Phosphorus undergoes many diagenetic transformations upon entering an estuary (Ruttenberg and Berner 1993; Faul et al. 2005). Relationships have been found between

the chemical forms in which P is bound in the sediment and its incidence in water column P concentrations (Böstrom et al. 1998; Koch et al. 2001; Tappin 2002). Various forms of P bind to sediments, either as long-term sinks or as short-term repositories, until P is released back to the environment through a series of "sorption" reactions (Froelich 1998). Factors influencing P retention in sediments are the flux of P to sediments, the depositional environment, and the fraction of this flux that is unavailable to microconsumers in the sediment and pore water (Ruttenberg and Berner 1993). Nutrient budgets in estuarine water columns could be better understood if the sediment dynamics that help drive retention and release of particulate nutrients were coupled with seasonal studies of particle-bound nutrients.

Natural particle-reactive geochemical tracers have been used for decades to examine sedimentation and sediment dynamics in coastal systems (e.g., Kirshnaswami et al. 1980; Olsen et al. 1986; Baskaran & Santschi 1993; Dellapenna et al. 1998; Giffin and Corbett 2003). One such geochemical tracer is the short-lived radioisotope, beryllium-7 (^{7}Be; $t_{1/2}$ = 53.3 days), which is a widely used tracer of short-term sediment dynamics across the sediment-water interface (e.g. Kirshnaswami et al. 1980; Wallbrink and Murray 1996; Feng et al. 1999; Fitzgerald et al. 2001; Blake et al. 2002). This naturally occurring cosmogenic radionuclide is produced in the atmosphere by the cosmic ray spallation of oxygen and nitrogen and deposited on the Earth's surface through wet or dry deposition. Greater proportions of ^{7}Be washouts are associated with precipitation events, and it enters aquatic systems directly with precipitation or indirectly with overland flow, where it adheres to suspended particles in surface waters (Kim et al. 1999; Wallbrink and Murray 1994). Beryllium-7 generally has a short residence time in the water column with removal rates of 1 to 20 days (Olsen et al. 1986; Baskaran and Santschi 1993; Baskaran et al. 1997). It is deposited with sediments and can be used to track sedimentation and

resuspension in aquatic environments such as lakes, lagoons, and estuaries (e.g. Fitzgerald et al. 2001; Canuel et al. 1989; DeMaster et al. 1985).

Another particle reactive tracer, lead-210 (^{210}Pb, $t_{1/2}$ = 22.3 years), can be used to approximate sedimentation rates on decadal time-scales when available in excess in sediments (e.g. Kirshnaswami et al. 1980; Dellapenna et al. 1998). Lead-210 has two input sources to sediment. Supported levels of ^{210}Pb is produced from the *in situ* decay of the parent isotope radium-226 (^{226}Ra, $t_{1/2}$ = 1620 years). Particle-bound ^{226}Ra decays to the gas radon-222 (^{222}Rn, $t_{1/2}$ = 3.82 days), and is released from sediment grains, where it subsequently decays to ^{210}Pb, re-adsorbs to the sediment, and can remain buried (Appleby and Oldfield, 1992). Excess ^{210}Pb is delivered to a system through a number of sources. One source is through atmospheric deposition, in which atmospheric ^{222}Rn decays to ^{210}Pb, the ^{210}Pb is scavenged by aerosols, and is subsequently deposited on the Earth's surface via wet or dry deposition, similar to ^{7}Be. The second method of delivery is from terrestrial weathering of radium-bearing rock, where ^{226}Ra is discharged to an aquatic system through runoff and decays to ^{210}Pb in the water column. As with ^{7}Be, the affinity of ^{210}Pb to bind to particles allows it to settle out of the water column and become buried with sediment deposition. Because of its longer half-life, excess ^{210}Pb can persist to greater depths than ^{7}Be, for the same burial rates, and thus can be used to estimate sedimentation rates over longer time scales.

The coupling between sediment dynamics and the potential for particulate P to be sequestered or readily used in estuarine environments requires quantification of various forms of P in the sediment, as well as understanding deposition and removal events. The effect of sediments on nutrient concentrations in the water column depends on the chemical form of P bound to the sediment (Ruttenberg 1992; Koch et al. 2001), while release of P from particles is strongly dependent on the concentration gradient in the pore waters and the overlying water column and the

particle-bound P (Cowen and Lee, 1976). The fine-grained nature of most marine sediments and low concentrations of sedimentary P make understanding P diagenesis difficult (Ruttenberg 1990). Sequential extraction methods provide a means to separate solid-phase P pools, and they are proving to be the most promising method for quantifying P fractions in sediments (e.g. Lucotte and d'Anglejan 1985; Ruttenberg 1992; Koch et al. 2001; Akhurst et al. 2004; Coelho et al. 2004; Sutula et al. 2004; Faul et al. 2005). Extracting various forms of sediment-bound P helps identify the exchangeable, labile, and refractory forms of P. It also helps determine the forms of P most likely to be buried or potentially made available for primary productivity if reintroduced to the water column. Aspila (1976) developed a method to separate P into total, inorganic, and organic pools. The SEDEX method, developed by Ruttenberg (1992), separates five major reservoirs of sediment P: (1) loosely sorbed or exchangeable P, (2) ferric (Fe^{3+}) bound P, (3) authigenic carbonate fluorapatite (CFA) + biogenic apatite (such as fish debris) + $CaCO_3$ bound P, (4) detrital apatite P of igneous and metamorphic origins, and (5) organic P. The SEDEX method has been applied extensively when examining sediment P in large estuaries and continental shelf regimes (Ruttenberg and Berner 1993; Sutula et al. 2004; Faul et al. 2005), but it has been applied rarely to shallow estuaries. Vink et al. (1997) examined suspended load and benthic sediment P compositions using the SEDEX procedure and determined driving factors regulating P concentrations in the upper 40 cm of shallow estuary sediments are bioturbation and non-steady state sediment deposition, while P concentrations in sediments analyzed below 40 cm are regulated by diagenetic shifts in the forms of sediment-bound P.

In the SEDEX extraction procedure, labile P, formed by the degradation of biological particulate matter, is most readily available for immediate biological uptake (Faul et al. 2005). The authigenic CFA-bound fraction is considered the primary diagenetic sink, especially in marine carbonate sediments (Ruttenberg and Berner 1993; Koch et al. 2001). Additionally, the separation

between the detrital apatite-bound phase and the CFA-bound phase is unique to the SEDEX procedure and represents an important distinction. Because of its lithogenic origins, detrital-bound P has been found to be a large contributor to the total P fraction on the California Coast (e.g. Pilskaln et al. 1996; Faul et al. 2005, and references therein). Though both forms represent sinks over geologic timescales, CFA-bound P is produced primarily in the ocean while detrital-bound P is of terrigenous origin. Thus, separation of detrital apatite from CFA is critical to assessing provenance in estuarine sediments.

Ferric-bound P may act as a sink for P, but under suitable oxidation-reduction (redox) conditions, it can be released to pore waters and become available for biological uptake. In anoxic sediments, insoluble ferric iron (Fe^{3+}) is reduced to dissolved ferrous iron (Fe^{2+}) and Fe dissolution can then release P to pore water. If the sediment-water interface is oxic, the Fe^{2+} will diffuse upward and oxidize to become Fe^{3+}, which can then adsorb to phosphate ions and precipitate out of solution. This redox-dependent flux can redistribute solid-phase P and create a barrier for diffusive loss of P from sediments (Froelich et al. 1988; Ruttenberg and Berner 1991). However, in marine environments the upward flux of Fe^{2+} to the oxidized surface layer can be inhibited by iron sulfide formation in the anoxic layer. Pyritization reduces the Fe^{3+} concentration in the oxidized surface layer and may reduce the P concentration removed from the water column (Lehtoranta and Pitkänen 2003).

Organic P becomes available for primary productivity after P-containing materials decompose, either in the water column or the sediments, yielding soluble inorganic forms (Vink et al. 1997; Mitsch and Gosselink 2000). Benthic P-rich organic matter can be partially mineralized and become partitioned between pore waters and surface adsorption sites in sediments (Lehtoranta et al. 2004). If organic matter and associated organic-bound P are released to pore water, dissolved P can: (1) diffuse back into the water column and become available for uptake, or (2)

precipitate out of solution (Ruttenberg, 1990). Vink et al. (1997) determined that organic P in sediments acts as a sink only over long time scales (i.e. buried in deeper sediments), and the diffusive loss of organic P in shallower sediments greatly outweighs its contribution as a sink for P. Oxic sediments are more effective at degrading organic matter than anoxic sediments (Froelich et al. 1979), and redox potential influences the rates at which organic-bound P can be released back to the water column.

This study examines the magnitude and variability of short-term sediment deposition and resuspension characteristics using the radioisotopes ^{7}Be and ^{210}Pb and the fractionation of sedimentary phosphorus in the upper sediment layers (6 cm) of Upper Newport Bay (UNB), California, during 2004. The SEDEX and Aspila methods of phosphorus extraction were used to quantify five fractions of P in the upper sediments of Newport Estuary. These data were coupled with estimates of sediment deposition and resuspension to determine the potential for sediment-bound P to become a benthic nutrient source by introducing bioavailable P to the water column.

FIELD SITE

Upper Newport Bay (UNB) is one of the largest estuaries remaining in southern California (Boyle et al. 2004) and is located approximately 105 km south of Los Angeles, California (Fig. 2). Newport Bay is divided geographically into two distinct sections, the upper bay and lower bay, separated by the Pacific Coast Highway. The lower bay runs parallel to the coast and receives high sediment loading from offshore sands. This study was conducted in the upper bay which is orientated perpendicular to the coast and has a surface area of 4 km^2. UNB is a drowned river valley bordered by steep sedimentary bluffs up to 30 m high, and it is geologically much older than the lower estuary (Trimble 2003). The headwaters of UNB remain largely undeveloped as it is a California Department of Fish and Game State Ecological Reserve, while the lower reaches have been developed for commercial and recreational use. Freshwater inputs come primarily from precipitation and stream flow, particularly San Diego Creek, located at the head of the estuary, and smaller tributaries that enter the estuary from the sides, including the Santa Ana Delhi Channel and Big Canyon Wash. The San Diego Creek watershed is approximately 450 km^2, and it is associated with a broad alluvial valley called the Tustin Plain. Headwaters originate in the Santa Ana Mountains to the east and the San Joaquin Hills to the south (Smith and Klimas 2004). Average daily discharge in San Diego Creek is 1.5 m^3/sec, and the creek is the source for approximately 94 percent of the sediment that enters the upper bay (Masters and Inman 2000) with over one half of this sediment attributed to upstream channel erosion (Trimble 2003).

Average annual precipitation (over the period 1971-2000) for Newport Bay Harbor is 296 mm (NCDC 2005). In general, summer is the dry season for the estuary due to the northward migration of the semi-permanent Pacific high pressure system that causes most storm tracks deflect far to the north (WRCC 2005). Winds are predominantly from the west or northwest (off

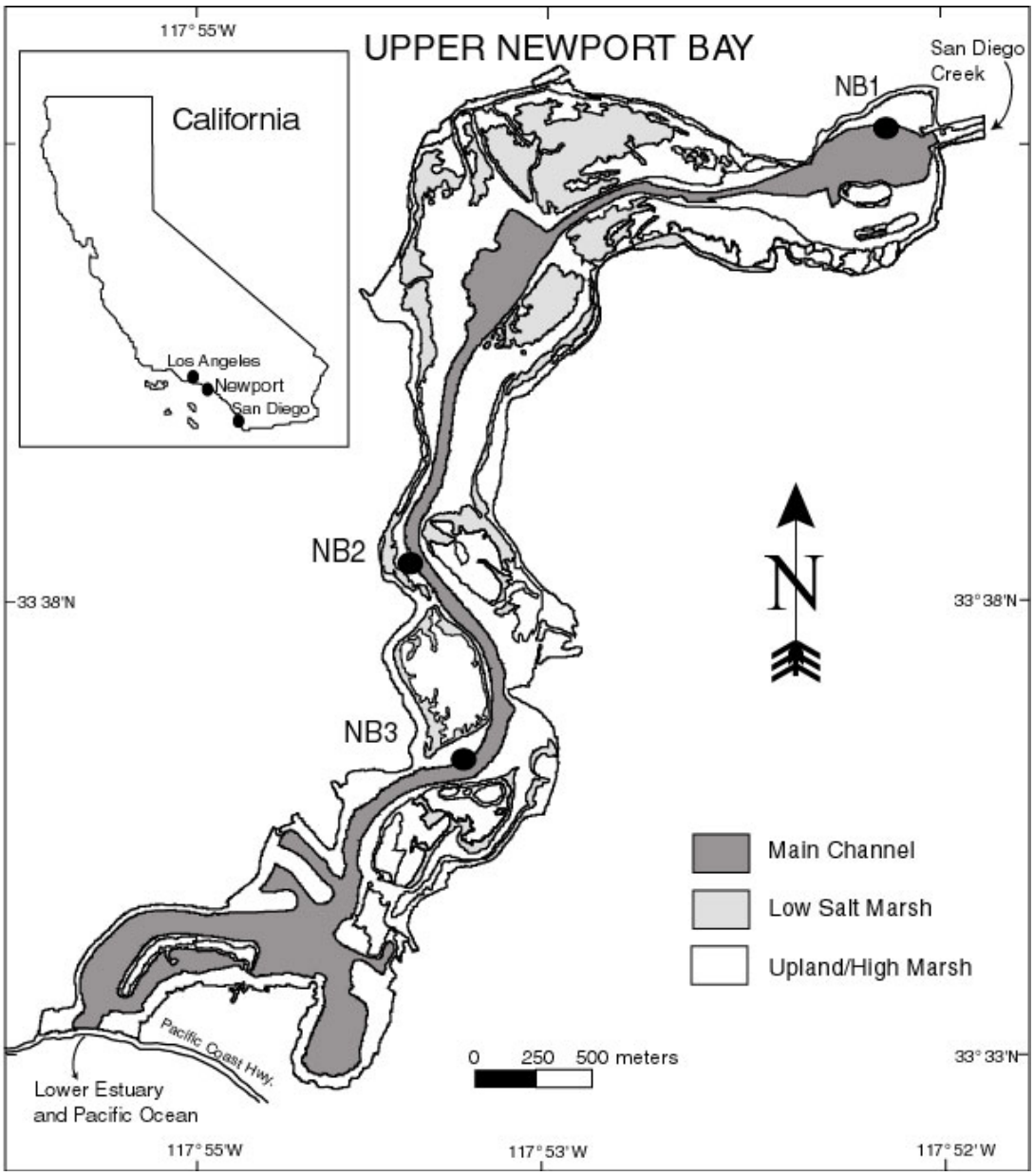

Figure 2. Map of Upper Newport Bay, California (USA).

the Pacific Ocean). The estuary is macrotidal with a mixed semi-diurnal tidal range up to 9 m, and the residence time of seawater in the upper bay is about three to four days. Sediment transport processes within Upper Newport Estuary are assumed to be driven primarily by tidal currents and storm flow (USACE 1997).

During the 2004 field study daily precipitation, creek discharge, and suspended sediment concentrations were collected approximately 2 km upstream from the mouth of San Diego Creek

by the County of Orange Watershed and Coastal Resources Office (Fig. 3). Annual precipitation was 446.5 mm with the largest events occurring in the spring, and no rain during the summer (June through September). Average daily discharge in San Diego Creek during this time appears to correlate to local precipitation events (Figure 3). Unseasonably large rain events occurred over two weeks in October, 2004, leading to the largest single recorded water discharge event from San Diego Creek (79.3 m^3/s). Suspended sediment in San Diego Creek and sediment discharge (calculated by multiplying creek discharge and suspended sediment values) varied seasonally as well, with highest consistent suspended sediment load during the spring. Unlike precipitation and creek discharge, which decreased during April, suspended sediment concentrations in San Diego Creek remained high through May.

San Diego Creek was found to be a major source of sediment to the upper bay in the late 1970s, largely due to erosion from surrounding agricultural fields and housing developments (Trimble 2003). In 1982, the San Diego Creek Comprehensive Stormwater Control Plan was initiated to decrease sediment accumulation within UNB (Boyle Engineers 1982), which primarily involved dredging retention basins at the head of UNB and in San Diego Creek. By 1998, the retention basins were completely filled with sediments (Boyle Engineers 1982). UNB was subsequently placed on the federal 303(d) list of impaired water bodies, and total maximum daily loads (TMDL) for nitrogen and phosphorus into the upper estuary were adopted with the primary goal being to decrease nutrient loading and sediment discharge to the upper estuary from San Diego Creek (USACE 2000).

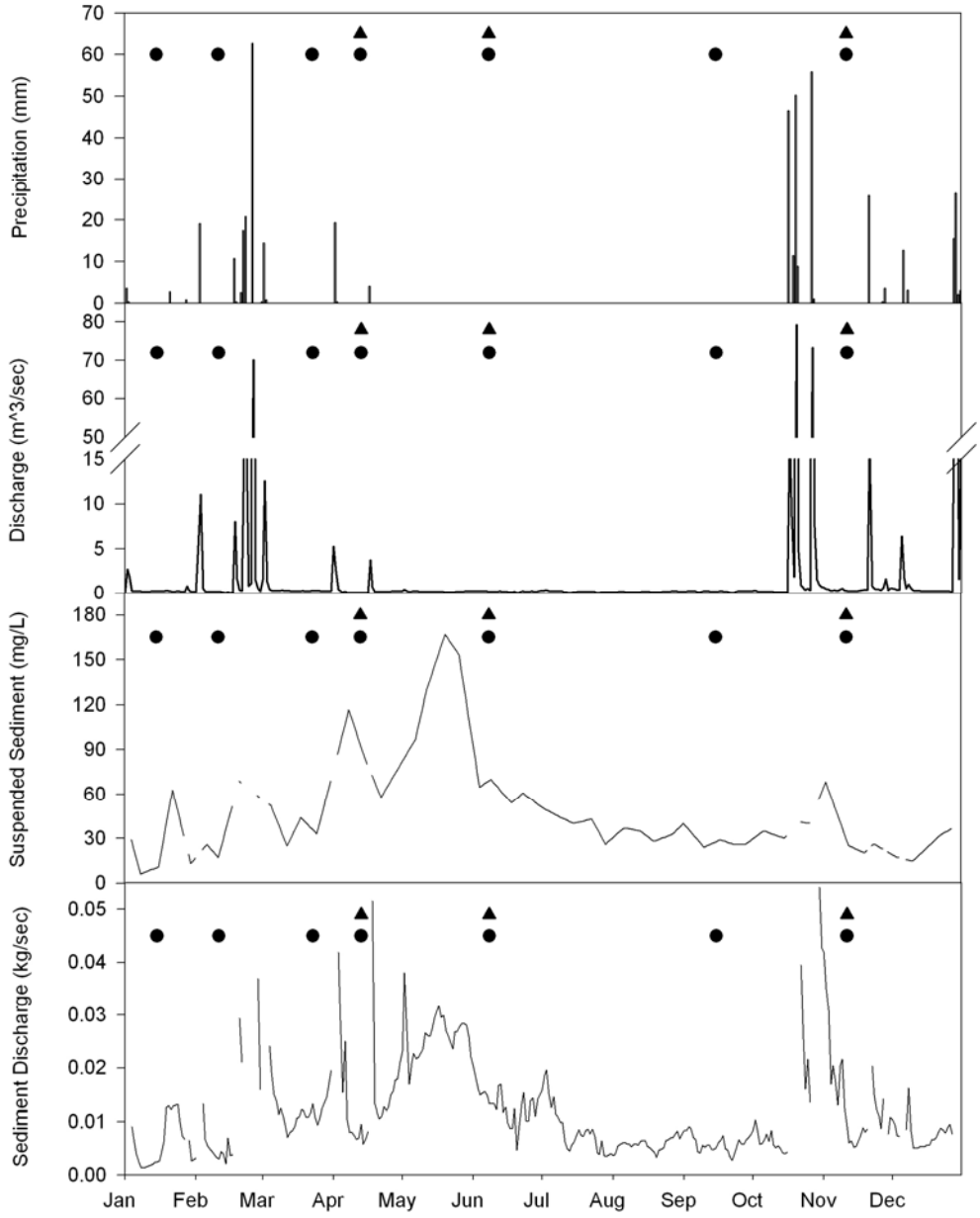

Figure 3. San Diego Creek daily (a) precipitation, (b) creek discharge, (c) suspended sediment, and (d) sediment discharge into Upper Newport Estuary are shown for 2004. Black circles on the graphs represent sediment core collection times, and triangles represents months when P was analyzed.

METHODS

Sample Collection

Seven sampling trips were conducted during 2004 at each of the three sites (Fig. 2). NB1 was located in the uppermost bay site, closest to the mouth of San Diego Creek in a wider area of the estuary on a slight bend away from the main channel. NB2 was the middle site and was in a narrower area located in the main channel. NB3 was the most southern station in the upper estuary, located on a point bar. Each site was divided into a continuously submerged subtidal zone and an intertidal zone that was exposed during low tide. Surface areas for the intertidal and subtidal zones are similar (1.0 and 0.9 km^2, respectively). One push core (~20 cm) was collected from each subtidal and intertidal zone at each site every field trip. Sampling was conducted monthly during the wet season (January through April) and then approximately bimonthly during the dry season (June, September, and November). After collection, sediment cores were immediately sectioned at 1-cm intervals for the upper 6 cm. The sectioned samples were sealed in plastic bags and transported to Louisiana State University for analysis.

During April, 2005, an additional field survey was conducted to (a) obtain cores to assess within-site spatial variability using randomly distributed cores collected ~1 m apart at the NB1 subtidal zone, (b) determine the long-term sediment deposition rate of the estuary using one long core (~50 cm) collected from a protected (i.e., non-dredged) area of the upper estuary (Fig. 2), and (c) examine physical structure within the sediments at each site using x-radiography of push cores.

Sediment Physical Characteristics

Porosity and Bulk Density

In the laboratory, all samples were weighed, dried at 60°C to constant weight, and then re-weighed to determine porosity and bulk density. Porosity (ϕ) was determined using the wet weight (f_{wet}) and dry weight (f_{dry}) fractions of sediment:

$$\phi = \frac{\frac{f_{wet}}{\rho_f}}{\left(\frac{f_{wet}}{\rho_f} + \frac{f_{dry}}{\rho_s}\right)} \qquad (1)$$

where ρ_f is the density of fluid (1.025 g/cm^3), and ρ_s is the dry grain density (~2.0 g/cm^3). Bulk density ($\rho_{bulk,}$ g/cm^3) was determined from the porosity:

$$\rho_{bulk} = (\phi - \rho_f) + (1 - \phi)\rho_s \qquad (2)$$

Grain Size

For each sample, grain size fractions of sand, silt, and clay were determined following Milner (1962). Approximately 10 g of dry sediment were added to 50-mL centrifuge tubes, soaked with 0.05% sodium metaphosphate solution, and shaken in a sonic dismembrator bath for 10 minutes to disaggregate the sediment. After 10 minutes, a 62-μm mesh sieve was used to separate the sand and gravel fractions from the fine sediments (silt and clay). The sand fraction (grain size diameter coarser than 4 phi) was transferred into a pre-weighed beaker, dried at 60°C to constant weight and reweighed.

The remaining sample was transferred to a 100-mL glass graduated cylinder and remaining volume filled with the sodium metaphosphate solution. Sediment in the cylinder was homogenized by vigorously stirring until all the sediment was suspended. Twenty-five mL of sample solution were removed 20 seconds after stirring from a depth of 10 cm within the cylinder and transferred to a pre-weighed weigh boat. The sample was left to settle for one hour and 51 minutes, and then another 25-mL sample solution was removed from a depth of 10 cm and transferred to a separate pre-weighed weigh boat. Both samples were weighed wet, transferred to a 60°C oven, dried to a constant weight, and re-weighed. The sample collected 20 seconds after sediments were suspended comprised the silt fraction (grain size diameter range

was 4 to 8 phi), and the sample collected one hour and 51 minutes after suspension comprised the clay fraction (grain size diameter finer than 8 phi).

X-radiography

Three 20-cm cores for x-radiographic imaging were collected from the subtidal zone of each site (NB1, NB2, and NB3) in April, 2005. One aluminum push core was collected from the subtidal zone of each site and transported intact back to Louisiana State University for analysis. In the laboratory, cores were sliced longitudinally into 2-cm-thick rectangular slabs, and placed on Plexiglas trays for imaging. Images (16-bit TIFF format) were collected using a Thales Flashcan 35 digital X-ray panel detector, illuminated with a Medson-Acoma PH15-HF veterinary x-ray generator.

Radioisotopic Analysis

A 10-g subsample of dried sediment was homogenized with a mortar and pestle, and approximately 2 g of this subsample were packed into 10-mm diameter vials to a standard height of 33 mm. Radionuclide activities were measured via gamma spectrometry on an intrinsic germanium well detector at 477.1 keV for ^{7}Be within one week of sample collection. During the April, 2005, field survey, five short cores (10 cm) were collected randomly from the subtidal zone of site NB1 and analyzed for ^{7}Be to determine if significant spatial variability in ^{7}Be concentrations existed within a site. Decadal time-scale sedimentation rates were determined using excess ^{210}Pb activities on a separate core collected during the April 2005 field survey. This core was sectioned in 1-cm intervals up to 10 cm, then every 2 cm to 20 cm. Samples were ground and packed into vials in the same fashion as the ^{7}Be samples, sealed with epoxy to allow ingrowth of the ^{226}Ra progeny to secular equilibrium (about 3 to 4 weeks), and analyzed on the germanium detector at 46.5 keV for ^{210}Pb. Excess ^{210}Pb values were calculated by subtracting the supported activity derived from the parent isotope ^{226}Ra from the total measured ^{210}Pb

activities are decay-corrected to the time of sampling. The supported activities were determined by averaging the activities of ^{226}Ra's daughter isotope, ^{214}Pb, which is measured at two photon peaks, 295.1 keV and 351.7 keV. Efficiencies were calculated using an International Atomic Energy Agency (IAEA) reference standard. Net peak area was recorded for each nuclide of interest (^{7}Be and ^{210}Pb), and activities (A; dpm/g) were calculated using the following equation:

$$A = \frac{(cpm_{sample} - cpm_{background})}{(f_{\text{int}ensity} * f_{eff} * Wt_{sample})} \quad (3)$$

where *cpm* is count rate per minute of sample or background, Wt_{sample} is sample mass, $f_{intensity}$ is γ-ray intensity, and f_{eff} is system efficiency for a particular photon energy. Activities below detection were reported as zero, and the average background count rate was 0.02 cpm. From these ^{7}Be activities, downcore sediment inventories were quantified using the equation:

$$I_{total} = \sum_{z=0}^{n} (A_z * \rho_z * h_z) \quad (4)$$

where I_{total} is total ^{7}Be inventory (dpm/cm^2), A_z is the activity at depth z, ρ is sample bulk density, and h is sample thickness (cm). Total ^{7}Be inventories at each site for each sampling event were corrected for the residual activities remaining from previous events. This residual inventory was estimated by correcting the previous month's total inventory for radioactive decay using the following equation:

$$I_R = I_T e^{-\lambda t} \quad (5)$$

where I_R is the residual inventory (dpm/cm^2), I_T is the total inventory from Eq. 5, λ is the decay constant for ^{7}Be (0.0130 d^{-1}), and t is the time between sampling periods (days). New inventory (I_N) for the current sample month was then calculated by subtracting the calculated residual inventory remaining from a previous month from the total inventory. New inventory physically represents the portion of the total inventory associated with recent sediment deposition/

resuspension events. A positive new inventory represents a deposition event while a negative new inventory indicates a removal event. Net ^{7}Be flux (dpm/cm^2 d) into or out of the sediments between sampling periods was calculated by dividing the new inventory by the time interval between sampling (Fitzgerald et al. 2001).

The time-dependent ^{7}Be flux, used here to determine short-term sediment accumulation/removal rates, was estimated as

$$\psi = I_N / A_{new} \tag{6}$$

where ψ is the short-term sediment deposition/removal rate (g/cm^2 d), and A_{new} is the average sample activity after subtracting the decay-corrected activity that existed from the previous sampling period.

To calculate long-term sedimentation rates using ^{210}Pb, the Constant Flux Constant Supply (CF:CS) model was used This model assumes the rate of supply of ^{210}Pb and sediment are constant and at steady state, and the initial concentration of excess ^{210}Pb is the same for each sediment interval (Appleby and Oldfield 1992). The sedimentation rate was calculated as

$$A_z = A_o e^{-\lambda t} \tag{7}$$

where A_o is the excess ^{210}Pb activity at the sediment-water interface, A_z, is excess ^{210}Pb activity at depth z, λ is the decay constant for ^{210}Pb (0.03112 yr^{-1}), and t is the time since the sediment was deposited. The log-linear regression coefficients of excess ^{210}Pb activities versus depth represent the rate of change of sediment accumulation through time (i.e., sediment accumulation is the decay constant divided by the slope of the line).

Phosphorus Analytical Procedure

Sediment P analyses were conducted for three distinct seasons during the months of April, June, and November, 2004, on sediment collected from Upper Newport Bay sites NB1,

NB2, and NB3. These months were chosen as representative of seasonal variations in sediment-bound P during periods of increased precipitation and sediment input (April), no precipitation or sediment input (June), and event-driven inputs (November) following an unseasonably large rain event that occurred in October. Sediments were taken from the same cores used in radioisotopic analyses. Prior to analysis, all sediment samples were dried at 60°C, homogenized, and ground to less than 125 μm. All glassware and centrifuge tubes were acid washed in 10% HCl for approximately 24 hours, triple-rinsed with deionized water and dried completely prior to use.

Total, Inorganic and Organic Phosphorus (Aspila Method)

Initially, total phosphorus (tot-P), inorganic phosphorus (inorg-P) and organic phosphorus (org-P) concentrations in the upper sediment were analyzed for each season (Aspila et al. 1976; see also Appendix A). Tot-P values were obtained by weighing duplicate sets of 0.3 g dry, homogenized sediment for each depth interval and sample month into 150-mL Erlenmeyer flasks and 50-mL centrifuge tubes. Sediments were combusted at 550°C for 2 hours. All flasks and centrifuge tube samples were washed with 30 mL of 1N HCl, covered, and placed in a shaker box for 16 hours. Combusted sediments were used to determine the tot-P concentration, and uncombusted sediments were used to determine the inorg-P concentration. After 16 hours, tot-P samples were transferred to 50-mL centrifuge tubes and all samples were centrifuged for 10 minutes at 80 rpm (Beckman Model TJ-6 Centrifuge). A portion of the supernatant was decanted into 30-mL beakers. Dissolved phosphate was determined using the phosphomolybdate blue method (Strickland and Parsons 1972). Org-P was determined as the difference between the total and inorganic P fractions.

Sequential Phosphorus Extraction (SEDEX method)

While the Aspila method allows for the assessment of P in sediments, it can not truly characterize the potentially bioavailable portion of sediment-bound P since portions of the

bioavailable P are summed in the inorganic P with refractory P. To obtain this information, five major forms of solid-phase P in sediments were determined for April, June, and November using the SEDEX sequential extraction procedure (Ruttenberg 1992; modified by Akhurst 2004). The five phases of sediment-bound P isolated with this procedure are: (1) exchangeable or loosely-bound labile P (lab-P), (2) ferric-bound (oxide associated) P (Fe-P), (3) authigenic carbonate fluorapatite (CFA), biogenic apatite and calcium carbonate associated P (Ca-P), (4) detrital apatite P of igneous or metamorphic origin (detr-P), and (5) organic P (org-P). (Table 1, see also Appendix A). For the sake of this paper, three classes of bioavailability are defined: (1) readily bioavailable, which is made up of the highly reactive lab-P fraction, (2) potentially bioavailable over ecological timescales (given the right redox conditions), which is composed of the reactive Fe-P and org-P fractions, and (3) refractory, because it represents the least reactive and least bioavailable fraction buried for geologically long time periods, and is composed of the detr-P and Ca-P fractions.

Duplicate sediment samples were prepared by weighing 0.3 g of dry ground sediment into 50-mL polyethylene centrifuge tubes. Extractant volumes were always 30 mL. Samples were mixed in a shaker box at 25°C for the time specified for each step (see Table 1) to ensure complete dissolution and centrifuged for 10 minutes at 80 rpm. Supernatants for each step were combined and either frozen (Steps I to III) or kept at room temperature (Steps IV and V) until analysis.

For all steps excluding step III (Fe-P), the combined extractants were analyzed for P spectrophotometrically (885 nm, Carey WinUV Spectrophotometer) in duplicate with the phosphomolybdate blue method (Strickland and Parsons 1972). This technique could not be used to analyze the Fe-bound P extracted in step III because the citrate dithionate-bicarbonate

Table 1. SEDEX extraction procedure and reaction mechanisms as developed by Ruttenberg (1992) and modified by Akhurst et al. (2004). The modifications involve excluding secondary washes of D.I. water from step I and 1M $MgCl_2$ from Step III.

STEP	FRACTION REMOVED	PROCEDURE	REACTION
I	Labile-P Loosely sorbed to clay or mineral particles	▪ 2X wash w/1M $MgCl_2$ for 2 h (pH 8) ▪ 1X wash w/deionized water for 2 h	▪ Formation of $MgPO_4^-$ complexes and/or mass action displacement by Cl^- ▪ Readily bioavailable
II	Fe-P Oxide associated, ferric-bound P	▪ 1X wash w/CDB soln. (pH 7.6) for 8 h ▪ 1X wash w/1M HCl for 2 h ▪ 1X wash w/deionized water for 2 h	▪ Reduction of Fe^{3+} by dithionite followed by chelation by citrate. ▪ Potentially bioavailable
III	Ca-P CFA + biogenic apatite + $CaCO_3$ associated P	▪ 1X wash w/1M Na-acetate buffered w/acetic acid (pH 4) for 6 h ▪ 1X wash w/1M HCl for 2 h ▪ 1X wash w/deionized water for 2 h	▪ Acid dissolution at a moderately low pH ▪ Refractory
IV	Detrital-P Detrital apatite associated P of igneous or metamorphic origin	▪ 1X wash w/1M HCl for 16 h	▪ Acid dissolution at a low pH ▪ Refractory
V	Organic-P	▪ Ash remaining residue for 2 h at 550 °C. ▪ 1X ash w/1M HCl for 16 h	▪ Dry oxidation ▪ Acid dissolution of residue at a low pH ▪ Potentially bioavailable

(CDB) extractant interferes with the reduction of the molybdate blue complex by reducing the dye and destroying the color absorbance. To analyze step III, the extractant was reacted with a 1% vol/vol $FeCl_3$ solution (Lucotte and d'Anglejan, 1985), extracted with isobutanol (Wantanabe and Olsen 1962; Ruttenberg 1992), and analyzed spectrophotometrically at 660 nm. The five different P fractions were summed to determine a total P (Σ-P) value that was compared to the Aspila method (tot-P). Studies have found that the SEDEX procedure usually produces 10 to 16% lower tot-P values than the Aspila method (Ruttenberg 1991; Sutula et al. 2004).

Standard curves were developed using blanks (18 mega-ohm deionized water) and calibration standards prepared using the same chemical matrix as the extracted sample. To test the accuracy of the standards, standard curves were established on two different spectrophotometers, the Varian Carey 50 Win dual beam UV-vis spectrophotometer and the Helios single beam Vis spectrophotometer. No significant difference was found between standard curves calculated for the two separate spectrophotometers (r^2>0.99). The Aspila and SEDEX methods were applied to duplicate samples of a tomato leaf standard purchased from the National Institute of Standards and Technology (NIST standard reference material #1573a) with a tot-P concentration of 69.7 μmol/g. The tot-P concentration determined using the Aspila method was 80.6 μmol/g, and the tot-P concentration determined by summing the five steps of the SEDEX procedure was 27.2 μmol/g (Table 2). Total P concentrations determined using the SEDEX method have been shown to be 10 to 20% lower compared to the Aspila method (Ruttenberg 1992; Sutula et al. 2004), but the tomato leaf standard was approximately 40% lower. The lower tot-P values determined using the SEDEX method are attributed to methodological problems that developed as a result of the fine, powder-like nature of the standard. The NIST standard was a fine grained organic material that made separation with a

centrifuge difficult. Thus, a small portion of the tomato leaf standard was lost between each ofthe five steps, resulting in lower Σ-P value.

Table 2. Tomato leaf tot-P concentrations that were determined using the Aspila and SEDEX methods compared to the NIST standard reference value.

NIST Value (μmol/g)	**Aspila** (tot-P)	**SEDEX** (Σ-P)
69.67	80.63	26.71
	80.66	28.92

RESULTS

Spatial and temporal variability for ^{7}Be inventories and P fractionation were evaluated in Upper Newport Bay, where temporal variability was seasonal based on sediment and water fluxes from the watershed into the upper bay. Spatial distributions were evaluated for horizontal variability (intertidal and subtidal zone distribution) as well as for longitudinal variability (down estuary from site NB1 to NB3). All statistical tests were run using a single-factor ANOVA, p-value$_{\alpha=0.05}$ < 0.05 indicating significant difference. For all figures with error bars, the error bars are reported as ± 1 standard error, ± SE, to visually display significant difference. All references to significant difference in the text were determined quantitatively using ANOVA, and then displayed in the figures using error bars. Significance can not be determined conclusively from error bars that do not overlap, however if error bars overlap, the difference between samples is not significant.

Bulk Sediment Characteristics

The grain size distribution of sediments shows considerable spatial variability with respect to longitudinal location within the estuary as well as temporal variability (Table 3, see also Appendix B). The upper estuary site (NB1) had larger average percentages of fine sediments (56% silt/clay for the intertidal zone and 61% silt/clay for the subtidal zone), and these values decreased with increasing proximity to the lower estuary (32% silt/clay for the intertidal zone and 29% silt/clay for the subtidal zone at site NB3). Average sand fractions increased down the estuary from NB1 (45% and 33% sand at the intertidal and subtidal zones) to site NB3 (68% and 71% sand at the intertidal and subtidal zones, respectively). Sediments at this lower site showed a high concentration of sand throughout the year at both the intertidal and subtidal zones (62-89% sand). While fine-grained sediments are discharged to the estuary from San

Diego Creek, these results also suggest coarser materials are imported tidally from the coast into the upper bay by tidal currents.

The upper site (NB1) and middle site (NB2) exhibited a strong seasonal variation in grain size, with larger percentages of silt/clay materials being deposited during the wet season (February to April) when water and sediment discharge from San Diego Creek was greatest (Fig. 3). Sand concentrations increased at both NB1 and NB2 during times when discharge from San Diego Creek was low. NB3 displayed no detectable seasonal variation in grain size.

Table 3. Mean (±1σ) grain size, percent (%) sand, silt, and clay for intertidal and subtidal zones for all sites and months samples for Upper Newport Bay.

Intertidal Zone									
Month		**NB1**			**NB2**			**NB3**	
	% Sand	% Silt	% Clay	% Sand	% Silt	% Clay	% Sand	% Silt	% Clay
Jan	57.5	27.1	15.4	32.1	30.9	36.9	62.0	8.8	29.2
Feb	36.5	27.2	36.3	34.4	34.1	31.5	73.3	5.9	20.9
Mar	25.1	29.1	45.7	50.9	23.3	25.8	38.9	32.9	28.2
April	51.1	4.7	44.1	63.8	0.0	36.7	78.1	0.0	23.9
June	53.2	0.0	48.5	70.4	0.0	34.2	78.0	3.1	19.0
Sept	48.7	0.0	53.2	33.1	2.5	64.4	78.1	0.0	34.9
Nov	39.2	13.9	46.8	37.6	36.8	25.6	70.1	0.0	30.4
Average	44.5	14.1	41.4	46.0	17.5	36.5	68.3	5.0	26.6
Subtidal Zone									
Month		**NB1**			**NB2**			**NB3**	
	% Sand	% Silt	% Clay	% Sand	% Silt	% Clay	% Sand	% Silt	% Clay
Jan	51.1	25.8	23.1	41.6	28.1	30.3	62.6	16.3	21.1
Feb	25.3	32.1	42.6	45.2	22.2	32.6	56.9	24.2	18.9
Mar	27.1	37.0	35.9	33.7	29.5	36.8	69.3	11.3	19.5
April	31.9	8.9	59.3	56.9	9.7	33.4	67.6	8.1	24.3
June	42.3	0.0	57.8	55.2	6.7	38.0	83.9	2.9	13.2
Sept	60.6	0.3	39.0	62.9	0.0	38.4	67.8	0.0	37.2
Nov	32.9	36.9	30.2	59.5	6.5	34.1	89.3	2.2	8.5
Average	38.8	20.1	41.1	50.7	14.5	34.8	71.0	8.6	20.4

Images obtained through x-radiography were used to examine sedimentary structures in the bed sediment (Fig. 4). Darker areas on the image indicate fine grained sediment, while lighter coloration indicates sand particles. Each image is approximately 20 cm in length and all

are presented with equal magnification. The cores for sites NB1 and NB3 contained bivalve shells and some of the core integrity was compromised when transferred to the Plexiglas tray, which makes site to site comparisons difficult. The image for site NB2 shows evidence of

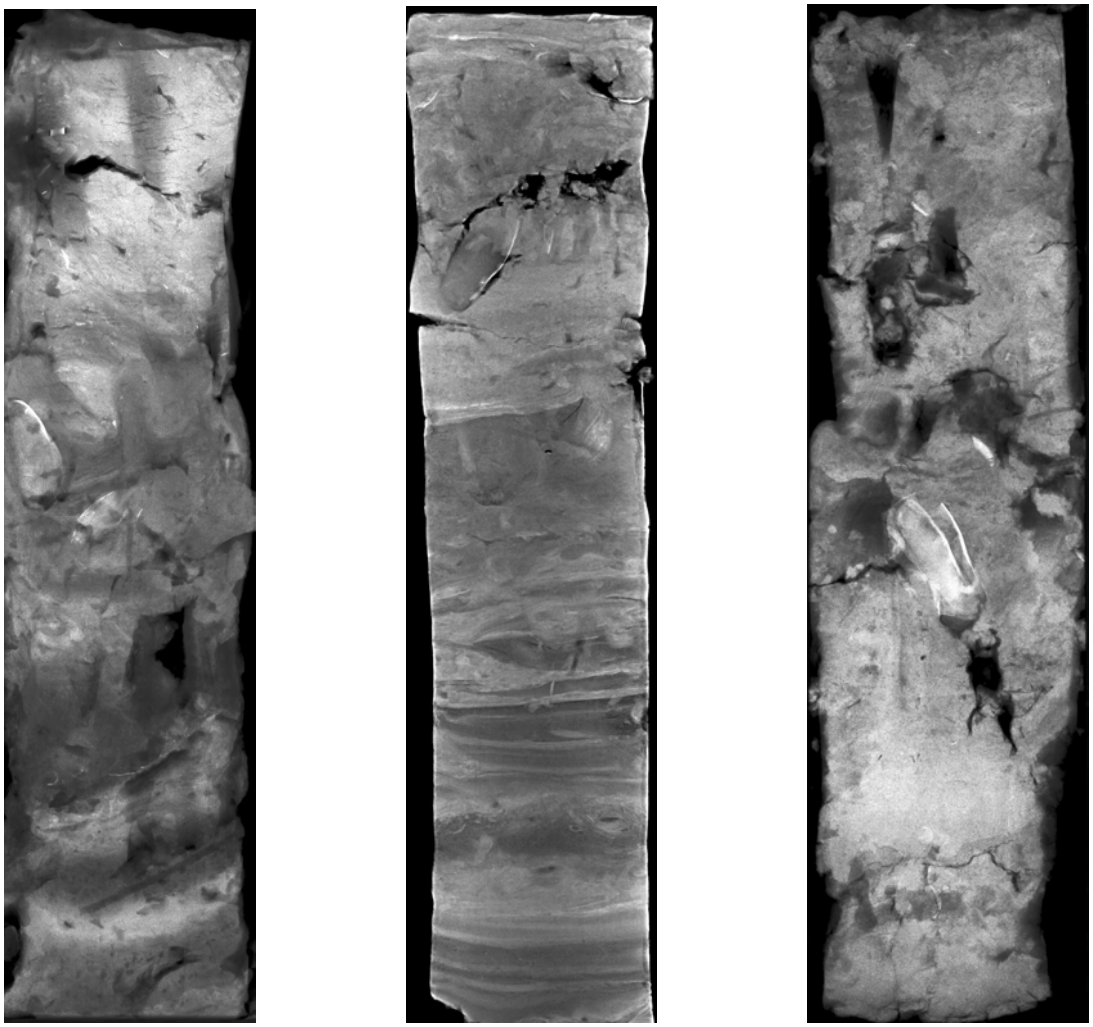

Figure 4. X-radiographic images of subtidal sediments at sites NB1 (left), NB2 (center), and NB3 (right). A distinct transition from mixed surface layer sediments to well stratified sediments appears in the lower portion of NB2 sediments. Large holes in the images (NB1, NB3) indicate areas where shells were deposited in the sediment and were removed prior to x-ray to allow the sample to fit into a slide.

mixed, unconsolidated sediment in the upper portion of the core, which transitions into distinct sedimentary layers down core. Large holes in the images indicate areas where bivalve shells

were removed to allow the sample to fit onto a slide. Bivalves in the upper sediments provide evidence for potential sediment resuspension from bioturbation.

Spatial Variability Within Sites

Five short cores were collected from the subtidal zone of NB1 to assess vertical and horizontal variability within a site (Fig. 5). Each core showed similar trends: a decrease in ^{7}Be inventory with depth in the upper 3 cm, followed by a maximum in ^{7}Be inventory at depths between 3 and 7 cm. This maximum inventory layer may be an indicator of bioturbation, recent sediment resuspension, or a combination of the two. Comparison of total inventories summed for each core provided an estimate of horizontal variability. No significant difference between the total ^{7}Be inventories for each core was found. Thus, spatial variability within sites was not considered a factor when examining short-term sediment dynamics in the upper estuary.

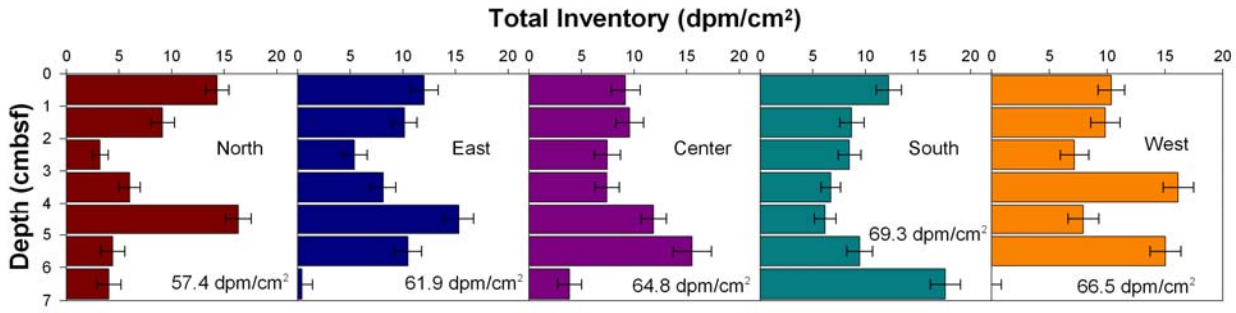

Figure 5. Vertical total inventory profiles (± SE) are shown for five cores collected at the subtidal zone of NB1 in a random pattern approximately 1 m apart. Total inventory summations for each core are displayed at the bottom of each profile.

Vertical Inventory Distributions

Intertidal zone and subtidal zone inventories are a direct function of activities in the sediments (see Appendix C for activity data). Inventories of ^{7}Be as a function of depth in the sediment were used to examine vertical variability such as event deposits or mixing of surface sediments (Figs. 6 to 8). Following a large precipitation event in February and March, the ^{7}Be

inventories increased with depth in the sediments, especially in the subtidal zone. Inventories decreased with depth in the sediment in June, and increased again slightly in September and November.

Seasonal trends for the vertical distributions of ^{7}Be at sites NB2 and NB3 were similar to site NB1 with an increase in ^{7}Be concentrations in March and April (Figs. 7 and 8). During March, ^{7}Be in the intertidal zone of NB2 was detected at a greater depth than the subtidal zone (^{7}Be was detected to 5 cm in the intertidal zone as opposed to 2 cm in the subtidal zone) which is indicative of either a larger volume of new sediment deposition or increased particle reworking down into the sediment. During the spring at site NB3, greater ^{7}Be inventories were detected in the intertidal zone than in the subtidal zone. Evidence of new sediment deposition and reworking in September was observed at both NB2 and NB3, as shown by relatively large ^{7}Be inventories compared to those in June. Beryllium-7 inventories were also found deeper in the profiles during September. The subtidal zones of NB2 and NB3 showed a slight increase in ^{7}Be deposition in November following the October storm, though not as great as that observed at site NB1.

Total Activities and Inventories

Total ^{7}Be inventories were summed for each sampling event and used in approximating sediment deposition (Fig. 9). Horizontal variability (between the intertidal and subtidal zones) was observed only during storm events. At site NB1, an increase in ^{7}Be deposition was observed in the subtidal zone during the spring wet season and following a large October storm. Site NB2 displayed no difference in deposition between the intertidal and subtidal zones. Following spring precipitation events, an increase in ^{7}Be deposition in the intertidal zone was observed at site NB3.

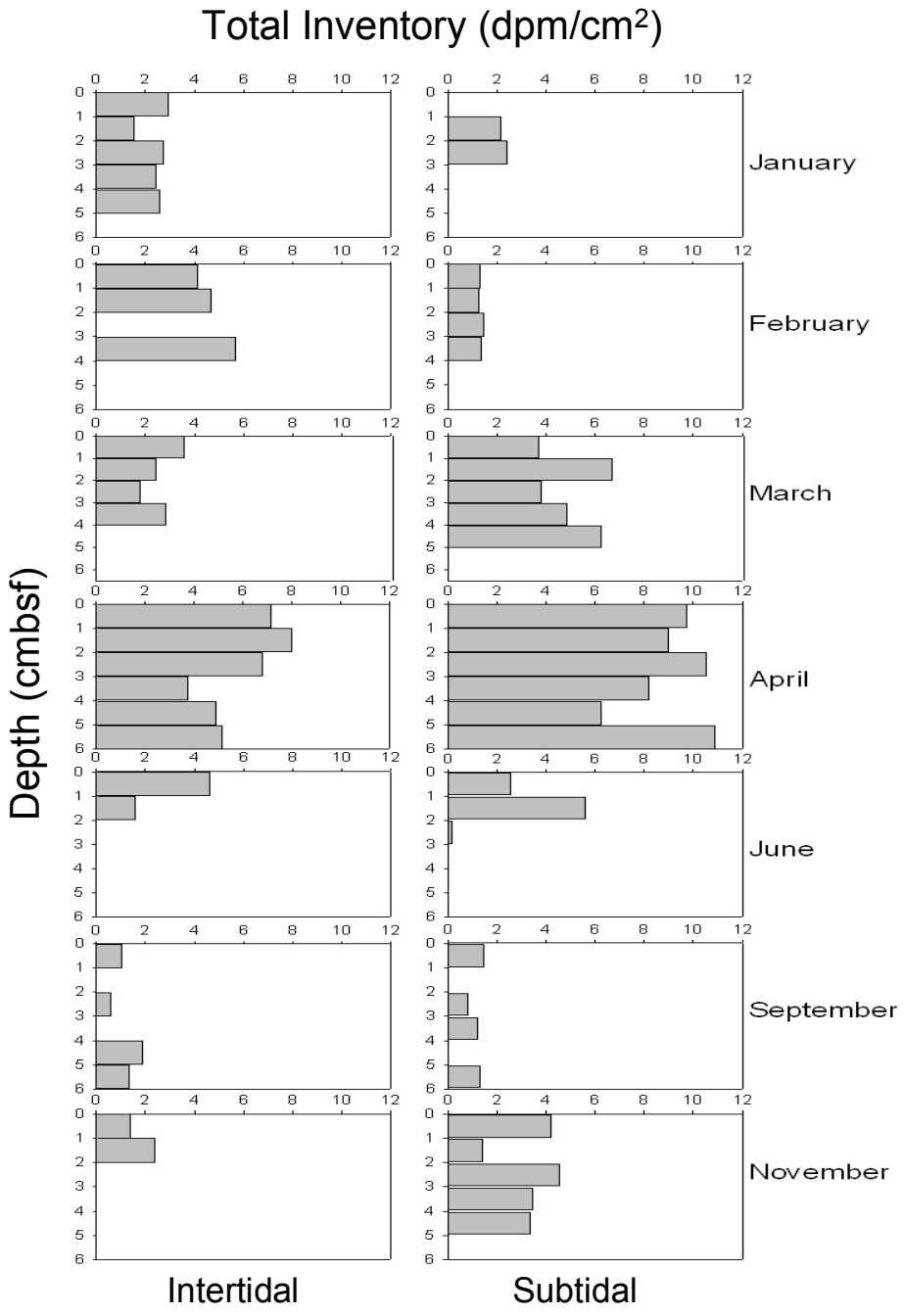

Figure 6. Monthly total ^{7}Be inventories in the upper estuary site (NB1) are shown with depth in the sediments (cmbsf) for the intertidal (left panel) and subtidal zones (right panel).

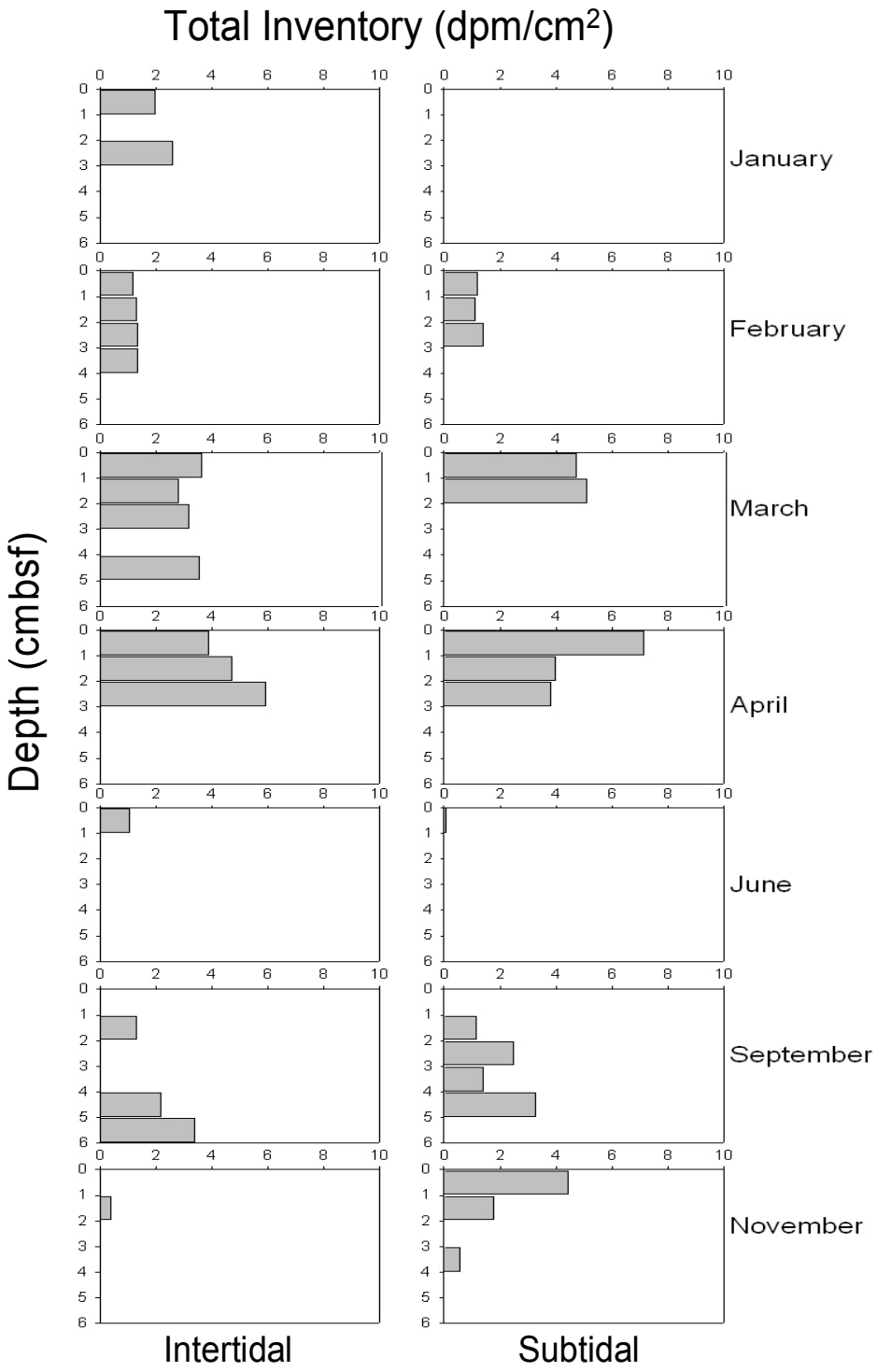

Figure 7. Monthly total ^{7}Be inventories in the upper estuary site (NB2) are shown with depth in the sediments (cmbsf) for the intertidal (left panel) and subtidal zones (right panel).

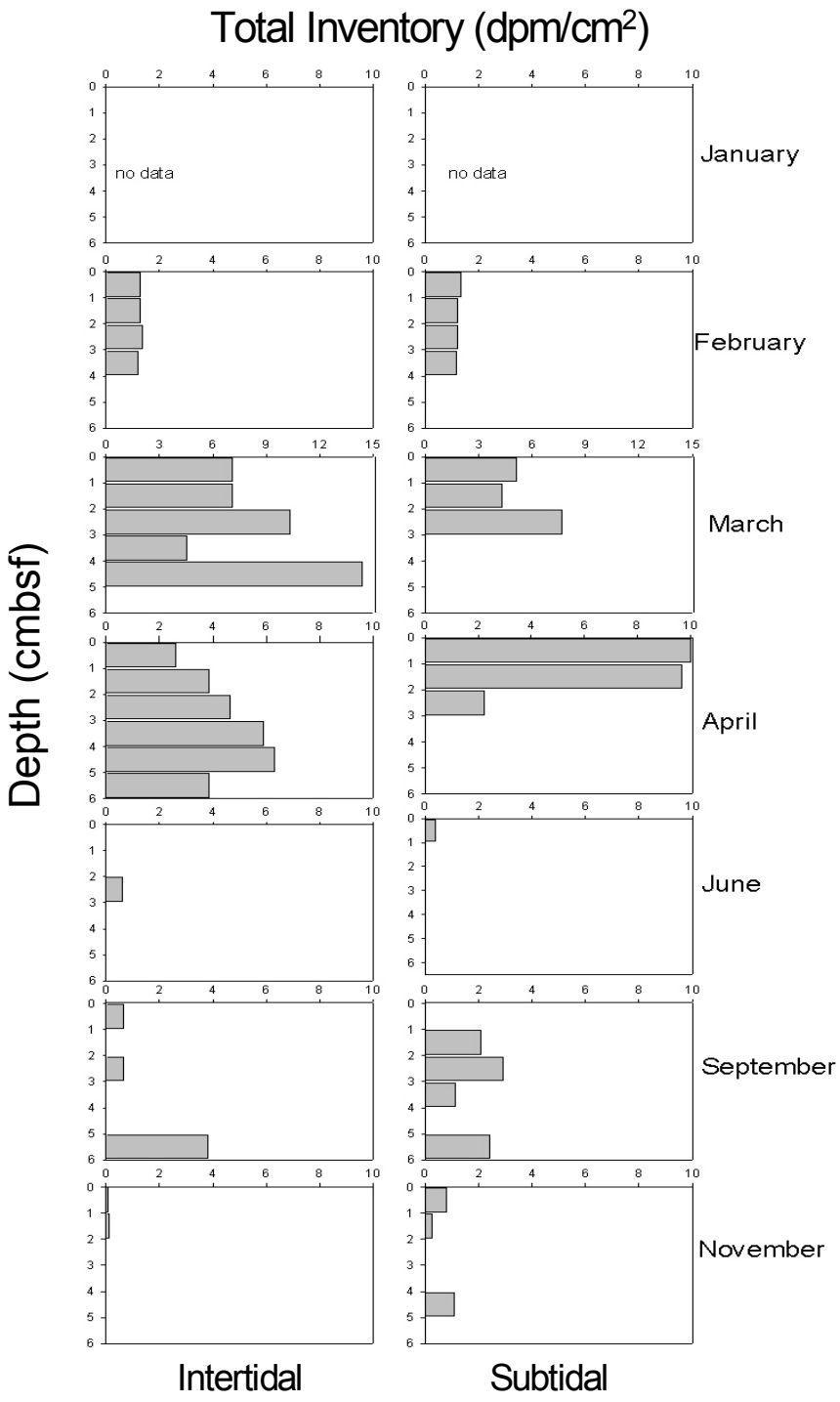

Figure 8. Monthly total ^{7}Be inventories in the upper estuary site (NB3) are shown with depth in the sediments (cmbsf) for the intertidal (left panel) and subtidal zones (right panel).

Longitudinal variability in ^{7}Be total inventories was observed within the upper estuary. NB1 was located proximal to the mouth of San Diego Creek and received the greatest total input of ^{7}Be during the course of the study for both the intertidal and subtidal zones (75.6 and 125.0 dpm/cm^2, respectively. Fig. 9). NB2 received the lowest total ^{7}Be inputs for the year (50.4 dpm/cm^2 at the intertidal zone and 49.3 dpm/cm^2 at the subtidal zone), while ^{7}Be inventories at the distal site (NB3) were intermediate between NB1 and NB2 inventories (84.7 dpm/cm^2 at the intertidal zone and 55.6 dpm/cm^2 at the subtidal zone). The increased inventories observed at NB3 may have resulted from increased deposition associated with decreased velocities around a point bar in the channel. January inventory calculations were not included in the annual summations because not all samples were analyzed for that sampling time, and their inclusion in only a few of the sites would have created biased conclusions regarding deposition.

A distinct seasonal trend of increased ^{7}Be deposition in March and April was observed for both the intertidal and subtidal zones at all sites due to high rates of precipitation, runoff, and sediment discharge from San Diego Creek (180 mm January to April; Fig. 3). Be-7 inventories were lowest during June following a period with no rainfall. Interestingly, ^{7}Be inventories increased in November after the large October precipitation event, but they were not nearly as large as the inventories observed in April following a similar magnitude of precipitation.

Total, Inorganic and Organic Phosphorus (Aspila method)

Total phosphorus (tot-P) concentrations revealed no discernable vertical trends among April, June, and November sediments (tot-P, inorg-P, and org-P values are provided in Appendix D). Thus all tot-P values reported here were averaged with depth to examine seasonal and temporal variability (Fig. 10). No consistent horizontal variability was observed for tot-P concentrations between subtidal and intertidal zones. Longitudinal variation differed across

sampling events. For example, mean tot-P values for April decreased significantly down estuary (53.9 ± 5.3, 45.7 ± 2.5, and 43.0 ± 5.7 μmol P/g for NB1, NB2, and NB3, respectively). However, June tot-P concentrations were similar (41.9 ± 2.0, 44.9 ± 1.2, and 42.4 ± 2.1 μmol P/g for NB1, NB2, and NB3, respectively), with the mid-estuary (NB2) tot-P concentration slightly higher. Tot-P concentrations appeared to increase down estuary in November, but this increase

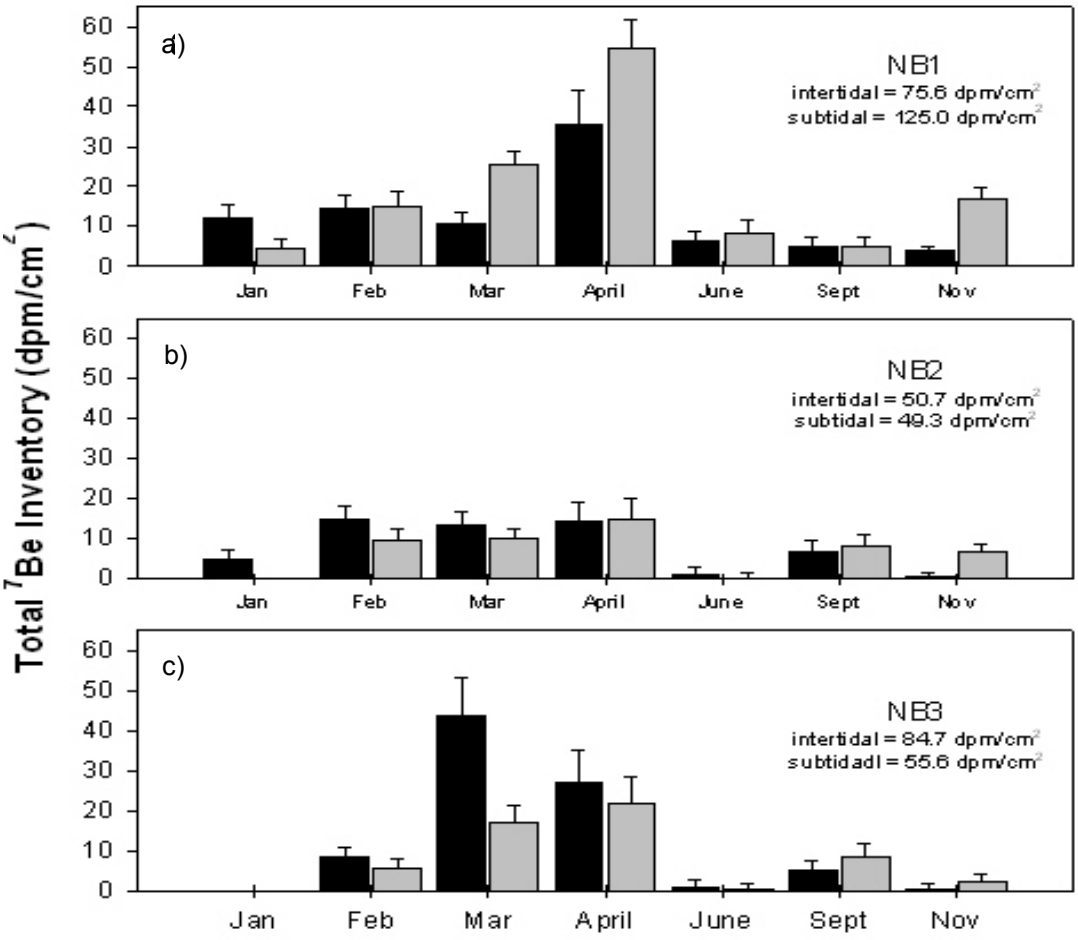

Figure 9. Total ^{7}Be inventories (± SE) in sediments are given for each site during 2004, where each site was subdivided into intertidal (black bars) and subtidal zones (grey bars). Values in each box indicate average ^{7}Be inventory for all sample events. A) Site NB1, located closest to San Diego Creek in a wide embayment, had the largest total inventories for the year. B) NB2, located about midway down the upper estuary in a narrow section with high current velocities, had the lowest total ^{7}Be inventories with no discernable trend between the intertidal and subtidal areas. C) NB3, located on a point bar at the lower end of the study area, had the greatest total ^{7}Be inventories in the intertidal zone.

was not statistically significant (37.9 ± 4.4, 43.2 ± 6.2, and 44.4 ± 4.5 μmol P/g for NB1, NB2, and NB3, respectively).

Mean org-P and inorg-P concentrations in the intertidal and subtidal zones were used at each site to examine spatial and temporal P trends in the upper estuary (Fig. 11). Org-P concentrations in April and June were observed to increase between sites NB1 and NB2, but org-P concentrations decreased significantly at site NB3 (Fig. 11**,** top panel). No significant variation in org-P concentrations existed among any of the November sites. Inorg-P concentration was highest in April at site NB1 (49.8 ± 4.8 μmol P/g) and decreased significantly during June (37.2 ± 1.2 μmol P/g) and November (35.0 ± 3.2 μmol P/g. Fig. 11, bottom panel). Inorg-P concentrations at site NB2 and NB3 were similar for all months and did not vary significantly (inorg-P concentrations were between 39.2 ± 4.9 and 41.3 ± 2.0 μmol P/g).

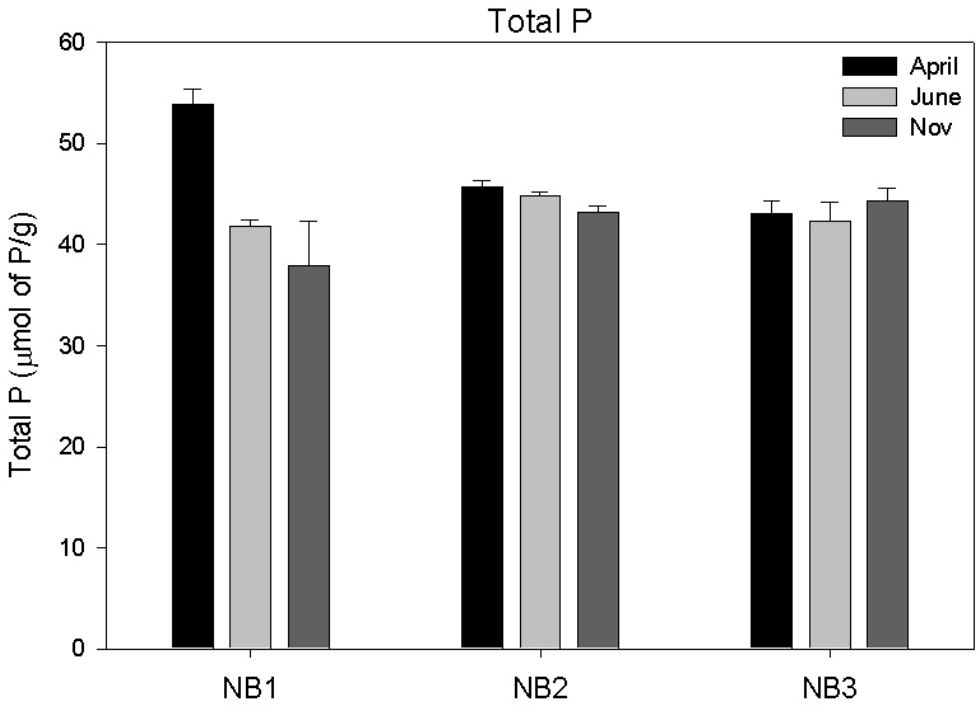

Figure 10. Mean Aspila tot-P concentrations (± SE) are shown for all sites for April, June, and November at Upper Newport Bay.

Sequential Phosphorus Extraction (SEDEX method)

Initially, the SEDEX procedure was run for each depth interval for all sites in April, June, and November (Appendix E), and phosphorus values for all months sampled were averaged for each depth interval to evaluate vertical variability (Fig. 12). Of the five extractions, lab-P and org-P phases exhibited the lowest concentrations and were the only fractions to display vertical gradients. Because vertical variability was not observed in the fractions with the highest concentrations of P, spatial and temporal variability of P distributions in the upper sediments were examined by homogenizing equal portions from each depth interval, then analyzing whole-core bulk sediment using SEDEX. Any P concentrations reported for the rest of this paper will refer to whole-core concentrations obtained with homogenized sediments analyzed using the SEDEX method.

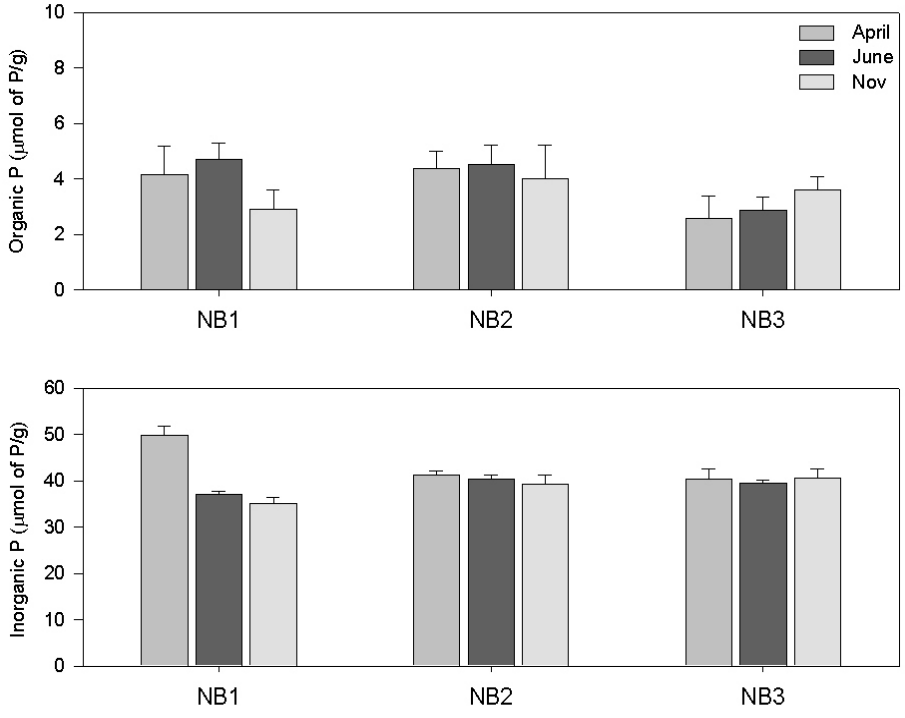

Figure 11. Mean org-P (top) and inorg-P (bottom) concentrations (± SE) for all sites sampled during April, June, and November are shown Note inorg-P is six times greater than org-P.

Total P concentrations determined from the SEDEX method (Σ-P) were lower than the Aspila method (tot-P; Table 4), which corresponds to previous studies that found lower total P values (10 to 20%) using the SEDEX method compared to the Aspila method (Ruttenberg 1991; Sutula et al. 2004). In this study Σ-P values obtained with the SEDEX method were 12 to 39% lower than Aspila tot-P. Spatial and temporal trends in total P obtained with both methods were similar, with larger values being recorded in April and November, and higher P concentrations in the subtidal zones than the intertidal zones.

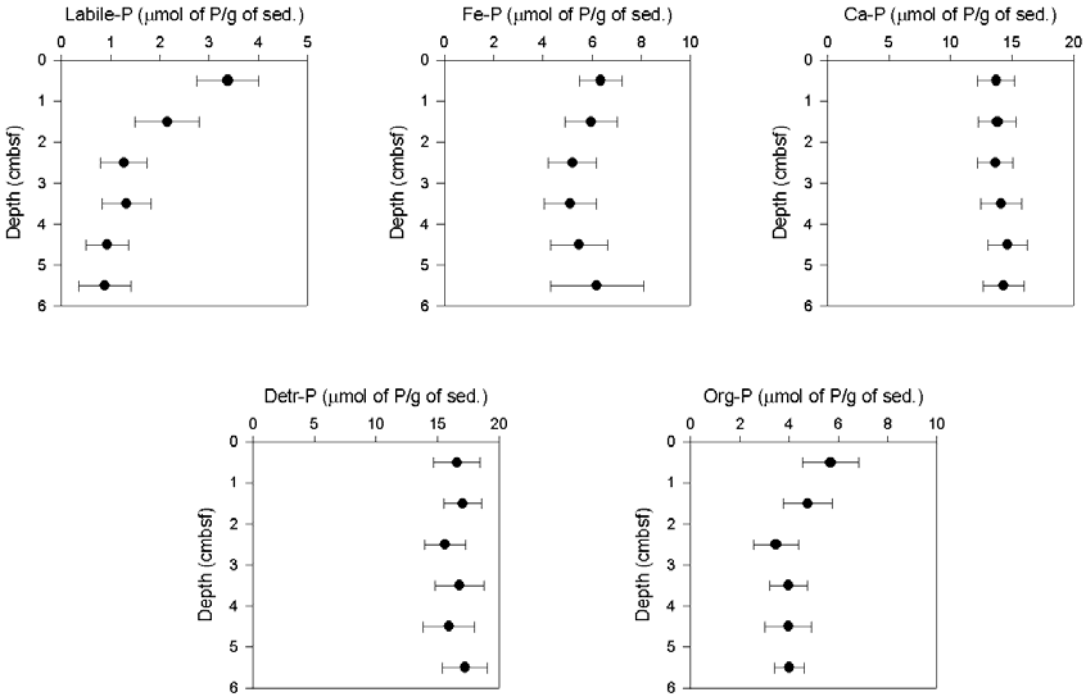

Figure 12. The five P fractions extracted using the SEDEX procedure are shown (± SE). P concentrations are average values for each site analyzed in April, June, and November.

Concentrations of phosphorus for the intertidal zones and subtidal zones varied based on the extracted fraction (Table 4). Generally, the Lab-P and Fe-P fractions were greater in the subtidal zone, while detr-P exhibited larger concentrations in the intertidal zone for all sites. Higher concentrations of Ca-P were observed in the subtidal zones at sites NB1 and NB3, but

were greater in the intertidal zone of NB2. Greater org-P concentrations were observed in the subtidal zone during April and in the intertidal zone in June, regardless of the site.

Distributions of the sediment P fractions in the upper estuary, with subtidal and intertidal zones averaged together for each site to examine longitudinal distribution, were variable with no consistent down estuary trend in Σ-P concentrations: Lab-P was 0.4 to 2.6 μmol/g; Fe-P was 6.0 to 8.1 μmol/g; Ca-P was 13.6 to 18.5 μmol/g; detr-P was 3.3-9.7 μmol/g; and org-P was 0.7-3.2 μmol/g (Fig. 13). Concentrations of Fe-P and Ca-P decreased down estuary, but only the Ca-P decrease was statistically significant along this gradient ($p<0.05$). Detr-P increased down estuary from NB1 to NB3, however this increase was not statistically significant. Lab-P and org-P varied down estuary with no discernable trend in concentrations. The refractory P phases (Ca-P and detr-P) comprised the largest fractions of sediment-bound P in the upper estuary. Ca-P and detr-P concentrations were significantly greater than the bioavailable fractions at every site and every month sampled, indicating that the majority of sediment-P is buried once the sediment is deposited.

Mean P concentrations for all sites from each extracted fraction for each month sampled were evaluated to examine seasonal variability (Table 5). The Σ-P was significantly higher in April when compared to June and November. Variation between months for the detr-P fraction was significant, but not for the Lab-P, Fe-P, Ca-P, and Org-P fractions. In general, values were highest in April and lowest in June, except for the Ca-P fraction which exhibited similar values across all months. The Ca-P fraction comprised the largest percent composition for each month (43 to 54%), followed by the Fe-P (20 to 24%), and detr-P (16 to 24%) fractions, with the org-P and lab-P fractions representing the lowest percent compositions (4 to 7%, and 3 to 5%, respectively).

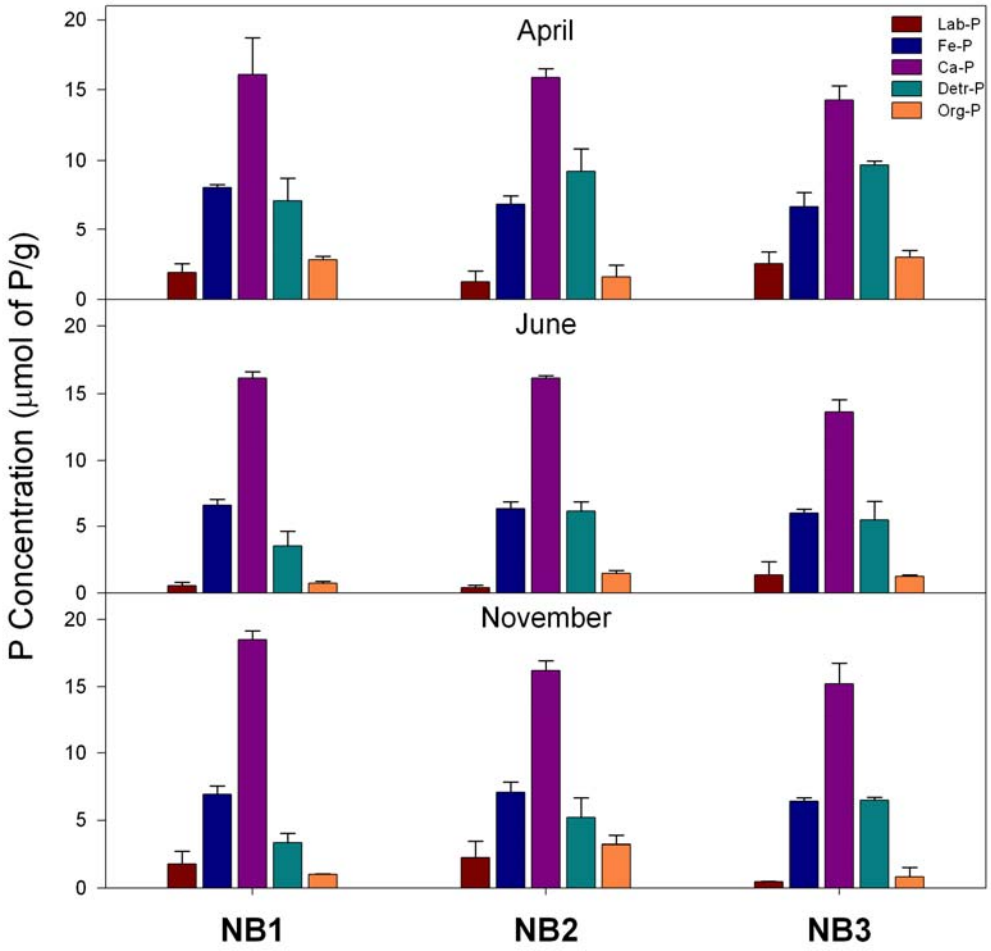

Figure 13. Whole core homogenized concentrations (± SE) obtained using the SEDEX extraction procedure for each site and month sampled (intertidal and subtidal sediments at each site are averaged).

Table 4. Phosphorus fractions (± 1σ) were determined using the SEDEX procedure for each site and month sampled. The summation (Σ-P) of the five fractions indicates total phosphorus concentrations and are compared to tot-P determined via the Aspila method.

APRIL	Lab-P	Fe-P	Ca-P	Detr-P	Org-P	Σ-P	Tot-P
Intertidal							
NB1	1.25 ± 0.66	7.87 ± 0.04	13.46 ± 1.50	8.73 ± 3.59	3.07 ± 3.05	34.38 ± 4.85	49.66 ± 2.61
NB2	0.46 ± 0.87	6.26 ± 0.89	16.51 ± 0.81	10.86 ± 0.23	0.77 ± 0.02	34.86 ± 6.85	44.39 ± 1.00
NB3	1.70 ± 1.03	5.71 ± 1.26	13.22 ± 2.95	9.96 ± 4.38	2.52 ± 1.08	33.11 ± 4.91	37.69 ± 1.70
Subtidal							
NB1	2.55 ± 0.62	8.27 ± 0.88	18.71 ± 2.59	5.52 ± 1.15	2.58 ± 0.91	37.64 ± 6.69	58.21 ± 3.29
NB2	2.04 ± 1.29	7.51 ± 0.36	15.30 ± 2.07	7.58 ± 0.10	2.44 ± 0.02	34.87 ± 5.36	47.01 ± 2.80
NB3	3.39 ± 0.23	7.75 ± 1.71	15.31 ± 3.14	9.47 ± 4.34	3.49 ± 1.76	39.40 ± 4.93	47.46 ± 3.40
JUNE	**Lab-P**	**Fe-P**	**Ca-P**	**Detr-P**	**Org-P**	**Σ-P**	**Tot-P**
Intertidal							
NB1	0.28 ± 0.41	6.12 ± 0.22	15.70 ± 1.84	4.63 ± 0.11	0.88 ± 0.54	27.60 ± 6.20	40.29 ± 0.55
NB2	1.09 ± 0.39	6.28 ± 1.79	16.95 ± 1.18	3.75 ± 0.06	2.6 ± 3.08	30.51 ± 6.15	45.16 ± 1.53
NB3	0.42 ± 0.13	6.18 ± 1.43	16.77 ± 2.20	6.29 ± 0.11	1.55 ± 0.08	24.65 ± 4.91	41.35 ± 1.22
Subtidal							
NB1	0.82 ± 0.68	7.01 ± 0.04	16.65 ± 2.63	2.40 ± 0.11	0.56 ± 0.96	27.44 ± 6.76	43.76 ± 1.30
NB2	3.44 ± 0.27	7.83 ± 2.17	15.46 ± 0.60	6.67 ± 0.04	3.89 ± 4.55	30.39 ± 6.33	44.58 ± 0.60
NB3	0.51 ± 0.15	6.67 ± 0.24	13.63 ± 0.05	6.69 ± 0.04	0.11 ± 0.02	30.59 ± 5.28	43.18 ± 2.26
NOVEMBER	**Lab-P**	**Fe-P**	**Ca-P**	**Detr-P**	**Org-P**	**Σ-P**	**Tot-P**
Intertidal							
NB1	0.87 ± 0.65	6.26 ± 2.00	17.90 ± 2.47	4.05 ± 0.02	0.95 ± 0.60	30.04 ± 7.03	34.22 ± 1.63
NB2	1.09 ± 0.39	6.28 ± 1.79	16.95 ± 1.18	3.75 ± 0.06	2.60 ± 3.08	30.66 ± 6.34	38.06 ± 2.94
NB3	0.42 ± 0.13	6.18 ± 1.43	16.77 ± 2.20	6.29 ± 0.11	1.55 ± 0.08	31.21 ± 6.46	47.14 ± 2.91
Subtidal							
NB1	2.74 ± 0.75	7.55 ± 2.38	19.16 ± 4.00	2.58 ± 0.30	1.07 ± 0.41	33.11 ± 7.42	42.33 ± 1.09
NB2	3.44 ± 0.27	7.83 ± 2.17	15.46 ± 0.60	6.67 ± 0.04	3.89 ± 4.55	37.29 ± 4.84	48.35 ± 3.93
NB3	0.51 ± 0.15	6.67 ± 0.24	13.63 ± 0.05	6.69 ± 0.04	0.11 ± 0.02	27.60 ± 5.54	41.68 ± 4.00

Table 5. Average (± 1σ) P concentrations in sequentially extracted fractions are given for all sites in April, June, and November 2004. Values in parentheses represent the percent composition for each extracted fraction.

	Lab-P (μmol P/g)	Fe-P	Ca-P	Detr-P	Org-P	Σ-P
April	2.0 ± 1.0 (5)	7.2 ± 1.0 (20)	15.4 ± 2.0 (43)	8.7 ± 1.9 (25)	2.5 ± 0.9 (7)	35.7 ± 2.3
June	0.8 ± 0.8 (3)	6.3 ± 0.5 (22)	15.3 ± 1.5 (54)	5.0 ± 1.7 (17)	1.1 ± 0.4 (4)	28.5 ± 2.4
Nov	1.5 ± 1.3 (5)	6.8 ± 0.7 (21)	16.7 ± 1.9 (53)	5.0 ± 1.8 (16)	1.7 ± 1.4 (5)	31.7 ± 3.3

DISCUSSION

Evaluating Sediment Dynamics Using Particle-Reactive Tracers

Estuaries are effective sediment transport and storage basins as sediments move between terrestrial and open ocean systems (Dellapenna et al. 2003). Flocculation of particles can occur as terrigenous sediments carried in freshwater interact with seawater at the head of the estuary (Dyer 1995). Sediment deposition in estuaries tends to be larger at river mouths and is enhanced by the geomorphology of the estuary because water velocities slow as river runoff discharges into a wider estuary basin, allowing sediments to settle out of suspension (Sommerfield and Lee 2003). In this study, the greatest sediment inputs to Upper Newport Bay occurred at the uppermost site (NB1), located proximal to the mouth of San Diego Creek, which provides over 90% of the sediment input to the upper estuary (Masters and Inman 2000). Previous findings indicated that during both peak and base flow conditions, most deposition occurs in the lower energy areas bordering the main channel, primarily where the cross-sectional area of the channel expands (USACE 1997).

Total new inventories of ^{7}Be to the upper estuary, net ^{7}Be flux to the sediment, and short-term sediment deposition and resuspension rates were calculated for UNB (Table 6.). When positive new inventory values were summed for each sampling event (per explanation in the methods), the highest value occurred in the subtidal zone of NB1 (69.1 dpm/cm^2). New inventory values were lowest at NB2 and intermediate at NB3, similar to the trend observed for total ^{7}Be inventories. New inventory values were negative at every site in June, suggesting sediment loss.

Average short-term sedimentation rates for the year suggest that sediment is accreting fastest at site NB1. Site NB1 is located closer to the mouth of San Diego Creek, thus it is

subjected to larger sediment inputs than the two downstream sites, allowing sedimentation rates to exceed erosion rates. Because much of the sediments are deposited at NB1, sites NB2 and NB3 have diminished loading rates, and thus the erosional forces acting on these sites are not offset by new sediment inputs from San Diego Creek. Another possibility is strong tidal or wind events may resuspend previously deposited sediments and redistribute them downstream, but this could not be confirmed with the evidence at hand. In a 2-D hydrodynamic and sediment budget model, the USACE (1997) predicted estuarine depositional patterns similar to those observed in this ^{7}Be study, where deposition would be greater in the upper estuary, decrease through the middle estuary and increase again at the lower estuary. Increased deposition in the lower site could also be due to sediment input from the lower bay, however sediment input data from the lower estuary was not available for this study.

The highest short-term sediment accumulation rates occurred between February and April, presumably in response to large precipitation events during which large new sediment inputs were discharged from San Diego Creek (Table 6). This calculation provides an estimate of net deposition or resuspension between sampling periods using the ^{7}Be tracer. The largest short-term sedimentation rates were observed at NB1 during late spring (April: 0.35 g/cm^2 d, intertidal zone; 0.26 g/cm^2 d, subtidal zone). Sediment accumulation rates in the fall (September and November) were consistently smaller than those calculated for the spring wet season.

All sample sites in June exhibited resuspension, which is indicative of an erosional regime, and was likely due to the influence of resuspension/erosion plus the lack of new sediment input from San Diego Creek during the summer dry season. Probable forces leading to resuspension of sediment were tidal currents and bioturbation acting on the shallow sediments. The NB2 intertidal zone and the NB3 intertidal and subtidal zones also experienced sediment

removal during November (-0.19, -0.63, and -0.07 g/cm^2 d, respectively). Resuspension rates are assumed to be the upper limit of remobilization potential within the upper estuary. Because the elapsed time between sampling events in summer and fall exceeded the mean life of 7Be ($^1/_\lambda$ = 77 days) it is likely residual inventory effects were not detected.

Table 6. Calculated new inventory, net ^{7}Be flux, and short-term sediment accumulation rates for sites sampled in Upper Newport Bay during 2004. Note the new inventory summation only includes months where deposition occurred (positive new inventory) and excludes data from February where some sites did not have measurements.

	Feb.	**Mar**	**Apr**	**Jun**	**Sept.**	**Nov.**	$\sum_{deposition}$
Elapsed Time (days)	26	41	21	56	99	57	dpm/cm^2
NB1 – intertidal							
new inventory (dpm/cm^2)	5.74	2.16	27.63	-10.92	3.14	1.48	**34.41**
net ^{7}Be flux (dpm/cm^2 d)	0.22	0.05	1.32	-0.19	0.03	0.03	
acc./removal rate (g/cm^2 d)	0.04	0.11	0.35	-0.09	0.04	0.05	
NB1 – subtidal							
new inventory (dpm/cm^2)	11.73	16.59	35.34	-17.96	2.51	14.67	**69.11**
net ^{7}Be flux (dpm/cm^2 d)	0.45	0.40	1.68	-0.32	0.03	0.26	
acc./removal rate (g/cm^2 d)	0.21	0.15	0.26	-0.26	0.04	0.12	
NB2 – intertidal							
new inventory (dpm/cm^2)	11.53	4.52	4.52	-5.92	6.55	-2.87	**15.59**
net ^{7}Be flux (dpm/cm^2 d)	0.44	0.11	0.22	-0.11	0.07	-0.05	
acc./removal rate (g/cm^2 d)	0.15	0.14	0.13	-0.14	0.04	-0.19	
NB2 - subtidal							
new inventory (dpm/cm^2)		4.22	7.50	-7.10	8.24	2.86	**22.82**
net ^{7}Be flux (dpm/cm^2 d)	no data	0.10	0.36	-0.13	0.08	0.05	
acc. rate (g/cm^2 d)		0.07	0.13	-2.20	0.06	0.02	
NB3 - intertidal							
new inventory (dpm/cm^2)		38.65	-5.85	-12.46	4.83	-2.19	**43.48**
net ^{7}Be flux (dpm/cm^2 d)	no data	0.94	-0.28	-0.22	0.05	-0.04	
acc./removal rate (g/cm^2 d)		0.18	-0.09	-0.54	0.05	-0.63	
NB3 - subtidal							
new inventory (dpm/cm^2)		13.84	8.96	-10.18	8.49	-1.97	**31.29**
net ^{7}Be flux (dpm/cm^2 d)	no data	0.34	0.43	-0.18	0.09	-0.03	
acc./removal rate (g/cm^2 d)		0.10	0.06	-0.67	0.09	-0.07	

Vertical total ^{7}Be inventories showed fine scale spatial and temporal variability in the upper sediments (Figures 6 to 8). During 2004, the highest rates of total ^{7}Be deposition occurred in subtidal environments. Most vertical trends observed in the Upper Newport Bay displayed variable ^{7}Be concentrations throughout the upper 6 cm. This variability is indicative of a more dynamic system in which sediments are reworked due to strong bed currents, storm events, or bioturbation (Fitzgerald et al. 2001; Sutula et al. 2006).

Temporal variability of ^{7}Be inventories in UNB corresponded well with seasonal variations in precipitation and San Diego Creek discharge to the upper estuary. Likewise, mean sediment discharge in the spring (1589.3 kg/d) was twice that of the summer (796.2 kg/d). The wet season in southern California generally occurs from October to April, and studies have shown a direct correlation between ^{7}Be fluxes from the atmosphere and precipitation events (Olsen et al. 1986; Vogler et al. 1996). The largest 2004 precipitation events occurred during spring and discharge from San Diego creek introduced large amounts of suspended sediment to the upper estuary, which led to the highest short-term deposition rates in the estuary in the spring.

A temporal lag occurred between precipitation events and observations of increasing ^{7}Be inventories. The largest quantity of rainfall in UNB occurred in February (133.6 cm), while most of the new ^{7}Be inventory at the upper intertidal and subtidal zones occurred during March and April. High seasonal flows, storms, or human perturbations can keep sediments in suspension for extended time periods and also re-introduce previously deposited ^{7}Be back to the water column (Olsen et al. 1986). Although ^{7}Be generally has a short residence time in the water column of approximately 1 to 20 days (Baskaran et al. 1997), these disturbances can prolong the residence time of particle-bound ^{7}Be in the water column by as much as 50 days. Because storm events not only deliver new sediments from San Diego Creek but can also resuspend sediments

from the bed, ^{7}Be can be scavenged by both sediment sources. Thus, a massive influx of sediment to the water column may increase settling times and result in the observed time delay between precipitation events and ^{7}Be appearance in the sediment bed.

The unexpectedly low ^{7}Be input following the large precipitation event in October may be linked to ^{7}Be production in the upper atmosphere. Beryllium-7 concentrations have been found to vary temporally in the troposphere. Most ^{7}Be is produced in the stratosphere and is readily transferred into the troposphere during the spring when seasonal thinning and folding of the tropopause into the stratosphere leads to an increased interaction between the two layers (Olsen et al. 1986; Baskaran et al. 1993; Rehfeld and Heimann 1995). Decreased atmospheric transport of ^{7}Be downward in the fall could lead to a decrease in ^{7}Be delivery to the Earth's surface (Dibb and Meeker 1994; Baskaran 1995). As a result, precipitation events during fall may be less effective at delivering ^{7}Be to UNB and may explain the low ^{7}Be inventories observed during this time of year.

Most arguments of seasonal atmospheric deposition favor increases in ^{7}Be fluxes from the atmosphere during the spring, but certain studies have found episodic increases in ^{7}Be atmospheric fluxes during the fall as well (Yoshimori et al. 2003). In Upper Newport Estuary, a deposition event was recorded in the sediments based on ^{7}Be inventories in September following a four month period without precipitation and very little creek discharge. If atmospheric ^{7}Be concentrations did occur in the late summer/early fall, dry atmospheric deposition may be responsible for delivering ^{7}Be to the bay, where it adsorbs to sediments resuspended by winds, bioturbation, and/or tides.

Comparing Short-term and Long-term Accumulation

Using the CF:CS model, excess ^{210}Pb activities in the NB1 subtidal zone were evaluated to determine a long-term sedimentation rate of 0.15 cm/yr in UNB (Fig. 14). By comparison, the

average of all short-term sedimentation rates determined from ^{7}Be new inventories across the entire year for all sites yields a mean short-term sedimentation rate of 24.7 cm/yr. From this analysis less than 1% of the new sediment deposited throughout the year will be buried in the system over decadal timescales. This difference in sedimentation rates highlights the dynamic nature of shallow sediments in the estuary. The remaining sediments not buried are presumably resuspended and redistributed within the estuary or exported to the ocean.

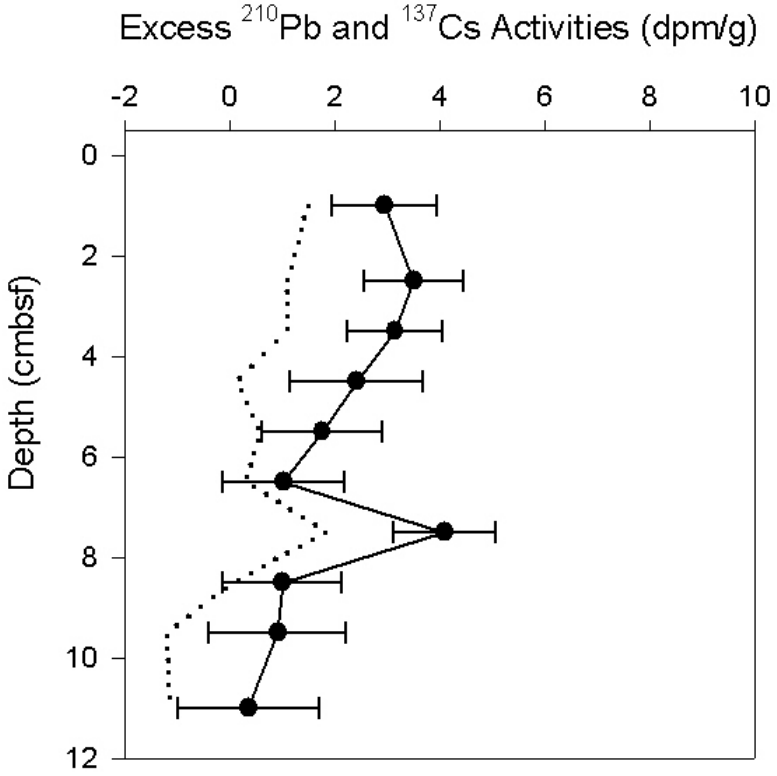

Figure 14. Excess ^{210}Pb (bold line) and ^{137}Cs (dotted line) activities (± SE) are shown versus depth in the sediments. The long-term sedimentation rate for Upper Newport Estuary is 0.15 cm/yr.

Current and wind-induced physical processes are important forcing mechanisms for sediment transport in coastal environments (e.g. Booth et al. 2000 and references therein). New sediment delivered to the bay via runoff from San Diego Creek can be transported down estuary by tidal and storm-induced flow or wind-generated wave orbitals during low tide (USACE 1997). Daily

wind speed data obtained from an offshore buoy (National Buoy Data Center 46025) were used to estimate depth and fetch-limited wave heights, lengths, and periods using equations developed by the USACE Coastal Engineering Research Center (USACE 1984). These values were in turn used to calculate wind-induced shear stress, critical shear velocity, and maximum orbital velocity at the estuary bed (Wright 1995). For all sites, these estimates suggest wind speeds alone were not large enough to resuspend sediments, as the fetch distances (250 to 455 m) and water depth (2 to 4 m) were too small to generate orbital velocities that would affect the estuary bed. Wind-induced wave orbital velocities alone were not substantial enough to mobilize sediment, however it is likely winds enhance the daily tidal and episodic storm current velocities and potentially generate enough force to transport sediment within or out of the estuary.

Although tidal currents are often assumed to be the driving force behind sediment transport within Upper Newport Estuary (Trinast 1974; USACE 1997; Sutula et al. 2006), no substantial measurements of near-bed tidal current velocities exist to make quantitative estimates of resuspension potential. A 2-D sediment transport model estimated the critical bed shear stress to be 0.12 N/m^2 (USACE 1997). Taking the square root of this value divided by the average bulk density of the sediments near the sediment-water interface (1360.6 kg/m^3) provides a critical bed shear velocity of 0.01 m/sec in Upper Newport Bay. Sediment deposition can occur when actual shear velocity is less than the critical bed shear velocity (Dyer 1995). The quadratic stress law was used to approximate mean flow velocity 1 m above the bed ($\bar{U}_{100}$):

$$U_* = C_{100}^{1/2} \overline{U}_{100} \tag{8}$$

where U_* is the critical bed shear velocity and C_{100} is a dimensionless drag coefficient with a range of 0.002 to 0.004 (Sternberg 1972). Based on these values, current velocities capable of transporting sediment within the upper estuary would be between 0.15 and 0.21 m/sec. A single

suite of synoptic velocity measurements collected at a depth of approximately 0.5 m from the water surface in April, 2005 revealed flows between 0.15 and 0.22 m/sec in the middle of the channel at high tide. Thus, tidal currents appear to be fully capable of eroding and transporting sediments in UNB. Actual measurements of current velocities near the bed would not only provide information regarding when conditions were favorable for deposition or resuspension, but also whether conditions were conducive for significant transport events within and out of the upper estuary.

Sediment Dynamics and Phosphorus Concentrations

Sediment-bound P concentrations in Upper Newport Bay followed the seasonal trends of sediment deposition and resuspension. Total P values measured using the Aspila and SEDEX methods show increased concentrations in April following periods of high sediment discharge. June total P concentrations decreased, corresponding to increased resuspension rates. November total P concentrations increased slightly, which is likely the result of decreased biological activity and small sediment inputs from San Diego Creek.

During periods of low sediment input (June), tot-P concentrations in the sediment decreased, corresponding to periods of increased resuspension from bottom sediments, greater amounts of particulate P are introduced to the water column (Sutula et al. 2006). Increased microalgae growth occurred in June, which tends to decrease P concentrations in the water column, and with no new input of P from creek discharge, conditions favored upward diffusion of interstitial or soluble P to the water column (Sutula et al. 2006). Increased P uptake subsequently increased total P flux from the pore waters, which would lead to desorption of phosphorus from sediment in response to the pore water concentration gradient (Cowen and Lee 1976).

For both methods (Aspila and SEDEX), org-P was greatest at NB1, especially in the subtidal zone, and was likely due to an increase in organic matter being discharged with suspended sediment from San Diego Creek. Silt and clay content at the upper site also increased during April, and have been shown to have a higher organic matter content (Froelich 1988; Sutula et al. 2006). Org-P concentrations decreased in June, indicating a possible release of org-P from sediment as water column phosphorus was utilized by microalgae growth during the summer. The org-P fraction removed from the sediments using the Aspila method produced slightly higher concentrations than those removed using the SEDEX procedure. However, the Aspila method has been found to overestimate org-P concentrations due to solubilization of inorg-P following the ashing step (Ruttenberg 1992). The org-P extraction is the final step in the five-step SEDEX procedure and procedural loss of P during extractions increase with each step.

Increased particulate P concentrations in the open ocean show seasonal patterns linked to times of increased primary productivity (Faul et al. 2005). However, nearshore locations show larger increases of particulate P during periods of large storm events, which would increase lithogenic fluxes of sediment and also increase resuspension and lateral advection of sediments (and sediment-bound P). Thus, greater P fluxes occur due to new sediment input than from particles sinking in coastal environments (Pilskaln et al. 1996). This study corroborates these findings, as total P concentrations consistently increased with high sediment discharge from San Diego Creek to the upper estuary, but during times of increased primary productivity (June), total P values in the sediment decreased. Sediment bound total P concentrations showed significant seasonal variation for both the Aspila and SEDEX methods. Total P concentrations in the sediment were greatest during April when sediment deposition was largest, and decreased in

June. November total P increased slightly as a result of a small increase in sediment entering the upper estuary, and a decrease in biological productivity in the water column.

Phosphorus Fractionation Potential Bioavailability

Burial or release of P in sediments is governed by five main processes: (1) the input of sediments; (2) the subsequent sedimentation rate, i.e., P is buried at a rate greater than upward diffusion and advective rates releasing P to the water column; (3) grain properties (composition and grain size or surface area of the sediments); (4) resuspension frequency, i.e., how often sediments (and pore waters) are reworked through physical or biological forces; and (5) the diagenetic shift of P within the sediments from a labile to a more refractory state (Ruttenberg and Berner 1993; Vink et al. 1997). Particle-bound inorganic P is released from sediments to compensate for a decrease in pore water P concentrations (Cowen and Lee 1976). Vink et al. (1997) found the driving factors regulating phosphorus concentrations in the upper 40 cm of shallow estuary sediments are bioturbation and non-steady state deposition of sediment, while phosphorus concentrations in sediments analyzed below 40 cm were regulated by diagenetic redistribution of P forms.

Certain components of sediment-bound P are readily available to organisms, while others are considered sinks (Ellison and Brett 2006). In this study, we classified 3 different levels of bioavailability based on how rapidly the fraction would be available for biological uptake: (1) readily bioavailable phosphorus, i.e., lab-P fraction; (2) potentially bioavailable phosphorus, or phosphorus that can become available following diagenetic reactions in the sediment, i.e., Fe-P and org-P; and (3) refractory phosphorus, or the phase biologically unavailable over timescales of years to decades, i.e., Ca-P and detr-P. The most biologically available or potentially available fractions (lab-P and org-P) decreased with depth over 6 cm, indicating a flux of P into

the sediment with subsequent consumption in the upper sediments (Fig. 13). This consumption is likely due to a release of sediment-bound P to the pore waters to compensate for upward advection-diffusion of soluble P from pore waters to the water column. As interstitial P enters the water column, particle-bound P must be released to pore waters in response to the concentration gradient. Interestingly, depth-averaged lab-P and org-P concentrations were consistently the lowest values measured, regardless of time or location within the upper estuary, and indicate how quickly these fractions must be consumed. Faul et al. (2005) found decreased lab-P and org-P concentrations in suspended sediment as water depth increased, indicating uptake of this fraction in the water column as well. Lab-P concentrations decreased vertically in the upper sediments of Tomales Bay, California, to less than 0.6 μmol P/g (Vink et al. 1997), which is consistent with values observed in this study of Upper Newport Bay.

The potential for Fe-P to become bioavailable is dependent upon the redox conditions in the sediment. If P is released from reduced Fe(II) and diffuses upward into oxic sediments, it can re-bind to Fe(III) and precipitate out of solution (Froelich et al. 1988). However, if sediments are anoxic, SO_4^{-2} is being reduced to S^{-2}, which binds to Fe(II) and precipitates out of solution, leaving the P free to move into the water column through diffusive or advective-diffusive transport (Krom and Berner 1981; Lehtoranta and Pitkänen 2003). In anoxic conditions, the release of biologically available P from Fe(III) can be two to five times greater (Sutula et al. 2006). Pore water S^{-2} concentrations were low in the surficial sediments during the months P was sampled (Sutula et al. 2006). A decrease in Fe-P occurred in June, indicating a release of potentially bioavailable P to the water column. However, site specific concentrations of Fe-P show less variation among months, indicating sulfate reduction in sediments is not large

enough to bind all reduced Fe, which would ultimately facilitate the release to the water column significant amounts of P previously bound to Fe(III).

The Σ-P determined using the SEDEX method is likely an underestimate of total P since the potential for P loss increases with each extraction step. The average Σ-P concentration across all sample sites for the year was 32.0 μmol P/g. This value, multiplied by the long-term sediment deposition rate (0.15 cm/yr) and the average dry bulk density (1.45 g/cm^3), provides an estimate of the burial rate of phosphorus in the sediment (1.5 μmol P/cm^2 yr or 46.5 μg P/cm^2 year). However, only a portion of the Σ-P deposited in the sediment is rendered unavailable for biological uptake over ecological timescales (the refractory Ca-P and detr-P fractions). The average concentration for these two fractions across all sample sites for the year is 15.8 μmol P/g for Ca-P and 6.2 μmol P/g for detr-P. Thus, a more accurate phosphorus burial rate in Upper Newport Bay is 0.97 μmol P/cm^2 yr (30.1 μg P/cm^2 year; approximately 66% of the total P in the sediment).

Many studies examining sediment-bound P concentrations and their potential influence on water column P have been conducted (Table 7). Sutula et al. (2004) quantified the potential P solubilized from particles in the Mississippi River to better constrain reactive P budgets exported from large river systems. The study estimated that 31% of reactive P exported from the Mississippi River is released from sediments. Total sediment-bound P values determined in UNB are similar to those determined in other California study sites (Vink et al. 1997; Faul et al. 2005). Vink et al. (1997) examined P desorption from sediments to the water column in Tomales Bay, California, a small estuary with larger organic P concentrations than those calculated for UNB, and determined that bioturbation and non-steady state deposition of sediments were driving factors controlling P release from shallow sediments. However, Vink et al (1997) did not

compare phosphorus fractionation in sediment with sediment deposition and removal events. The continuous deposition and resuspension of sediments, and the digenetic transformation and potential release of phosphorus fractions from sediments, control distributions of P found in UNB sediments. During periods of low water column P concentrations, pools of sediment-bound P could shift productivity by releasing sediment-bound P to the system. The links among sediment dynamics, phosphorus concentrations in the sediment, and P uptake in the water column are an important factors that should be considered when constructing nutrient budgets in aquatic environments.

Table 7. Mean phosphorus distributions (± 1σ) of the five fractions removed using the SEDEX extraction procedure for various sample locations along the coasts of California and Louisiana.

Site	Mean Depth (m)	Lab-P	Fe-P	Ca-P	Detr-P	Org-P	Σ-P	Tot-P	Reference
		µmol P/g of sed.							
Upper Newport Bay, 2004	3	1.4 ± 1.1	6.8 ± 0.8	15.8 ± 1.8	6.2 ± 2.5	1.7 ± 1.1	32.0 ± 5.7	44.1 ± 5.3	This study
Tomales Bay, CA., November 1990	3	1.6 ± 0.1	below detection	0.9 ± 0.1	2.5 ± 0.2	20.3 ± 0.5	25.3 ± 0.6	24.5 ± 0.8	Vink et al. 1997
Tomales Bay, CA, March 1991	3	0.8 ± 0.0		0.7 ± 0.1	3.3 ± 0.0	16.8 ± 0.4	21.6 ± 0.7	23.2 ± 0.0	Vink et al. 1997
Monterey Bay, CA 1996	1800	1.2 ± 0.0	4.5 ± 0.2	12.1 ± 0.1	10.5 ± 0.3	7.9 ± 0.9	36.3 ± 1.0		Faul et al. 2005
Northern C.A. Coast, 1998	2829	0.6 ± 0.1	2.3 ± 0.2	8.5 ± 0.1	8.4 ± 0.2	6.6 ± 0.3	26.3 ± 0.4		Faul et al. 2005
Mississippi River, April 1999 – May 2000	25-60	3.5	10.9	5.2	2.8	4.4	26.7		Sutula et al. 2004
Gulf of Mexico Continental Shelf, April 1999 – May 2000	40	1.2	3.5	2.9	7.3	3.5	18.4		Sutula et al. 2004

CONCLUSION

The greatest overall sediment deposition observed in Upper Newport Bay occurred in the spring (February through April). This seasonal deposition can be attributed to increased freshwater delivery to the watershed via precipitation and subsequent creek discharge and increased suspended sediment loads. In contrast, an unseasonably large rain event in October delivered very little ^{7}Be to the system relative to the precipitation events in the spring. This low ^{7}Be input with a high precipitation event in the late fall was likely caused by decreased atmospheric ^{7}Be fluxes at the time. The lowest ^{7}Be delivery to the system was observed during the summer when atmospheric production of ^{7}Be is low and no precipitation or creek discharge occurred to deliver ^{7}Be to the estuary. Spatial variations in deposition were generally consistent with proximity to the primary sediment source and changes in channel morphology down estuary. The largest delivery of ^{7}Be to the system was observed at the upper bay site located proximal to the mouth of San Diego Creek. A decrease in ^{7}Be inventories at the middle estuary site occurred as the channel narrows and water velocities increased. The estuary channel width increases around a point bar at the lowest site and velocities are likely to slow, resulting in an increase in ^{7}Be deposition, especially at the intertidal area.

Resuspension and removal rates are generally greater in the summer following long periods without fresh sediment input. Short-term sedimentation rates were largest in the spring (0.1 to 0.4 g/cm^2 d), while resuspension rates were calculated for all sites during the summer (-0.1 to -2.2 g/cm^2 d). The average annual short-term, sediment deposition rate calculated from the ^{7}Be was 24.7 cm/yr during the study period. A long-term sediment deposition rate was found to be 0.15 cm/year. These values indicate that less than 1% of the annual sediment deposited in Upper Newport Bay is permanently buried. The remaining sediment is subject to resuspending

forces such as tidal currents, wind orbital velocities, discharge currents, and bioirrigation that could potentially export sediment out of the upper estuary to the ocean. Tidal currents are generally regarded as the primary force driving sediment transport in Upper Newport Bay, with a critical erosion shear velocity estimated to be 0.01 m/sec, but more research on the estuarine physics should be conducted to quantify tidal and storm-induced influences on sediment movement within the upper estuary.

The labile P and organic P fractions appear to be the most readily available for biological uptake in Upper Newport Bay. Sediment concentrations were enriched during spring sediment deposition, and decreased during June, when pore water total P concentrations decreased and P flux from the sediments increased. The labile and organic P fractions comprised 12% of the total sediment P in April, and decreased to 7% in June. A decrease in another potentially bioavailable P fraction, iron-bound P, was observed from April to June when concentrations were averaged for all sites; however, this observation was not obvious for site to site comparisons. The refractory forms of P indicated approximately 66% of sediment-bound P is unavailable for biological uptake over ecological timescales with an estimated burial rate of 0.97 μmol P/cm^2 year.

The continual deposition and resuspension of sediments, and the diagenetic transformation and potential release of phosphorus fractions from sediments, control distributions of P found in Upper Newport Bay sediments, and potentially influence pore water and water column concentrations of P. During periods of low water column P concentrations, pools of sediment-bound P could shift productivity by releasing sediment bound P to the system. Many studies have been conducted to examine sediment-bound P concentrations, both along the California coast and the Gulf of Mexico; however, none have compared phosphorus fractionation

in sediment with the dynamic nature of sediment deposition and removal. The links among sediment dynamics, phosphorus concentrations in the sediment, and P uptake in the water column are an important factors that should be considered when constructing nutrient budgets in aquatic environments.

REFERENCES

Akhurst, D., G.B. Jones, and D.M. McConchie. 2004. The application of sediment capping agents on phosphorus speciation and mobility in a sub-tropical dunal lake. *Marine and Freshwater Research* 55: 715-725.

Appleby, P.G., and F. Oldfield. 1992. Application of Lead-210 to sedimentation studies. pp. 731-751. *In* M. Inanovic, and R.S. Harmon [ed], Uranium-Series Disequilibrium: Applications to Earth, Marine, and Environmental Sciences. Oxford, U.K.

Aspila, K.I., H. Agemian, and A.S.Y. Chau. 1976. A semi-automated method for the determination of inorganic, organic and total phosphate in sediment. *Analyst London* 101: 187-197.

Aviles, A. and F.X. Niell. 2005. Pattern of phosphorus forms in a Mediterranean shallow estuary: Effects of flooding events. *Estuarine, Coastal and Shelf Science* 64: 786-794.

Baskaran, M. 1995. A search for the seasonal variability on the depositional fluxes of Be-7 and Pb-210. *Journal of Geophysical Research* 100 (D2): 2833-2840.

Baskaran, M., C.H. Coleman, and P.H. Santschi. 1993. Atmospheric depositional fluxes of ^{7}Be and ^{210}Pb at Galveston and College Station, Texas. *Journal of Geophysical Research* 98(11): 20,555-20,571.

Baskaran, M., M. Ravichandran, and T.S. Bianchi. 1997. Cycling of ^{7}Be and ^{210}Pb in a high DOC, shallow, turbid estuary of South-east Texas. *Estuarine, Coastal and Shelf Science* 45: 165-176.

Baskaran, M. and P.H. Santschi. 1993. The role of particles and colloids in the transport of radionuclides in coastal environments of Texas. *Marine Chemistry* 43: 95-114.

Benitez-Nelson, C.R. 2000. Phosphorus in the upper ocean. *Ciencia al Dia Internacional* 3: 1-13.

Blake, W.H., D.E. Walling, and Q. He. 2002. Using cosmogenic beryllium-7 as a tracer in sediment budget investigations. *Geografiska Annaler* 84 A(2): 89-102.

Boers, P.C.M., W. Van Raaphorst, and D.T. Van der Molen. 1998. Phosphorus retention in sediments. *Water Science and Technology* 37(3): 31-39.

Booth, J.G., R.L. Miller, B.A. McKee, and R.A. Leathers. 2000. Wind-induced bottom sediment resuspension in a microtidal coastal environment. *Continental Shelf Research* 20: 785-806.

Böstrom, B., J.M. Anderson, S. Fleisher, and M. Jansson. 1988. Exchange of phosphorus across the sediment-water interface. *Hydrobiologia* 170: 229-244.

Boyle Engineering Corporation. 1983. "Newport Bay Watershed, San Diego Creek Comprehensive Stormwater Sedimentation Control Plan." Report prepared for the Cities of Irvine and Newport Beach, and the Southern California Association of Governments, Newport Beach, CA.

Boyle, K.A., K. Kamer and P. Fong. 2004. Spatial and temporal patterns in sediment and water column nutrients in a eutrophic southern California estuary. *Estuaries* 27(3): 378-388.

Canuel, E.A., C.S. Martens and L.K. Benninger. 1990. Seasonal variations in ^{7}Be activity in the sediment of Cape Lookout Bight, North Carolina. *Geochimica et Cosmochimica Acta* 54: 237-245.

Chambers, R.M., J.W. Fourqurean, J.T. Hollibaugh and S.M. Vink. 1995. Importance of terrestrially-derived particulate phosphorus to phosphorus dynamics in a West Coast estuary. *Estuaries* 18(3): 518-526.

Clavaro, V., J.J. Izquierdo, J.A. Fernandez, and F.X. Neil. 1999. Water management and climate changes increases the phosphorus accumulation in the small shallow estuary of the Palmones River (southern Spain). *The Science of the Total Environment* 228: 193-202.

Coelho, J.P., M.R. Flindt, H.S. Jensen, A.I. Lillebo, and M.A. Pardal. 2004. Phosphorus speciation and availability in intertidal sediments of a temperate estuary: relation to eutrophication and annual P-fluxes. *Estuarine, Coastal and Shelf Science* 61: 583-590.

Cowen, W.F., and G.F. Lee. 1976. Phosphorus availability in particulate materials transported by urban runoff. *Journal of Water Pollution Control Federation* 48: 580-591.

Conley, D.J., W.M. Smith, J.C. Cornwell, and T.R. Fisher. 1995. Transformation of particle-bound phosphorus at the land-sea interface. *Estuarine, Coastal and Shelf Science* 40: 161-176.

Dellapenna, T.M., S.A. Kuehl and L.C. Schaffner. 1998. Sea-bed mixing and particle residence times in biologically and physically dominated estuarine systems: a comparison of Lower Chesapeake Bay and the York River Subestuary. *Estuarine, Coastal and Shelf Science* 46: 777-795.

Dellapenna, T.M., S.A. Kuehl and L.C. Schaffner. 2003. Ephemeral deposition, seabed mixing and fine-scale strata formation in the York River estuary, Chesapeake Bay. *Estuarine, Coastal and Shelf Science* 58: 621-643.

DeMaster, D.J., B.A. McKee, C.A. Nittrouer, Q. Jiangchu and C. Guodong. 1985. Rates of sediment accumulation and particle reworking based on radiochemical measurements from continental shelf deposits in the East China Sea. *Continental Shelf Research* 4(1/2): 143-158.

Dibb, J.E. and L.D. Meeker. 1994. Estimation of stratospheric input to the Arctic troposphere: Be-7 and Be-10 in aerosols at Alert, Canada. *Journal of Geophysical Research* 99: 12855-12864.

Dyer, K.R., 1995, Sediment transport processes in estuaries. Perillo, G.M.E. pp. 423-449. *Geomorphology and Sedimentology of Estuaries*. Elsevier Science B.V. Amsterdam.

Fanning, K.A., L.C. Carder, and P.R. Betzer. 1982. Sediment Resuspension by coastal waters: a potential mechanism for nutrient recycling on the ocean's margin. *Deep Sea Research* 29 (8A): 953-965.

Faul, K.L., A. Paytan, and M.L. Delaney. 2005. Phosphorus distribution in sinking oceanic particulate matter. *Marine Chemistry* 97: 307-333.

Fitzgerald, S., J. Val Klump, P. Swarzenski, R. MacKenzie, and K. Richards. 2001. Beryllium-7 as a tracer of short-term sediment deposition and resuspension in the Fox River, Wisconsin. *Environmental Science and Technology* 35:300-305.

Froelich, P.N., M.L. Bender, N.A. Luedtke, G.R. Heath, and T. DeVries. 1982. The marine phosphorus cycle. *American Journal of Science* 282: 474-511.

Froelich, P.N. 1988. Kinetic control of dissolved phosphate in natural rivers and estuaries: A primer on the phosphate buffer mechanism. *Limnology and Oceanography* 33(4): 649-668.

Froelich, P. N., G.P. Klinkhammer, M.L. Bender, N.A. Luedtke, G.R. Heath, D. Cullen, D. Dauphin, D. Hammond, B. Hartman, and V. Maynard. 1979. Early oxidation of organic matter in pelagic sediments of the eastern equatorial Atlantic: suboxic diagenesis. *Geochimica et Cosmochimica Acta* 43: 1075-90.

Giffin, D. and D.R. Corbett. 2003. Evaluation of sediment dynamics in coastal systems via short-lived radioisotopes. *Journal of Marine Systems* 42: 83-96.

Kim, G., L.Y. Alleman, and T.M. Church. 1999. Atmospheric depositional fluxes of trace elements, ^{210}Pb and ^{7}Be, to the Sargasso Sea. *Global Biogeochemical Cycles* 13(4): 1183-1192.

Kirshnaswami, S., L.K. Benninger, R.C. Aller, and K.L. Von Damn. 1980. Atmospherically-derived radionuclides as tracers of sediment mixing and accumulation in near-shore marine and lake sediments: evidence from ^{7}Be, ^{210}Pb, and $^{239, 240}$Pu. *Earth and Planetary Science Letters* 47: 307-318.

Koch, M.S., R.E. Benz, and D.T. Rudnick. 2001. Solid-phase phosphorus pools in highly organic carbonate sediments of north-eastern Florida Bay. *Estuarine, Coastal and Shelf Science* 52: 279-291.

Krom, M.D., and R.A. Berner. 1981. The diagenesis of phosphorus in nearshore marine sediment. *Geochimica et Cosmochimica Acta* 45: 207-216.

Lehtoranta, J; A.S. Heiskanen, and H. Pitkanen. 2004. Particulate N and P characterizing the fate of nutrients along the estuarine gradient of the River Neva (Baltic Sea). *Estuarine Coastal and Shelf Science* 61: 275-287.

Lehtoranta, J. and H. Pitkänen. 2003. Binding of phosphate in sediment accumulation areas of the eastern Gulf of Finland, Baltic Sea. *Hydrobiologia* 492: 55-67.

Lucotte, M. and B. d'Anglejan. 1985. A comparison of several methods for the determination of iron hydroxides and associated orthophosphate in estuarine particulate matter. *Chemical Geology* 48: 257-264.

Masters, P.M. and D.L. Inman. 2000. Transport and fate of organochlorines discharged to the salt marsh at Upper Newport Bay, California, USA. *Environmental Toxicology and Chemistry* 19(8): 2076-2084.

Milner, H.B. 1962. Sedimentary Petrography. Macmillian Company: New York.

Mitsch, W.J. and J.G. Gosselink. 2000. Wetlands. John Wiley & Sons, Inc. New York. pp. 920.

NCDC. 2005. U.S. Climate Normals (1971-2000). National Climate Data Center. (http://www.ncdc.noaa.gov).

Olsen, C.R., I.L. Larsen, P.D. Lowrey, and N.H. Cutshall. 1986. Geochemistry and deposition of ^{7}Be in river, estuarine and coastal waters. *Journal of Geophysical Research* 91(C1): 896-908.

Pilskaln, C.H., J.B. Paduan, F.P. Chavez, R.Y. Anderson, and W.M. Berelson. 1996. Carbon export and regeneration in the coastal upwelling system of Monterey Bay, central California. *Journal of Marine Research* 54: 1149-1178.

Rehfeld, S. and M. Heimann. 1995. Three dimensional atmospheric transport simulation of the radioactive tracers ^{210}Pb, ^{7}Be, ^{10}Be, and ^{90}Sr. *Journal of Geophysical Research* 100(D12): 26141-16161.

Ruttenberg, K.C. 1990. Diagenesis and burial of phosphorus in marine sediments: Implications for the marine phosphorus budget. Ph.D. Dissertation. Yale University. pp. 375.

Ruttenberg, K.C. 1992. Development of a sequential extraction method for different forms of phosphorus in marine sediments. *Limnology and Oceanography* 37: 1460-1482.

Ruttenberg, K.C. and R.A. Berner. 1993. Authigenic apatite formation and burial in sediments from non-upwelling continental margin environments. *Geochimica et Cosmochimica Acta* 57: 991-1007.

Smith, R.D. and C.V. Klimas. 2004. San Diego Creek Watershed riparian ecosystem restoration plan: general design criteria. U.S. Army Engineer Research Development Center, Waterways Experiment Station, Vicksburg, MS. Draft Report to the U.S. Army Corps of Engineers, Los Angeles District, Regulatory Branch. p. 1-85.

Sommerfield, C.K. and H.J. Lee. 2003. Magnitude and variability of Holocene sediment accumulation in Santa Monica Bay, California. *Marine Environmental Research* 56: 151-176.

Sommerfield, C.K., C.A. Nittrouer and C.R. Alexander. 1999. ^{7}Be as a tracer of flood sedimentation on the northern California continental margin. *Continental Shelf Research* 19: 335-361.

Strickland, J.D. and T.R. Parsons. 1972. A Practical Handbook of Seawater Analysis. Fisheries Research Board of Canada: pp. 317.

Sutula, M., T.S. Bianchi, and B.A. McKee. 2004. Effect of seasonal sediment storage in the lower Mississippi River on the flux of reactive particulate phosphorus to the Gulf of Mexico. *Limnology and Oceanography* 49(6): 2223-2235.

Sutula, M., K. Kamer, J. Cable, H. Collis, William Berelson, and Jeff Mendez. 2006. Sediments as an internal source of nutrients to Upper Newport Bay, California. Southern California Coastal Water Resource Project Technical Report No. 482.

Tappin, A.D. 2002. An examination of the fluxes of nitrogen and phosphorus in temperate and tropical estuaries: current estimates and uncertainties. *Estuarine, Coastal and Shelf Science* 55: 885-901.

Trimble, S. 2003. Historical hydrographic and hydrologic changes in the San Diego Creek watershed, Newport Bay, California. *Journal of Historical Geography* 29(3): 422-444.

Trinast, E.M. 1975. Tidal currents and *Acartia* distribution in Newport Bay, California. *Estuarine, Coastal and Marine Science* 3: 165-176.

US Army Corps of Engineers (USACE) Coastal Research Center. 1984. Shore protection manual. Vol. I: 4th Ed. U.S. Army Coastal Engineering Center, Fort Belvoir, VA, p. 603.

US Army Corps of Engineers (USACE). 1997. Feasibility Report: Upper Newport Bay. *Final Model and GUI Development and Implementation Report.* pp. 118.

US Army Corps of Engineers (USACE). 2000. Upper Newport Bay Ecosystem Restoration Feasibility Study. *Final Report, Environmental Impact Statement*. pp. 171.

Vink, S., R.M. Chambers, and S.V. Smilth. 1997. Distribution of phosphorus in sediments from Tomales Bay, California. *Marine Geology* 139: 157-179.

Vogler, S., M. Jung and A. Mangini. 1996. Scavenging of ^{234}Th and ^{7}Be in Lake Constance. *Limnology and Oceanography* 41(7):1384-1393.

Wallbrink, P. and A. Murray. 1994. Fallout of ^{7}Be in South Eastern Australia. *Journal of Environmental Radioactivity* 25:213-228.

Wallbrink, P.J. and A.S. Murray. 1996. Distribution and variability of ^{7}Be in soils under different surface cover conditions and its potential for describing soil redistribution processes. *Water Resources Research*. 32(2): 467-476.

Wantanabe, F.S., and S.R. Olsen. 1962. Colorimetric determination of phosphorus in water extracts of soils. *Soil Science* 93: 183-188.

WRCC 2005. Climate Narrative for Each State. Western Regional Climate Center. (http://www.wrcc.dri.edu).

Wright, L.D.1995. Morphodynamics of Inner Continental Shelves. CRC Press: pp. 241.

Zwolsman, J.J.G. 1994. Seasonal variability and biogeochemistry of phosphorus in the Scheld Estuary, South-west Netherlands. *Estuarine, Coastal and Shelf Science* 39: 227-248.

APPENDIX A: PHOSPHORUS EXTRACTION PROCEDURES

Aspila Method – Total, Inorganic, and Organic Phosphorus
(Aspila 1976)

Purpose: To obtain the approximate magnitude of refractory and bioavailable P fractions

Preparation:
- Samples should be completely dried prior to analysis (60°C oven).
- Grind samples to <125µm
- All laboratory equipment should be acid washed in a 10% HCl bath, rinsed 3 times with D.I. H_2O, and dried completely prior to analysis.

Reagent:
- 1 N HCl solution – add 85.3 mL concentrated HCl to 1 L D.I. H_2O
    - **CAUTION!** – always pour acid into water!

Equipment and Supplies:
- Muffle furnace
- Shaker box or shaker table
- Analytical Balance
- Acid washed glassware and 50 mL centrifuge tubes
- Centrifuge

Procedure:
- It is suggested that all samples be run in duplicate.
- Preheat muffle furnace to 550ºC.
- Add 0.3 g of dry ground sediment to 125 mL Erlenmeyer flask for total P determination.
- Add 0.3 g of dry ground sediment to 50 mL centrifuge tube for inorganic P determination.
- Place flasks into the preheated muffle furnace for 2 hours
    - Samples must remain in the furnace for 2 hours **AFTER** temperatures reach 550ºC (when samples are put into the furnace, the temperatures will decrease).
- Remove flasks from furnace and allow them to return to room temperature.
- Add 30 mL of 1 N HCl to all Erlenmeyer flasks and centrifuge tubes.
- Cover Erlenmeyer flasks with Parafilm and screw tops on centrifuge tubes.
- Place Erlenmeyer flaks and centrifuge tubes in the shaker box (or on a shaker table) at a rate that allows samples to mix thoroughly.
- Shake samples for 16 hours at room temperature.
- Transfer the samples in the Erlenmeyer flasks to 50 mL centrifuge tubes, keeping track of the treatments.
- Centrifuge all samples for 10 minutes at 8000 rpm.
- Filter the extractant through 0.45µm filters.
    - Discard the first 2ml and collect remaining filtrate for analysis.
- Store samples at room temperature until ready for analysis (see phosphomolybdate blue method).

SEDEX Method - Five Phase Sediment Phosphorus Sequential Extraction
(Ruttenberg 1992; Akhurst et al. 2004)

Purpose: Five step sequential extraction to determine labile and refractory sediment P.

I. Remove loosely sorbed or exchangeable P (labile or adsorbed P).
   a. Forms $MgPO4^-$ complex and/or mass action displacement by Cl^-
   b. Most readily available and reactive P

II. Remove ferric Fe-bound P (oxide associated)
   a. Reduction of Fe^{3+} by dithionite and subsequent chelation by citrate
   b. Bioavailable under correct redox conditions

III. Remove P associated with authigenic carbonate fluorapatite + biogenic apatite + $CaCO_3$
   a. Acid dissolution of moderately low pH and/or chelation of Ca^{2+} by acetate
   b. Oceanic sink over short time scales.

IV. Remove detrital apatite P of igneous or metaphoric origin (detrital-P)
   a. Acid dissolution
   b. Considered a weathering product of terrestrial origin

V. Remove organic P
   a. Dry oxidation at 550°C with 1M HCl extraction of ashed supernatant
   b. Generally a bioavailable P fraction

Preparation:

- Samples should be completely dried prior to analysis (60°C oven).
- Grind samples to <125µm
- Begin with 0.3 g sediment
- All laboratory equipment should be acid washed in a 10% HCl bath, rinsed 3 times with D.I. H_2O, and dried completely prior to analysis.

Reagents:

- 1 M $MgCl_2$ = 95.2 g/L
- Citrate dithionate-bicarbonate (CDB) for step II
  - CDB Solution:
    - 0.3 M Na_3-citrate = 88.23 g/L
    - 1 M $NaHCO_3$ (pH 7.6) = 84.01 g/L
  - 1.125 g of $Na_2S_2O_4$ dissolved in 45ml of the CDB solution
- 1 M Na-acetate = 136.08 g/L (use the chemical nomenclature for acetate)
- 1 M HCl = 36.46 g/L

Equipment and Supplies:

- Shaker box or shaker table
- Analytical Balance
- Acid washed glassware and centrifuge tubes
- Centrifuge

Notes:

- Extractant volumes are about 30 ml
- All samples are run in 50 ml centrifuge tubes

- Samples will be placed in a shaker box and mixed for the duration required for each step.

When removing extractant:

- Centrifuge all samples for 10 minutes at 8000 rpm.
- Filter through 0.45µm filters every time extractant is removed.
  - Discard the first 2 ml and collect remaining filtrate for analysis.
- At the end of each step, combine all the extractants and mix well before proceeding to the phosphomolybdate blue method.

Step I:

1. Mix 0.3g sediment with 1M $MgCl_2$ at pH of 8.0.
   a. Shake for 2 hours at 25°C
2. Remove extractant and repeat step 1.
3. Remove extractant, combine with initial extractant and wash solid with H_2O
   a. Shake for 2 hours at 25°C
4. Remove extractant and combine with initial extractants
5. Combined extractants may frozen until ready for analysis (see phosphomolybdate blue method).

Step II:

1. Mix remaining solid with CDB solution (pH = 7.6).
   a. Shake for 8 hours at 25°C
2. Remove extractant and mix remaining solid with 1 M $MgCl_2$ at pH of 8.0
   a. Shake for 2 hours at 25°C
3. Remove extractant, combine with extractant from step II, wash remaining solid with H_20
   a. Shake for 2 hours at 25°C
4. Remove extractant and combine with the rest of the extractants
5. Combined extractants may be frozen until ready for analysis (see phosphomolybdate blue method).

Step III:

1. Mix remaining solid with 1M Na-acetate buffered to pH of 4.0 using acetic acid.
   a. Shake for 6 hours at 25°C
2. Remove extractant and mix remaining solid with 1M $MgCl_2$ at pH of 8.0.
   a. Shake for 2 hours at 25°C
3. Remove extractant, combine with extractant from step II and wash remaining solid with H_2O.
   a. Shake for 2 hours at 25°C
4. Remove extractant and combine with the rest of the extractants. Combined extractants may be frozen until ready for analysis (see phosphomolybdate blue method).

Step IV:

1. Mix remaining solid with 1M HCl
    a. Shake for 16 hours at 25°C
        i. this could potentially be shortened
2. Remove extractant
3. Combined extractants may be stored at room temperature until ready for analysis (see phosphomolybdate blue method).

Step V:

1. Ash remaining solid at 550°C for 2 hours
2. Add 1M HCl to the remaining solid
    a. Shake for 16 hours at 25°C
3. Remove extractant
4. Combined extractants may stored at room temperature until ready for analysis (see phosphomolybdate blue method).

Phosphomolybdate Blue Method
(Strickland and Parsons 1972)

Purpose: This analytical procedure is used to analyze P concentrations using a spectrophotometer. It was used to run all the extractants for both the Aspila and SEDEX procedures, except for Step II of SEDEX.

Equipment:

- Spectrophotometer with an infrared phototube of 880 nm providing a light path of 2.5 cm or longer
- Acid-washed glassware

Reagents:

- Initial reagents for the Combined Reagent
  - 2.4 M Sulfuric Acid Solution
    - Add 70 ml concentrated H_2SO_4 to 450 ml D.I water.
    - Stable indefinitely
  - 0.004 M Potassium Antimonyl Tartrate Solution
    - Dissolve 0.272 g $C_8H_4K_2O_{12}Sb_3$ * $3H_2O$ in 250 ml D.I. water.
    - Dilute to a final volume of 300 ml.
    - Store in a glass-stopped bottle, and is stable for many months.
  - 0.024 M Ammonium Molybdate Solution
    - Dissolve 15 g $(NH_4)6Mo7O_{24}$ * 4H2O in 400 ml D.I. water.
    - Dilute to a final volume of 500 ml
    - Store in a plastic bottle at 4°C
  - Ascorbic Acid
    - See combined reagent section.

- Combined Reagent: dilute reagents in the following order and mix well before adding each reagent.
  - Dissolve completely 0.55 g ascorbic acid with 10 ml D.I. water.
  - Add 10 ml ammonium molybdate solution
    - Solution should turn yellow
    - Add 25 ml of 2.4 M sulfuric acid.
    - Add 5 ml of potassium animonyl tartrate solution
    - **This reagent is only stable for 4 hours**

- Standard Phosphate Solutions
  - Stock Phosphate Solution – **mix this first and store in refrigerator.**
    - Dissolve 219.5 mg anhydrous KH_2PO_4 in D.I. water
    - Dilute to 1000 ml (1 ml=50.0 µg PO_4-P), also called Potassium Phosphate Monobasic
    - Dilute 50 ml Stock Phosphate Solution to 1000 ml with deionized water (1 ml = 2.50 µg P)

Sample Preparation:

- It is suggested that all samples be run in duplicate
- Blank:
  - Auto-pipette 5 ml of same reagent used for a specific extraction step into a test tube.
  - For example: for Step I, use 2 parts of 1M $MgCl_2$ and 1 part D.I. water for the blank.
- Standard:
  - Auto-pipette the necessary volume of phosphate standard into a test tube to achieve desired concentration
  - Dilute the standard to 5 ml using the same reagent used for a specific extraction step (similar to making the blank).
- Sample:
  - Pipette 5 ml of the sample into duplicate clean test tubes.
  - Add 0.5 ml of the combined reagent to each test tube and mix evenly.
  - Wait approximately 10 minutes for color to develop.
    - Samples should be analyzed as quickly as possible following the color development (within 30 minutes).
  - Measure extinction using a spectrophotometer at 885 nm.
    - Use blanks and standards to create a standard curve
    - Measure sample absorbence against the standard curve to obtain the phosphate concentration.

Calculation:

$$\text{mg/L of P} = \frac{\text{Mass (mg P)} * 1000}{\text{Volume (ml sample)}}$$

Fe-bound Phosphorus Analysis
(Wantanabe & Olsen 1961)

Purpose: This procedure was used to analyze P concentrations in extractant from step II of the SEDEX procedure instead of the phosphomolybdate blue method, because the CDB solution used to extract Fe-P interferes with the molybdate blue reagent in the phosphomolybdate blue method. The molybdate blue is reduced by the CDB and the color development in the dye does not form.

Equipment:

- 125 ml Sepratory Funnel
- Ring stand and ring
- Acid-washed glassware

Reagents:

- Ammonium molybdate
- 10 *N* H_2SO_4
  - dilute 140 ml of concentrated H_2SO_4 in 500 ml of D.I. water
- 1 *N* H_2SO_4
  - dilute 14 ml of concentrated H_2SO_4 in 500 ml of D.I. water
- Stannous Chloride – $SnCl_2$ * $6H_2O$
- Isobutyl Alcohol – commercial grade
- Ethyl Alcohol – 99.5% (less than this can cause the molybdenum blue color to become unstable)

- Combined Reagents (from above list):
  - Molybdate Reagent
    - Dissolve 50 g of ammonium molybdate in 500 ml of water
    - Add 400 ml of 10*N* H_2SO_4
    - Dilute to 1 L
    - Store in a polyethylene bottle
  - Sulfuric Acid (approximately *N*)
  - Stannous Chloride (**stock** solution)
    - Dissolve 10 g of $SnCl_2$*$6H_2O$ in 25 ml concentrated HCl
    - Store **refrigerated** in a polyethylene bottle
  - Stannous Chloride (**dilute** solution)
    - Dilute 1 ml of stock solution to 200 ml 1 *N* H_2SO_4
    - **Do this just before use**

- Standards
  - Developed in the same fashion as the standards for the Phosphomolybdate Blue Method above.
  - Recommended range is between 2 and 20 µg
  - Run the standards with the same procedure as below

Procedure:

1. Pipette 15 ml of sample into a 125 ml sepratory funnel sepratory funnel

- Works best if inorganic P range is between 2 and 20µg

2. Add 5 ml of the molybdate-sulfuric acid reagent
    - If using less than 15 ml of sample, dilute the reagent to 20 ml with deionized water after adding 5 ml of molybdate reagent
3. Add 10 ml isobutyl alcohol and shake for 2 minutes
4. Allow the solution to stratify in two layers. Drain and discard the bottom (aqueous) layer
5. Add 10 ml of 1*N* H_2SO_4 and "wash" by shaking once
6. Allow the two layers to form. Drain and discard the bottom (aqueous) layer
7. Add 15 ml of the dilute stannous chloride solution and shake for 1 minute
8. Again allow the two layers to form. Drain and discard the bottom (aqueous) layer
9. The top layer should be blue
10. **VERY CAREFULLY** transfer the blue isobutyl alcohol layer into a 25 ml volumetric flask
11. Wash the sepratory funnel with ethyl alcohol and drain entire volume into the 25 ml volumetric flask
12. Allow color to develop for 30 minutes (color is stable for 4 hours)
13. Analyze on a spectrophotometer at wavelengths of 660 or 720 nm.

APPENDIX B: BULK SEDIMENT CHARACTERISTICS

Table 1. January Grain Size – vertical distribution of % sand, silt, and clay for all sample sites in Upper Newport Bay in January 2004.

NB1						
Depth Interval (cm)	**Intertidal**			**Subtidal**		
	% Sand	% Silt	% Clay	% Sand	% Silt	% Clay
0-1	59.47	20.27	20.27	61.94	27.68	10.38
1-2	54.22	41.61	4.16	52.94	15.69	31.38
2-3	57.68	25.39	16.93	50.65	22.21	27.14
3-4	59.02	35.13	5.85	47.03	26.49	26.49
4-5	55.42	7.43	37.15	48.39	30.25	21.35
5-6	59.18	32.66	8.16	45.81	32.52	21.68

NB2						
Depth Interval (cm)	**Intertidal**			**Subtidal**		
	% Sand	% Silt	% Clay	% Sand	% Silt	% Clay
0-1	35.95	12.81	51.24	50.06	23.65	26.28
1-2	46.69	11.42	41.89	51.45	13.24	35.31
2-3	35.49	40.61	23.89	51.55	30.60	17.85
3-4	31.64	39.88	28.48	29.78	51.07	19.15
4-5	25.56	37.22	37.22	37.69	29.32	32.99
5-6	17.38	43.74	38.88	29.07	20.59	50.34

NB3						
Depth Interval (cm)	**Intertidal**			**Subtidal**		
	% Sand	% Silt	% Clay	% Sand	% Silt	% Clay
0-1	43.85	28.07	28.07	58.20	25.55	16.26
1-2	61.23	2.98	35.79	72.55	14.64	12.81
2-3	77.02	0.00	22.98	74.62	6.92	18.46
3-4	68.53	13.11	18.36	60.90	16.54	22.56
4-5	59.38	2.90	37.72	54.48	23.84	21.68
5-6	62.07	5.84	32.09	55.09	10.36	34.55

Table 2. February Grain Size – vertical distribution of % sand, silt, and slay for all sample sites in Upper Newport Bay in February 2004. Blank spaces reflect times when to little sediment was available for analysis.

NB1						
Depth Interval (cm)	**Intertidal**			**Subtidal**		
	% Sand	% Silt	% Clay	% Sand	% Silt	% Clay
0-1	41.22	19.59	39.18	25.90	42.34	31.76
1-2	38.63	29.55	31.82	22.70	0.00	77.30
2-3	38.23	25.27	36.50	22.78	45.27	31.95
3-4	40.25	19.92	39.83	24.29	31.33	44.38
4-5	32.56	31.61	35.83	25.85	48.36	25.79
5-6	28.29	37.09	34.62	30.37	25.07	44.56

NB2						
Depth Interval (cm)	**Intertidal**			**Subtidal**		
	% Sand	% Silt	% Clay	% Sand	% Silt	% Clay
0-1	46.69	22.85	30.46	54.53	18.94	26.52
1-2	41.41	54.93	3.66	55.21	19.19	25.59
2-3	32.33	35.09	32.58	47.03	23.54	29.43
3-4	27.63	25.68	46.69	42.14	25.71	32.14
4-5	23.79	31.96	44.25	37.54	30.28	32.18
5-6				34.91	15.50	49.59

NB3						
Depth Interval (cm)	**Intertidal**			**Subtidal**		
	% Sand	% Silt	% Clay	% Sand	% Silt	% Clay
0-1	50.63	17.42	31.94	33.13	63.83	3.04
1-2	71.31	2.05	26.64	54.76	20.56	24.68
2-3	85.21	0.00	14.79	66.05	7.83	26.11
3-4	77.15	1.76	21.10	72.98	10.39	16.63
4-5	79.33	7.52	13.16	57.46	18.50	24.05
5-6	76.02	6.40	17.59			

Table 3. March Grain Size – vertical distribution of % sand, silt, and clay for all sample sites in Upper Newport Bay in March 2004. Blank spaces reflect times when too little sediment was available for analysis.

NB1						
Depth Interval (cm)	**Intertidal**			**Subtidal**		
	% Sand	% Silt	% Clay	% Sand	% Silt	% Clay
0-1	50.56	20.36	29.08	39.64	22.36	38.01
1-2				36.43	29.34	34.23
2-3				29.99	38.90	31.12
3-4	28.71	28.52	42.77	22.42	51.72	25.86
4-5	17.24	46.55	36.21	7.23	42.52	50.25
5-6	3.99	21.08	74.93			

NB2						
Depth Interval (cm)	**Intertidal**			**Subtidal**		
	% Sand	% Silt	% Clay	% Sand	% Silt	% Clay
0-1	47.75	19.91	32.35			
1-2	56.52	20.87	22.61			
2-3	55.43	16.42	28.15			
3-4				32.47	30.70	36.83
4-5				32.73	28.46	38.81
5-6	44.01	35.83	20.16	36.03	29.32	34.65

NB3						
Depth Interval (cm)	**Intertidal**			**Subtidal**		
	% Sand	% Silt	% Clay	% Sand	% Silt	% Clay
0-1	28.74	47.51	23.75	68.82	7.20	23.99
1-2						
2-3	30.16	34.92	34.92	50.47	20.18	29.35
3-4	57.79	16.23	25.98	63.79	14.81	21.40
4-5				79.03	5.72	15.25
5-6				84.16	8.45	7.39

Table 4. April Grain Size – vertical distribution of % sand, silt, and clay for all sample sites in Upper Newport Bay in March 2004. Blank spaces reflect times when too little sediment was available for analysis.

NB1						
Depth Interval (cm)	**Intertidal**			**Subtidal**		
	% Sand	% Silt	% Clay	% Sand	% Silt	% Clay
0-1	66.89	5.70	27.41	19.02	-19.07	100.05
1-2				17.11	11.71	71.18
2-3	50.55	0.00	49.45	33.02	22.11	44.86
3-4	45.12	23.96	30.92	44.03	6.14	49.83
4-5	47.12	0.00	52.88	29.82	25.03	45.14
5-6	46.02	-5.95	59.92	48.12	7.33	44.55

NB2						
Depth Interval (cm)	**Intertidal**			**Subtidal**		
	% Sand	% Silt	% Clay	% Sand	% Silt	% Clay
0-1	64.21	6.62	29.18	57.92	6.24	35.84
1-2	67.32	0.00	39.57	62.92	6.67	30.41
2-3	68.32	4.27	27.40	61.72	11.06	27.22
3-4	66.32	0.00	36.04	57.52	19.56	22.92
4-5	60.92	0.00	43.36	52.62	2.23	45.15
5-6	55.62	0.00	44.38	48.82	12.17	39.01

NB3						
Depth Interval (cm)	**Intertidal**			**Subtidal**		
	% Sand	% Silt	% Clay	% Sand	% Silt	% Clay
0-1	81.84	0.00	23.27	46.22	0.00	58.84
1-2				67.62	8.00	24.37
2-3	76.72	0.00	30.54	98.46	0.36	1.18
3-4	72.22	0.00	31.22	69.22	13.97	16.80
4-5	74.82	1.24	23.93	60.32	5.61	34.07
5-6	84.72	4.77	10.51	63.52	25.77	10.70

Table 5. June Grain Size – vertical distribution of % sand, silt, and clay for all sample sites in Upper Newport Bay in March 2004. Blank spaces reflect times when too little sediment was available for analysis.

NB1						
Depth Interval (cm)	**Intertidal**			**Subtidal**		
	% Sand	% Silt	% Clay	% Sand	% Silt	% Clay
0-1	62.50	17.59	19.91			
1-2	57.60	3.39	39.01	42.50	2.74	54.76
2-3	53.70	0.00	55.57	38.60	3.24	58.17
3-4	54.10	0.00	58.43	40.70	14.32	44.98
4-5	48.50	0.00	58.87	38.80	0.00	88.43
5-6	43.10	0.00	58.94	50.80	6.72	42.49

NB2						
Depth Interval (cm)	**Intertidal**			**Subtidal**		
	% Sand	% Silt	% Clay	% Sand	% Silt	% Clay
0-1	79.60	2.55	17.85	62.72	0.00	39.39
1-2	81.30	0.00	20.40	61.10	14.02	24.89
2-3	78.30	0.00	31.36	60.62	6.14	33.23
3-4	64.30	0.00	40.17	51.32	10.48	38.20
4-5	64.20	0.00	52.35	45.20	0.00	60.03
5-6	55.00	1.80	43.20	50.50	17.08	32.42

NB3						
Depth Interval (cm)	**Intertidal**			**Subtidal**		
	% Sand	% Silt	% Clay	% Sand	% Silt	% Clay
0-1	82.85	5.09	12.07	76.70	9.47	13.83
1-2	80.22	2.67	17.11	80.90	1.98	17.12
2-3	77.32	5.96	16.72	83.40	6.39	10.21
3-4	77.92	6.13	15.95	88.30	0.94	10.77
4-5	72.02	0.00	30.66	89.30	0.00	11.83
5-6	77.42	1.17	21.40	84.70	0.00	15.30

Table 6. September Grain Size – vertical distribution of % sand, silt, and clay for all sample sites in Upper Newport Bay in March 2004. Blank spaces reflect times when too little sediment was available for analysis.

NB1						
Depth Interval (cm)	**Intertidal**			**Subtidal**		
	% Sand	% Silt	% Clay	% Sand	% Silt	% Clay
0-1	76.39	0.00	23.61	92.75	0.00	7.90
1-2	61.82	0.00	38.18	44.22	0.00	58.18
2-3	52.72	0.00	49.15	42.92	1.89	55.19
3-4	44.52	0.00	71.50	61.62	7.63	30.75
4-5	11.92	12.87	75.21	61.32	0.00	38.68
5-6	44.52	0.00	61.59	60.92	0.00	43.55

NB2						
Depth Interval (cm)	**Intertidal**			**Subtidal**		
	% Sand	% Silt	% Clay	% Sand	% Silt	% Clay
0-1	54.13	4.87	40.99	79.29	0.00	20.71
1-2	34.22	0.00	68.61	74.04	0.00	29.31
2-3	31.92	6.34	61.74	51.12	-8.42	57.29
3-4	28.62	0.00	74.21	57.32	0.00	59.55
4-5	25.92	12.23	61.85	59.22	12.56	28.22
5-6	23.72	0.00	79.19	56.42	8.11	35.46

NB3						
Depth Interval (cm)	**Intertidal**			**Subtidal**		
	% Sand	% Silt	% Clay	% Sand	% Silt	% Clay
0-1	82.00	7.98	10.02	68.72	0.00	42.17
1-2	82.10	0.00	28.59	72.94	0.00	30.03
2-3	57.90	0.00	63.04	63.12	1.59	35.29
3-4	83.60	0.00	65.10	65.62	0.00	41.78
4-5				71.22	0.00	33.79
5-6	84.80	7.56	7.64	65.42	0.00	39.85

Table 7. November Grain Size – vertical distribution of % sand, silt, and clay for all sample sites in Upper Newport Bay in November 2004.

NB1						
Depth Interval (cm)	**Intertidal**			**Subtidal**		
	% Sand	% Silt	% Clay	% Sand	% Silt	% Clay
0-1	48.70	13.66	37.64	17.97	46.81	35.22
1-2	49.90	0.00	50.10	23.70	42.86	33.43
2-3	39.50	23.50	37.00	39.10	46.51	14.38
3-4	41.30	14.66	44.04	43.60	33.14	23.26
4-5	23.30	19.16	57.54	43.00	17.07	39.93
5-6	32.70	12.60	54.70	30.10	34.90	35.00

NB2						
Depth Interval (cm)	**Intertidal**			**Subtidal**		
	% Sand	% Silt	% Clay	% Sand	% Silt	% Clay
0-1	51.10	4.88	44.02	43.01	17.51	39.49
1-2	46.50	26.70	26.79	41.39	0.00	65.92
2-3	38.10	23.77	38.13	62.10	11.64	26.25
3-4	30.70	55.36	13.93	68.70	7.81	23.49
4-5	31.60	58.54	9.85	71.80	0.00	28.20
5-6	27.60	51.64	20.76	69.70	9.31	20.99

NB3						
Depth Interval (cm)	**Intertidal**			**Subtidal**		
	% Sand	% Silt	% Clay	% Sand	% Silt	% Clay
0-1	79.10	0.00	20.90	96.60	0.00	3.40
1-2	73.20	2.23	24.57	90.10	5.93	3.97
2-3	60.90	0.00	39.10	83.50	2.06	14.44
3-4	63.50	0.00	36.50	92.10	0.00	7.90
4-5	63.70	0.00	39.59	90.30	0.00	11.31
5-6	80.00	0.00	21.99	83.10	6.73	10.17

APPENDIX C: RADIOISOTOPIC ACTIVITY AND INVENTORY DATA

Table 8. UNB Site 1 Intertidal Zone Activity (Act.) and Total Inventory (Inv.) Calculations.

Activity

Depth Int. (cm)	January Act. (dpm/g)		Std. Dev	February Act. (dpm/g)		Std. Dev	March Act. (dpm/g)		Std. Dev	April Act. (dpm/g)		Std. Dev	June Act. (dpm/g)		Std. Dev	September Act. (dpm/g)		Std. Dev	November Act. (dpm/g)		Std. Dev
0-1	2.09	±	0.93	2.93	±	1.12	2.54	±	0.93	5.07	±	1.61	3.29	±	1.18	0.74	±	0.65	0.99	±	0.70
1-2	1.06	±	0.93	3.20	±	1.22	1.67	±	0.91	5.48	±	1.75	1.10	±	1.23	0.00	±	0.00	1.64	±	0.52
2-3	1.84	±	0.93	0.00	±	0.00	1.20	±	1.08	4.59	±	1.78	0.00	±	0.00	0.39	±	0.70	0.00	±	0.00
3-4	1.67	±	0.94	3.87	±	1.46	1.93	±	0.96	2.57	±	1.63	0.00	±	0.00	0.00	±	0.00	0.00	±	0.00
4-5	1.76	±	0.92		±			±		3.33	±	1.72		±		1.29	±	1.06	0.00	±	0.00
5-6	0.00	±	0.00		±			±		3.55	±	4.35		±		0.93	±	1.07	0.00	±	0.00

Total Inventory

Depth Int. (cm)	Bulk Density (g/cm^3)	January Inv. (dpm/cm^2)		Std. Dev	February Inv. (dpm/cm^2)		Std. Dev	March Inv. (dpm/cm^2)		Std. Dev	April Inv. (dpm/cm^2)		Std. Dev	June Inv. (dpm/cm^2)		Std. Dev	September Inv. (dpm/cm^2)		Std. Dev	November Inv. (dpm/cm^2)		Std. Dev
0-1	1.41	2.95	±	1.32	4.13	±	1.59	3.58	±	1.31	7.16	±	2.27	4.65	±	1.67	1.05	±	0.92	1.39	±	0.99
1-2	1.46	1.55	±	1.35	4.66	±	1.77	2.43	±	1.32	7.98	±	2.55	1.60	±	1.80	0.00	±	0.00	2.39	±	0.76
2-3	1.48	2.71	±	1.38	0.00	±	0.00	1.78	±	1.60	6.78	±	2.63	0.00	±	0.00	0.58	±	1.04	0.00	±	0.00
3-4	1.46	2.44	±	1.37	5.65	±	2.13	2.81	±	1.40	3.75	±	2.38	0.00	±	0.00	0.00	±	0.00	0.00	±	0.00
4-5	1.46	2.57	±	1.35		±			±		4.87	±	2.51		±		1.88	±	1.56	0.00	±	0.00
5-6	1.45	0.00	±	0.00		±			±		5.15	±	6.31		±		1.34	±	1.55	0.00	±	0.00

Table 9. UNB Site 1 Subtidal Zone Activity (Act.) and Total Inventory (Inv.) Calculations.

Activity

Depth Int. (cm)	January Act. (dpm/g)		Std. Dev	February Act. (dpm/g)		Std. Dev	March Act. (dpm/g)		Std. Dev	April Act. (dpm/g)		Std. Dev	June Act. (dpm/g)		Std. Dev	September Act. (dpm/g)		Std. Dev	November Act. (dpm/g)		Std. Dev
0-1	0.00	±	0.00	2.05	±	1.25	2.82	±	1.03	7.41	±	2.08	1.96	±	1.44	1.11	±	0.79	3.20	±	0.69
1-2	1.58	±	1.45	2.96	±	1.21	4.95	±	1.04	6.65	±	2.04	4.12	±	1.43	0.00	±	0.00	1.04	±	0.76
2-3	1.76	±	1.13	2.85	±	1.72	2.77	±	1.14	7.64	±	1.97	0.11	±	1.32	0.60	±	1.01	3.28	±	0.78
3-4	0.00	±	0.00	3.09	±	1.46	3.46	±	1.23	5.82	±	1.96	0.00	±	0.00	0.86	±	1.01	2.44	±	0.77
4-5		±			±		4.51	±	1.36	4.50	±	2.20	0.00	±	0.00	0.00	±	0.00	2.42	±	1.13
5-6		±			±		0.00	±	0.00	7.68	±	2.15		±		0.91	±	1.09	0.00	±	0.00

Total Inventory

Depth Int. (cm)	Bulk Density (g/cm^3)	January Inv. (dpm/cm^2)		Std. Dev	February Inv. (dpm/cm^2)		Std. Dev	March Inv. (dpm/cm^2)		Std. Dev	April Inv. (dpm/cm^2)		Std. Dev	June Inv. (dpm/cm^2)		Std. Dev	September Inv. (dpm/cm^2)		Std. Dev	November Inv. (dpm/cm^2)		Std. Dev
0-1	1.31	0.00	±	0.00	2.69	±	1.64	3.70	±	1.35	9.72	±	2.73	2.57	±	1.88	1.45	±	1.04	4.20	±	0.90
1-2	1.36	2.14	±	1.97	4.02	±	1.65	6.71	±	1.41	9.01	±	2.76	5.58	±	1.94	0.00	±	0.00	1.41	±	1.03
2-3	1.38	2.42	±	1.56	3.93	±	2.37	3.82	±	1.57	10.54	±	2.72	0.15	±	1.82	0.82	±	1.40	4.53	±	1.08
3-4	1.41	0.00	±	0.00	4.35	±	2.06	4.87	±	1.73	8.20	±	2.75	0.00	±	0.00	1.21	±	1.43	3.43	±	1.09
4-5	1.39		±			±		6.26	±	1.88	6.26	±	3.05	0.00	±	0.00	0.00	±	0.00	3.37	±	1.58
5-6	1.42		±			±		0.00	±	0.00	10.89	±	3.05		±		1.29	±	1.54	0.00	±	0.00

Table 10. UNB Site 2 Intertidal Zone Activity (Act.) and Total Inventory (Inv.) Calculations.

Activity

Depth Int. (cm)	January Act. (dpm/g)		Std. Dev	February Act. (dpm/g)		Std. Dev	March Act. (dpm/g)		Std. Dev	April Act. (dpm/g)		Std. Dev	June Act. (dpm/g)		Std. Dev	September Act. (dpm/g)		Std. Dev	November Act. (dpm/g)		Std. Dev
0-1	1.40	±	1.21	2.77	±	1.05	2.61	±	1.15	2.79	±	1.75	0.76	±	1.16	0.00	±	0.00	0.00	±	0.00
1-2	0.00	±	0.00	4.00	±	1.33	1.93	±	1.19	3.24	±	2.01	0.00	±	0.00	0.89	±	0.85	0.26	±	0.73
2-3	1.74	±	1.12	3.41	±	1.39	2.11	±	1.19	3.96	±	1.57	0.00	±	0.00	0.00	±	0.00	0.00	±	0.00
3-4	0.00	±	0.00	0.00	±	0.00	0.00	±	0.00	0.00	±	0.00	0.00	±	0.00	0.00	±	0.00	0.00	±	0.00
4-5		±			±		2.39	±	1.23		±			±		1.47	±	1.03		±	
5-6		±			±		0.00	±	0.00		±			±		2.27	±	1.21		±	

Total Inventory

Depth Int. (cm)	Bulk Density (g/cm^3)	January Inv. (dpm/cm^2)		Std. Dev	February Inv. (dpm/cm^2)		Std. Dev	March Inv. (dpm/cm^2)		Std. Dev	April Inv. (dpm/cm^2)		Std. Dev	June Inv. (dpm/cm^2)		Std. Dev	September Inv. (dpm/cm^2)		Std. Dev	November Inv. (dpm/cm^2)		Std. Dev
0-1	1.39	1.95	±	1.68	3.84	±	1.45	3.63	±	1.60	3.87	±	2.43	1.06	±	1.62	0.00	±	0.00	0.00	±	0.00
1-2	1.46	0.00	±	0.00	5.83	±	1.93	2.81	±	1.73	4.72	±	2.93	0.00	±	0.00	1.29	±	1.24	0.38	±	1.06
2-3	1.50	2.60	±	1.68	5.10	±	2.08	3.16	±	1.79	5.93	±	2.35	0.00	±	0.00	0.00	±	0.00	0.00	±	0.00
3-4	1.45	0.00	±	0.00	0.00	±	0.00	0.00	±	0.00	0.00	±	0.00	0.00	±	0.00	0.00	±	0.00	0.00	±	0.00
4-5	1.49		±			±		3.56	±	1.83		±			±		2.18	±	1.53		±	
5-6	1.48		±			±		0.00	±	0.00		±			±		3.37	±	1.79		±	

Table 11. UNB Site 2 Subtidal Zone Activity and Total Inventory Calculations.

Activity

Depth Int. (cm)	January Act. (dpm/g)		Std. Dev	February Act. (dpm/g)		Std. Dev	March Act. (dpm/g)		Std. Dev	April Act. (dpm/g)		Std. Dev	June Act. (dpm/g)		Std. Dev	September Act. (dpm/g)		Std. Dev	November Act. (dpm/g)		Std. Dev
0-1		±		2.86	±	1.19	3.55	±	1.42	5.40	±	2.11	0.06	±	0.94	0.00	±	0.00	3.35	±	0.81
1-2		±		1.94	±	1.05	3.67	±	1.43	2.87	±	2.09	0.00	±	0.00	0.82	±	0.78	1.27	±	0.78
2-3		±		2.02	±	1.38	0.00	±	0.00	2.53	±	2.03	0.00	±	0.00	1.65	±	0.83	0.00	±	0.00
3-4		±			±			±			±		0.00	±	0.00	0.97	±	0.94	0.41	±	0.92
4-5		±			±			±			±			±		2.25	±	1.16	0.00	±	0.00
5-6		±			±			±			±			±		0.00	±	0.00	0.00	±	0.00

Total Inventory

Depth Int. (cm)	Bulk Density (g/cm^3)	January Inv. (dpm/cm^2)		Std. Dev	February Inv. (dpm/cm^2)		Std. Dev	March Inv. (dpm/cm^2)		Std. Dev	April Inv. (dpm/cm^2)		Std. Dev	June Inv. (dpm/cm^2)		Std. Dev	September Inv. (dpm/cm^2)		Std. Dev	November Inv. (dpm/cm^2)		Std. Dev
0-1	1.32		±		3.78	±	1.58	4.70	±	1.88	7.15	±	2.80	0.08	±	1.25	0.00	±	0.00	4.44	±	1.07
1-2	1.38		±		2.68	±	1.45	5.08	±	1.97	3.97	±	2.89	0.00	±	0.00	1.13	±	1.08	1.76	±	1.08
2-3	1.51		±		3.05	±	2.08	0.00	±	0.00	3.81	±	3.06	0.00	±	0.00	2.49	±	1.25	0.00	±	0.00
3-4	1.42		±			±			±			±		0.00	±	0.00	1.38	±	1.34	0.58	±	1.31
4-5	1.45		±			±			±			±			±		3.25	±	1.67	0.00	±	0.00
5-6	1.46		±			±			±			±			±		0.00	±	0.00	0.00	±	0.00

Table 12. UNB Site 3 Intertidal Zone Activity (Act.) and Total Inventory (Inv.) Calculations.

Activity

Depth Int. (cm)	January Act. (dpm/g)		Std. Dev	February Act. (dpm/g)		Std. Dev	March Act. (dpm/g)		Std. Dev	April Act. (dpm/g)		Std. Dev	June Act. (dpm/g)		Std. Dev	September Act. (dpm/g)		Std. Dev	November Act. (dpm/g)		Std. Dev
0-1		±		3.91	±	1.19	5.12	±	1.53	1.87	±	2.24	0.00	±	0.00	0.48	±	0.74	0.06	±	0.63
1-2		±		1.98	±	1.17	4.94	±	2.18	2.69	±	2.21	0.00	±	0.00	0.00	±	0.00	0.07	±	0.72
2-3		±		0.00	±	0.00	6.98	±	1.89	3.13	±	2.02	0.41	±	1.29	0.44	±	0.85	0.00	±	0.00
3-4		±		0.00	±	0.00	3.00	±	1.77	3.90	±	2.19	0.00	±	0.00	0.00	±	0.00	0.00	±	0.00
4-5		±			±		9.51	±	5.29	4.18	±	2.16		±		2.43	±	1.02		±	
5-6		±			±			±		2.47	±	2.06		±			±			±	

Total Inventory

Depth Int. (cm)	Bulk Density (g/cm^3)	January Inv. (dpm/cm^2)		Std. Dev	February Inv. (dpm/cm^2)		Std. Dev	March Inv. (dpm/cm^2)		Std. Dev	April Inv. (dpm/cm^2)		Std. Dev	June Inv. (dpm/cm^2)		Std. Dev	September Inv. (dpm/cm^2)		Std. Dev	November Inv. (dpm/cm^2)		Std. Dev
0-1	1.32		±		5.41	±	1.65	7.09	±	2.11	2.59	±	3.10	0.00	±	0.00	0.67	±	1.02	0.08	±	0.87
1-2	1.38		±		2.85	±	1.69	7.12	±	3.14	3.87	±	3.19	0.00	±	0.00	0.00	±	0.00	0.09	±	1.04
2-3	1.51		±		0.00	±	0.00	10.36	±	2.81	4.65	±	3.01	0.61	±	1.92	0.65	±	1.26	0.00	±	0.00
3-4	1.42		±		0.00	±	0.00	4.54	±	2.68	5.91	±	3.32	0.00	±	0.00	0.00	±	0.00	0.00	±	0.00
4-5	1.45		±			±		14.37	±	8.00	6.31	±	3.27		±		3.68	±	1.54		±	
5-6	1.46		±			±			±		3.85	±	3.22		±			±			±	

Table 13. UNB Site 3 Subtidal Zone Activity and Total Inventory Calculations.

Activity

Depth Int. (cm)	January Act. (dpm/g)		Std. Dev	February Act. (dpm/g)		Std. Dev	March Act. (dpm/g)		Std. Dev	April Act. (dpm/g)		Std. Dev	June Act. (dpm/g)		Std. Dev	September Act. (dpm/g)		Std. Dev	November Act. (dpm/g)		Std. Dev
0-1		±		0.00	±	0.00	3.82	±	1.76	7.49	±	2.77	0.27	±	1.09	0.00	±	0.00	0.59	±	0.69
1-2		±		0.00	±	0.00	2.95	±	1.79	6.65	±	2.40	0.00	±	0.00	1.43	±	0.86	0.17	±	0.74
2-3		±		1.71	±	1.22	5.20	±	1.79	1.50	±	2.67	0.00	±	0.00	1.99	±	0.92	0.00	±	0.00
3-4		±		2.00	±	1.15	0.00	±	0.00		±		0.00	±	0.00	0.76	±	1.03	0.00	±	0.00
4-5		±			±			±			±			±		0.00	±	0.00	0.73	±	0.92
5-6		±			±			±			±			±		1.62	±	1.16	0.00	±	0.00

Total Inventory

Depth Int. (cm)	Bulk Density (g/cm^3)	January Inv. (dpm/cm^2)		Std. Dev	February Inv. (dpm/cm^2)		Std. Dev	March Inv. (dpm/cm^2)		Std. Dev	April Inv. (dpm/cm^2)		Std. Dev	June Inv. (dpm/cm^2)		Std. Dev	September Inv. (dpm/cm^2)		Std. Dev	November Inv. (dpm/cm^2)		Std. Dev
0-1	1.34		±		0.00	±	0.00	5.12	±	2.35	10.03	±	3.71	0.37	±	1.45	0.00	±	0.00	0.78	±	0.93
1-2	1.46		±		0.00	±	0.00	4.29	±	2.61	9.69	±	3.50	0.00	±	0.00	2.09	±	1.26	0.25	±	1.08
2-3	1.47		±		2.53	±	1.80	7.67	±	2.65	2.21	±	3.94	0.00	±	0.00	2.93	±	1.36	0.00	±	0.00
3-4	1.50		±		3.01	±	1.73	0.00	±	0.00		±		0.00	±	0.00	1.15	±	1.55	0.00	±	0.00
4-5	1.48		±			±			±			±			±		0.00	±	0.00	1.08	±	1.36
5-6	1.50		±			±			±			±			±		2.42	±	1.73	0.00	±	0.00

Table 14. Upper Newport Bay Total, Residual and New Inventory Results.

	Intertidal			Subtidal		
	Total Inventory (dpm/cm^2)	**Residual Inventory** (dpm/cm^2)	**New Inventory** (dpm/cm^2)	**Total Inventory** (dpm/cm^2)	**Residual Inventory** (dpm/cm^2)	**New Inventory** (dpm/cm^2)
NB1						
Jan	12.22			4.57		
Feb	5.83	8.70	5.74	5.41	3.25	11.73
March	10.61	3.41	2.16	25.36	3.17	16.59
April	35.69	8.06	27.63	54.61	19.27	35.34
June	6.24	17.16	-10.92	8.30	26.26	-17.96
Sept	4.85	1.71	3.14	4.78	2.28	2.51
Nov	3.79	2.30	1.48	16.94	2.27	14.67
∑	**79.22**	**41.34**	**23.49**	**119.97**	**56.49**	**51.15**
NB2						
Jan	4.55			No data		
Feb	5.17	3.24	11.53	3.71		
March	13.16	3.02	4.52	9.78	2.17	4.22
April	14.52	10.00	4.52	14.93	7.43	7.50
June	1.06	6.98	-5.92	0.08	7.18	-7.10
Sept	6.84	0.29	6.55	8.26	0.02	8.24
Nov	0.38	3.25	-2.87	6.78	3.92	2.86
∑	**45.68**	**26.78**	**6.80**	**43.54**	**20.72**	**15.71**
NB3						
Jan	No data			No data		
Feb	5.07			4.97		
March	43.48	2.96	38.65	17.08	2.91	13.84
April	27.19	33.04	-5.85	21.94	12.98	8.96
June	0.61	13.07	-12.46	0.37	10.55	-10.18
Sept	5.12	0.17	4.83	8.59	0.10	8.49
Nov	0.18	2.43	-2.20	2.11	4.08	-1.97
∑	**81.64**	**51.67**	**22.97**	**55.05**	**30.51**	**19.14**

Table 15. Activities of the sediment collected for long-term sedimentation rates in Upper Newport Estuary.

Depth Interval (cm)	^{226}Ra			Excess ^{210}Pb			^{137}Cs		
	Activity (dpm/g)		Std. Dev	Inv. (dpm/g)		Std. Dev	Inv. (dpm/g)		Std. Dev
0-1	2.63	±	0.18	2.95	±	1.00	1.49	±	0.10
1-2	2.47	±	0.32	3.51	±	0.94	1.10	±	0.10
2-3	2.01	±	0.16	3.15	±	0.89	1.08	±	0.10
3-4	2.40	±	0.54	2.42	±	1.27	0.13	±	0.12
4-5	2.00	±	0.49	1.76	±	1.16	0.58	±	0.11
5-6	2.09	±	0.43	1.02	±	1.16	0.30	±	0.11
6-7	2.02	±	0.10	4.09	±	0.97	1.84	±	0.11
7-8	1.61	±	0.19	1.00	±	1.14	0.07	±	0.12
8-9	1.95	±	0.40	0.91	±	1.30	0.00	±	0.00
9-10	1.95	±	0.68	0.36	±	1.35	0.00	±	0.00
10-12	2.63	±	0.18	2.95	±	1.00	1.49	±	0.10

APPENDIX D: VERTICAL DISTRIBUTIONS OF SEDIMENT PHOSPHORUS (ASPILA)

Table 14. Vertical Total P, Inorganic P, and Organic P concentrations for NB1.

Depth (cmbsf)	NB1 - INTERTIDAL								
	April			June			November		
	Total P	Inorg-P	Org-P	Total P	Inorg-P	Org-P	Total P	Inorg-P	Org-P
	µmol of P/g of sed			µmol of P/g of sed			µmol of P/g of sed		
0-1	54.4 ± 1.3	51.4 ± 1.4	2.9 ± 2.7	40.9 ± 0.7	35.5 ± 0.2	5.3 ± 0.5	36.1 ± 0.3	32.2 ± 1.1	3.9 ± 1.4
1-2	49.8 ± 0.8	45.5 ± 5.9	4.3 ± 5.1	40.3 ± 0.4	36.5 ± 0.1	3.8 ± 0.4	33.9 ± 1.4	33.0 ± 0.2	1.0 ± 1.2
2-3	47.4 ± 0.5	43.8 ± 0.4	3.6 ± 0.9	39.6 ± 0.7	35.9 ± 0.6	3.7 ± 1.3	32.7 ± 2.5	31.7 ± 0.5	0.9 ± 3.0
3-4	46.7 ± 0.1	45.8 ± 0.4	0.9 ± 0.4	39.9 ± 0.1	36.9 ± 0.4	3.1 ± 0.3	33.4 ± 2.2	32.4 ± 0.1	0.9 ± 2.1
4-5	49.7 ± 0.1	45.6 ± 0.7	4.1 ± 0.8	40.5 ± 0.0	35.3 ± 0.8	5.2 ± 0.8	33.9 ± 0.0	32.2 ± 0.4	1.8 ± 0.4
5-6	50.0 ± 1.0	44.0 ± 0.6	6.1 ± 0..	40.6 ± 0.1	38.0 ± 1.4	2.5 ± 1.4	35.3 ± 0.2	32.2 ± 1.0	3.1 ± 0.8
Depth (cmbsf)	**NB1 - SUBTIDAL**								
	April			June			November		
	Total P	Inorg-P	Org-P	Total P	Inorg-P	Org-P	Total P	Inorg-P	Org-P
	µmol of P/g of sed			µmol of P/g of sed			µmol of P/g of sed		
0-1	63.9 ± 1.3	56.5 ± 0.3	7.4 ± 2.7	No Sample			No Sample		
1-2	58.4 ± 1.7	56.5 ± 1.4	1.9 ± 5.1	44.6 ± 0.1	38.4 ± 0.7	6.2 ± 0.7	41.8 ± 0.6	38.0 ± 0.4	3.8 ± 1.0
2-3	54.7 ± 0.5	52.4 ± 0.2	2.3 ± 0.9	45.2 ± 0.9	38.5 ± 0.1	6.7 ± 0.8	42.5 ± 0.7	38.5 ± 1.8	4.0 ± 1.1
3-4	56.4 ± 3.6	49.9 ± 1.3	6.5 ± 0.4	42.0 ± 0.2	37.4 ± 0.2	4.6 ± 0.1	44.1 ± 0.4	39.6 ± 0.2	4.5 ± 0.6
4-5	58.0 ± 2.1	53.5 ± 0.0	4.4 ± 0.8	43.3 ± 1.3	38.1 ± 0.2	5.2 ± 1.5	42.0 ± 0.2	38.3 ± 0.0	3.8 ± 0.1
5-6	57.9 ± 1.3	52.5 ± 0.1	5.4 ± 0.3	43.8 ± 0.5	38.3 ± 0.4	5.5 ± 0.0	41.3 ± 0.6	37.0 ± 0.0	4.3 ± 0.6

Table 15. Vertical Total P, Inorganic P, and Organic P concentrations for NB2.

Depth (cmbsf)	NB2 - INTERTIDAL								
	April			June			November		
	Total P	Inorg-P	Org-P	Total P	Inorg-P	Org-P	Total P	Inorg-P	Org-P
	µmol of P/g of sed			µmol of P/g of sed			µmol of P/g of sed		
0-1	44.6 ± 0.6	39.6 ± 0.3	4.9 ± 0.3	47.4 ± 1.4	42.1 ± 0.8	5.3 ± 2.0	39.7 ± 2.0	37.0 ± 1.0	2.7 ± 0.9
1-2	44.4 ± 0.0	40.4 ± 1.4	3.9 ± 1.3	46.1 ± 0.2	41.3 ± 0.3	4.7 ± 0.2	37.5 ± 0.2	35.4 ± 0.5	2.1 ± 0.7
2-3	45.9 ± 0.9	41.1 ± 0.2	4.8 ± 1.1	43.6 ± 0.4	41.1 ± 1.1	2.5 ± 6.4	41.5 ± 6.4	34.4 ± 0.6	7.1 ± 5.8
3-4	43.9 ± 0.3	41.4 ± 1.3	2.5 ± 1.0	45.0 ± 0.8	40.8 ± 0.5	4.2 ± 1.8	37.0 ± 1.8	34.2 ± 1.3	2.8 ± 3.1
4-5	42.9 ± 0.3	37.2 ± 0.0	5.8 ± 0.02	43.6 ± 0.7	37.9 ± 0.8	5.7 ± 1.2	36.7 ± 1.2	32.5 ± 1.6	4.2 ± 2.9
5-6	44.6 ± 0.6	42.0 ± 0.1	2.6 ± 0.7	45.2 ± 1.0	39.2 ± 1.0	6.0 ± 1.1	36.0 ± 1.1	34.7 ± 0.9	1.3 ± 0.2
Depth (cmbsf)	**NB2 - SUBTIDAL**								
	April			June			November		
	Total P	Inorg-P	Org-P	Total P	Inorg-P	Org-P	Total P	Inorg-P	Org-P
	µmol of P/g of sed			µmol of P/g of sed			µmol of P/g of sed		
0-1	52.3 ± 0.1	45.5 ± 0.4	6.8 ± 0.5	45.4 ± 0.2	44.6 ± 0.6	0.8 ± 0.5	54.8 ± 0.3	44.8 ± 1.7	10.0 ± 1.4
1-2	47.6 ± 1.2	42.9 ± 0.0	4.7 ± 1.2	44.2 ± 1.8	40.0 ± 1.4	4.1 ± 0.5	51.8 ± 0.1	45.9 ± 0.4	5.9 ± 0.4
2-3	44.6 ± 0.7	42.2 ± 0.6	2.4 ± 1.3	44.6 ± 1.6	40.1 ± 1.1	4.5 ± 2.2	46.6 ± 0.6	43.6 ± 0.6	3.0 ± 0.0
3-4	44.5 ± 0.6	40.9 ± 0.2	3.5 ± 0.7	45.1 ± 2.2	39.2 ± 2.0	5.9 ± 0.1	46.8 ± 0.9	43.1 ± 0.5	3.7 ± 1.4
4-5	47.1 ± 0.1	41.5 ± 0.7	5.6 ± 0.6	44.0 ± 0.2	38.6 ± 0.2	5.5 ± 1.2	45.6 ± 0.5	43.3 ± 0.7	2.3 ± 1.2
5-6	46.0 ± 0.2	41.3 ± 0.6	4.8 ± 0.8	44.1 ± 2.8	39.2 ± 2.6	4.9 ± 0.2	44.5 ± 0.2	41.5 ± 0.3	3.0 ± 0.8

Table 16. Vertical Total P, Inorganic P, and Organic P concentrations for NB3.

Depth (cmbsf)	NB3 - INTERTIDAL								
	April			June			November		
	Total P	Inorg-P	Org-P	Total P	Inorg-P	Org-P	Total P	Inorg-P	Org-P
	µmol of P/g of sed			µmol of P/g of sed			µmol of P/g of sed		
0-1	35.7 ± 0.5	34.5 ± 0.5	1.2 ± 1.0	42.7 ± 0.7	38.4 ± 0.0	4.3 ± 0.7	51.7 ± 0.3	48.4 ± 1.7	3.3 ± 1.4
1-2	No Sample			No Sample			50.5 ± 0.1	46.3 ± 0.4	4.3 ± 0.4
2-3	34.7 ± 1.2	34.4 ± 0.2	0.3 ± 1.4	41.0 ± 0.8	37.6 ± 0.1	3.4 ± 0.9	44.8 ± 0.6	41.2 ± 0.6	3.6 ± 0.0
3-4	34.8 ± 0.2	34.6 ± 0.2	0.2 ± 0.1	39.5 ± 0.0	36.9 ± 0.5	2.7 ± 0.5	45.3 ± 0.9	41.1 ± 0.5	4.2 ± 1.4
4-5	35.8 ± 0.5	34.8 ± 0.8	1.0 ± 0.3	41.5 ± 0.4	39.6 ± 0.6	1.9 ± 0.9	44.7 ± 0.5	41.0 ± 0.7	3.7 ± 1.2
5-6	35.1 ± 0.0	34.3 ± 0.5	0.8 ± 0.5	42.1 ± 0.7	40.1 ± 0.1	2.0 ± 0.8	45.8 ± 0.4	45.5 ± 0.5	0.4 ± 0.8
Depth (cmbsf)	**NB3 - SUBTIDAL**								
	April			June			November		
	Total P	Inorg-P	Org-P	Total P	Inorg-P	Org-P	Total P	Inorg-P	Org-P
	µmol of P/g of sed			µmol of P/g of sed			µmol of P/g of sed		
0-1	54.2 ± 0.3	47.0 ± 0.6	7.3 ± 0.2	28.1 ± 0.5	24.7 ± 0.4	3.4 ± 0.9	35.2 ± 0.6	31.7 ± 0.3	3.5 ± 0.9
1-2	44.9 ± 0.7	43.2 ± 0.1	1.7 ± 0.8	24.3 ± 1.0	22.4 ± 0.5	1.9 ± 1.5	38.4 ± 0.4	34.8 ± 1.4	3.5 ± 1.7
2-3	45.3 ± 0.6	43.5 ± 0.1	1.8 ± 0.7	24.3 ± 0.4	21.8 ± 0.2	2.5 ± 0.3	46.0 ± 0.9	41.9 ± 1.2	4.1 ± 2.0
3-4	45.3 ± 1.3	44.4 ± 0.7	0.9 ± 0.6	25.6 ± 0.2	21.2 ± 0.9	4.4 ± 0.7	42.8 ± 0.8	38.2 ± 0.2	4.6 ± 0.6
4-5	47.5 ± 0.5	45.3 ± 1.3	2.1 ± 0.8	23.9 ± 0.1	20.9 ± 0.3	3.0 ± 0.5	42.3 ± 0.4	38.7 ± 0.2	3.6 ± 0.5
5-6	47.6 ± 0.1	45.4 ± 1.0	2.2 ± 1.0	21.4 ± 0.4	20.4 ± 0.3	1.0 ± 0.1	45.3 ± 0.8	43.0 ± 0.5	2.3 ± 1.4

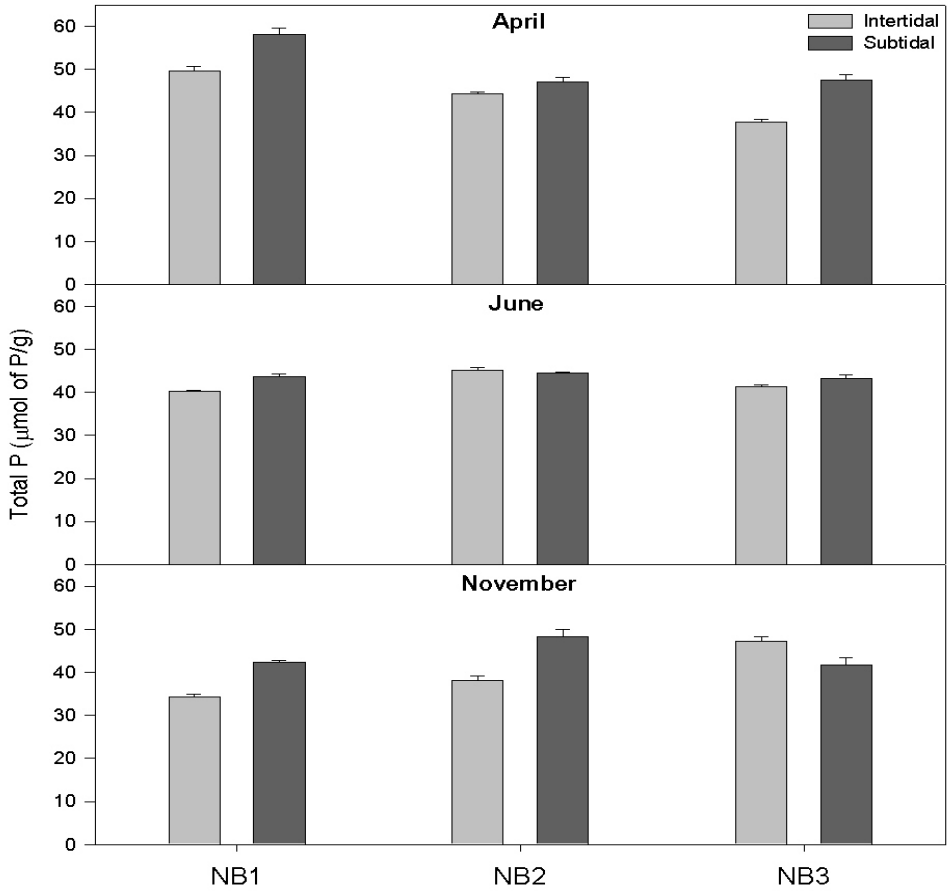

Figure 1. Mean tot-P values for the intertidal and subtidal zones of Upper Newport Estuary for April (top panel), June (middle panel) and November (bottom panel).

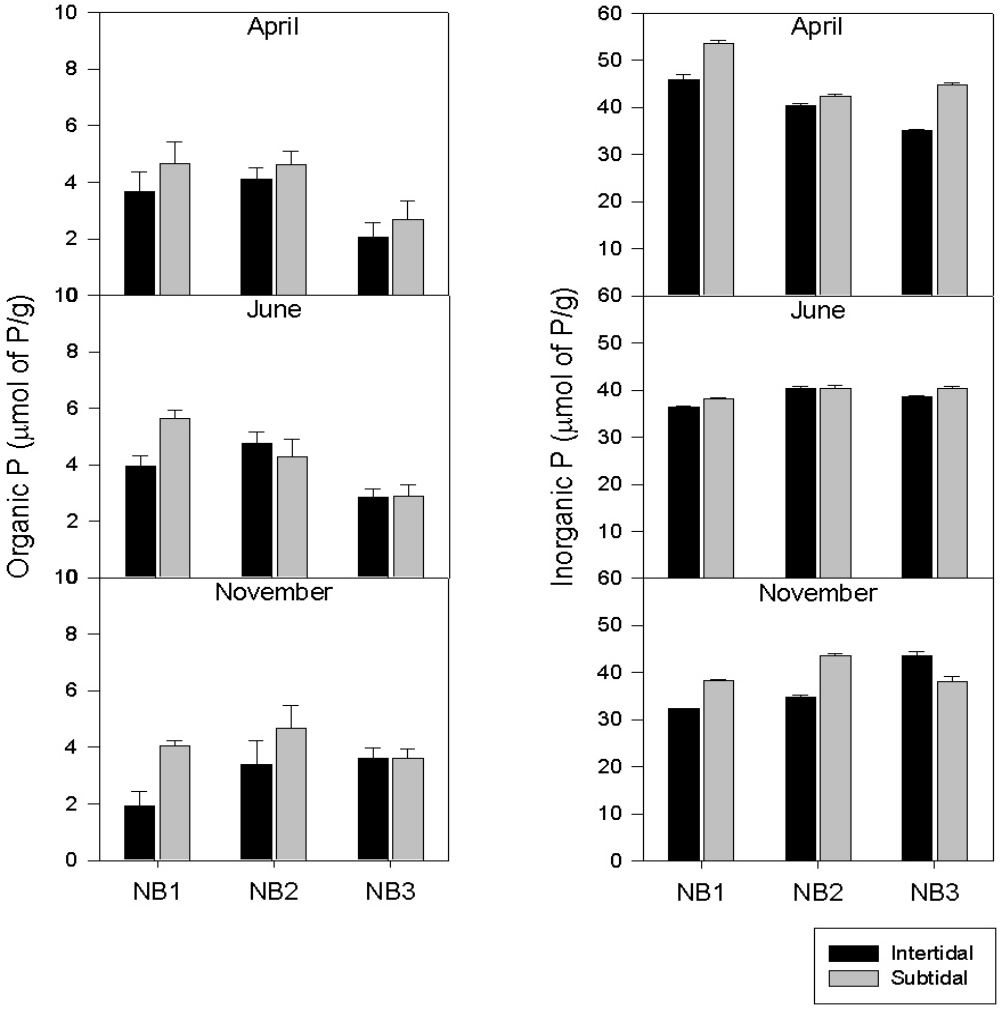

Figure 2. Mean org-P (left) and inorg-P (right) concentrations for the intertidal and subtidal zones for all three sites sampled in April, June, and November. Both org-P and inorg-P concentrations tended to be greater in the subtidal zone than the intertidal zone. The x-axis for the inorg-P fraction is six times greater than the org-P fraction.

APPENDIX E: VERTICAL DISTRIBUTIONS OF SEDIMENT PHOSPHORUS (SEDEX)

Table 1. April vertical phosphorus concentrations determined at site NB1 using SEDEX.

April – NB1 - Intertidal					
Depth Int. (cm)	**Lab-P** (μmol/g)	**Fe-P**	**Ca-P**	**Detr-P**	**Org-P**
0-1	6.72 ± 0.06	7.36 ± 0.11	11.62 ± 0.04	15.02 ± 0.23	14.33 ± 0.18
1-2	2.78 ± 0.01	7.58 ± 0.63	10.51 ± 0.14	16.09 ± 0.13	13.09 ± 0.65
2-3	1.36 ± 0.00	7.34 ± 0.25	10.41 ± 0.55	15.73 ± 0.03	7.83 ± .18
3-4	1.43 ± 0.01	7.36 ± 0.29	10.54 ± 0.09	14.84 ± 0.54	7.64 ± 0.96
4-5	1.11 ± 0.03	8.25 ± 1.09	11.43 ± 0.58	15.14 ± 0.33	3.63 ± 0.18
5-6	1.23 ± 0.04	9.11 ± 1.04	11.12 ± 0.13	14.12 ± 0.39	4.57 ± 0.02
Mean	4.75 ± 2.19	7.47 ± 0.72	11.07 ± 0.52	15.55 ± 0.69	13.71 ± 4.37
April – NB1 - Subtidal					
Depth Int. (cm)	**Lab-P** (μmol/g)	**Fe-P**	**Ca-P**	**Detr-P**	**Org-P**
0-1					
1-2	3.29 ± 0.05	8.37 ± 0.24	23.06 ± 0.38	6.98 ± 1.24	5.72 ± 0.06
2-3	2.36 ± 0.30	6.27 ± 1.04	22.65 ± 0.16	6.97 ± 1.29	7.84 ± 1.19
3-4	1.96 ± 0.05	5.83 ± 0.16	23.11 ± 0.45	6.47 ± 0.10	1.93 ± 0.06
4-5	2.28 ± 0.05	7.28 ± 0.12	23.56 ± 0.54	7.84 ± 0.02	3.03 ± 1.42
5-6	1.73 ± 0.20	6.04 ± 0.03	22.67 ± 0.25	9.64 ± 0.26	2.51 ± 0.79
Mean	3.29 ± 0.60	8.37 ± 1.06	23.06 ± 0.38	6.98 ± 1.25	5.72 ± 2.50

Table 2. April vertical phosphorus concentrations determined at site NB2 using SEDEX.

April – NB2 - Intertidal					
Depth Int. (cm)	**Lab-P** (μmol/g)	**Fe-P**	**Ca-P**	**Detr-P**	**Org-P**
0-1	0.24 ± 0.01	6.37 ± 0.56	11.63 ± 0.27		
1-2	0.00 ± 0.08	5.98 ± 0.07	14.82 ± 0.11		
2-3	0.00 ± 0.04	4.49 ± 0.11	13.59 ± 0.37		
3-4	0.00 ± 0.01	3.71 ± 0.08	12.77 ± 0.10		
4-5	0.00 ± 0.07	3.89 ± 0.63	18.48 ± 0.15		
5-6	0.00 ± 0.21	3.76 ± 0.04	19.41 ± 1.29		
Mean	0.12 ± 0.10	6.18 ± 1.18	13.22 ± 3.16		
April – NB2 - Subtidal					
Depth Int. (cm)	**Lab-P** (μmol/g)	**Fe-P**	**Ca-P**	**Detr-P**	**Org-P**
0-1	3.87 ± 0.15	10.10 ± 0.01	17.69 ± 1.29		
1-2	0.24 ± 0.00	7.28 ± 0.23	19.58 ± 0.08		
2-3	0.00 ± 0.01	5.77 ± 0.36	19.26 ± 0.25		
3-4	0.00 ± 0.01	5.91 ± 0.12	17.99 ± 0.33		
4-5	0.00 ± 0.06	4.62 ± 0.44	20.32 ± 1.85		
5-6	0.00 ± 0.09	7.52 ± 0.16	18.69 ± 0.82		
Mean	2.05 ± 1.56	8.69 ± 1.91	18.63 ± 1.00		

Table 3. April phosphorus concentrations determined at site NB3 using SEDEX.

April – NB3 - Intertidal					
Depth Int. (cm)	**Lab-P** (μmol/g)	**Fe-P**	**Ca-P**	**Detr-P**	**Org-P**
0-1	3.50 ± 0.92	4.95 ± 0.01	19.59 ± 0.12	13.55 ± 0.52	4.04 ± 0.37
1-2					
2-3	0.16 ± 0.01	3.16 ± 0.14	18.16 ± 0.41	16.34 ± 0.10	3.29 ± 1.58
3-4	0.00 ± 0.10	3.13 ± 0.22	19.81 ± 1.33	18.23 ± 0.75	5.29 ± 0.47
4-5	0.00 ± 0.06	3.23 ± 0.29	18.10 ± 0.62	19.53 ± 0.44	6.15 ± 0.79
5-6	0.00 ± 0.04	2.82 ± 0.03	16.53 ± 1.43	20.95 ± 1.18	3.47 ± 0.42
Mean	3.50 ± 1.55	4.95 ± 0.85	19.59 ± 1.33	13.55 ± 2.88	4.04 ± 1.23
April – NB3 - Subtidal					
Depth Int. (cm)	**Lab-P** (μmol/g)	**Fe-P**	**Ca-P**	**Detr-P**	**Org-P**
0-1	6.76 ± 0.20	6.80 ± 0.03	27.23 ± 0.28	9.31 ± 0.09	8.16 ± 0.04
1-2	1.83 ± 0.01	4.07 ± 0.03	18.95 ± 0.37	18.95 ± 0.20	6.94 ± 1.23
2-3	1.44 ± 0.01	3.83 ± 0.07	18.53 ± 0.07	17.88 ± 0.51	5.21 ± 0.01
3-4	2.63 ± 0.02	4.36 ± 0.19	18.95 ± 0.16	18.61 ± 1.81	5.86 ± 1.10
4-5	2.98 ± 0.10	4.55 ± 0.10	21.26 ± 1.17	17.06 ± 0.73	6.71 ± 0.18
5-6	2.28 ± 0.17	4.49 ± 0.17	20.41 ± 0.39	21.33 ± 1.43	6.90 ± 0.67
Mean	4.30 ± 1.93	5.44 ± 1.07	23.09 ± 3.27	14.13 ± 4.12	7.55 ± 1.01

Table 4. June phosphorus concentrations determined at site NB1 using SEDEX.

June – NB1 - Intertidal					
Depth Int. (cm)	**Lab-P** (μmol/g)	**Fe-P**	**Ca-P**	**Detr-P**	**Org-P**
0-1	1.65 ± 0.04	3.75 ± 0.16	12.10 ± 0.24	12.84 ± 0.09	1.00 ± 1.41
1-2	0.62 ± 0.03	2.67 ± 0.09	12.53 ± 0.50	11.30 ± 0.77	1.07 ± 0.09
2-3	0.87 ± 0.00	2.68 ± 0.20	12.66 ± 0.25	10.90 ± 1.89	2.20 ± 2.30
3-4	1.04 ± 0.02	2.54 ± 0.20	13.20 ± 0.06	11.15 ± 0.66	1.74 ± 0.72
4-5	0.98 ± 0.13	2.89 ± 0.26	12.51 ± 0.29	11.66 ± 0.37	1.35 ± 0.31
5-6	0.78 ± 0.02	3.07 ± 0.07	11.51 ± 1.27	11.93 ± 1.20	3.67 ± 0.70
Mean	1.65 ± 0.35	2.93 ± 0.44	12.42 ± 0.57	11.63 ± 0.70	2.01 ± 1.00
June – NB1 - Subtidal					
Depth Int. (cm)	**Lab-P** (μmol/g)	**Fe-P**	**Ca-P**	**Detr-P**	**Org-P**
0-1					
1-2	3.29 ± 0.12	7.87 ± 0.84	10.62 ± 1.15	17.16 ± 0.30	2.06 ± 0.24
2-3	2.31 ± 0.02	7.60 ± 0.95	11.98 ± 0.63	16.47 ± 0.66	2.16 ± 0.37
3-4	1.69 ± 0.34	5.93 ± 0.63	11.97 ± 0.31	17.21 ± 0.25	1.24 ± 0.74
4-5	1.43 ± 0.23	6.16 ± 0.35	12.17 ± 0.11	16.33 ± 0.16	2.81 ± 0.25
5-6	1.44 ± 0.20	6.69 ± 0.08	13.21 ± 0.62	16.44 ± 2.10	3.07 ± 0.67
Mean	2.43 ± 0.79	6.85 ± 0.86	11.99 ± 0.92	16.72 ± 0.43	2.27 ± 0.71

Table 5. June phosphorus concentrations determined at site NB2 using SEDEX.

June – NB2 - Intertidal					
Depth Int. (cm)	**Lab-P** (μmol/g)	**Fe-P**	**Ca-P**	**Detr-P**	**Org-P**
0-1	2.10 ± 0.02	2.24 ± 3.17	12.32 ± 0.49	18.98 ± 2.19	4.72 ± 0.05
1-2	0.73 ± 0.27	2.44 ± 0.20	12.13 ± 0.90	18.25 ± 3.36	1.20 ± 3.54
2-3	0.03 ± 0.06	0.96 ± 1.35	12.42 ± 0.30	16.12 ± 0.81	0.00 ± 6.01
3-4	0.27 ± 0.02	3.31 ± 0.22	12.64 ± 0.55	15.37 ± 1.43	4.27 ± 2.36
4-5	0.62 ± 0.63	3.69 ± 0.29	13.46 ± 0.13	13.23 ± 1.81	3.94 ± 0.96
5-6	0.28 ± 0.01	3.49 ± 0.47	10.64 ± 0.20	14.07 ± 0.07	4.01 ± 0.25
Mean	2.10 ± 0.75	2.69 ± 1.03	12.27 ± 0.92	16.00 ± 2.27	3.63 ± 1.93
June – NB2 - Subtidal					
Depth Int. (cm)	**Lab-P** (μmol/g)	**Fe-P**	**Ca-P**	**Detr-P**	**Org-P**
0-1	2.91 ± 0.15	6.42 ± 0.11	1.25 ± 0.09		
1-2	1.08 ± 0.10	5.98 ± 0.65	1.16 ± 0.10		
2-3	0.31 ± 0.12	5.13 ± 0.85	1.20 ± 0.00		
3-4	0.36 ± 0.02	4.44 ± 0.77	0.81 ± 0.58		
4-5	0.00 ± 0.33	6.67 ± 1.76	1.23 ± 0.39		
5-6	0.00 ± 0.01	5.16 ± 0.15	1.17 ± 0.12		
Mean	0.78 ± 1.12	5.63 ± 0.86	1.14 ± 0.16		

Table 6. June phosphorus concentrations determined at site NB3 using SEDEX.

June – NB3 - Intertidal					
Depth Int. (cm)	**Lab-P** (μmol/g)	**Fe-P**	**Ca-P**	**Detr-P**	**Org-P**
0-1	3.88 ± 0.32	16.77 ± 7.92	8.91 ± 1.17	6.54 ± 2.04	2.13 ± 0.09
1-2	2.58 ± 0.42	21.00 ± 3.62	9.68 ± 0.59	7.90 ± 5.15	1.58 ± 0.06
2-3	1.38 ± 0.09	19.68 ± 6.96	8.58 ± 3.73	6.14 ± 0.29	1.21 ± 0.83
3-4	1.08 ± 0.02	21.94 ± 8.18	8.16 ± 1.34	4.40 ± 3.21	1.65 ± 0.51
4-5	0.49 ± 1.05	23.52 ± 11.82	9.51 ± 1.66	6.94 ± 0.36	0.00 ± 0.22
5-6	0.00 ± 0.31	36.29 ± 2.80	6.96 ± 0.32	11.64 ± 2.98	2.75 ± 1.53
Mean	1.88 ± 1.43	23.20 ± 6.81	8.63 ± 1.00	7.26 ± 2.43	1.86 ± 0.93
June – NB3 - Subtidal					
Depth Int. (cm)	**Lab-P** (μmol/g)	**Fe-P**	**Ca-P**	**Detr-P**	**Org-P**
0-1	4.97 ± 5.19	7.28 ± 0.22	5.01 ± 0.41	11.10 ± 0.57	3.74 ± 2.06
1-2	9.06 ± 0.00	5.78 ± 0.53	2.99 ± 0.07	13.58 ± 3.08	4.12 ± 0.59
2-3	8.45 ± 0.39	6.12 ± 0.60	2.26 ± 0.40	5.96 ± 4.41	0.52 ± 2.09
3-4	8.89 ± 0.96	2.87 ± 1.32	1.98 ± 0.61	11.03 ± 0.73	1.61 ± 1.10
4-5	7.41 ± 0.44	5.01 ± 0.55	1.49 ± 0.12	5.49 ± 0.05	0.00 ± 1.80
5-6	9.24 ± 0.34	3.90 ± 1.58	2.79 ± 1.02	13.49 ± 0.02	1.98 ± 2.51
Mean	8.00 ± 1.63	5.16 ± 1.59	2.75 ± 1.23	10.11 ± 3.57	2.39 ± 1.66

Table 7. November phosphorus concentrations determined at site NB1 using SEDEX.

November – NB1 - Intertidal					
Depth Int. (cm)	**Lab-P** (μmol/g)	**Fe-P**	**Ca-P**	**Detr-P**	**Org-P**
0-1	0.92 ± 0.10	2.93 ± 0.11	22.43 ± 0.11	15.94 ± 0.65	0.68 ± 0.05
1-2	0.18 ± 0.04	2.39 ± 0.01	24.48 ± 1.13	18.69 ± 0.13	3.45 ± 0.29
2-3	0.00 ± 0.16	2.14 ± 0.06	19.64 ± 0.25	14.65 ± 0.48	1.30 ± 0.22
3-4	0.00 ± 0.07	2.68 ± 0.13	23.69 ± 0.62	12.52 ± 0.27	0.00 ± 5.30
4-5	0.05 ± 0.18	3.16 ± 0.57	21.20 ± 0.65	8.58 ± 0.40	4.86 ± 0.48
5-6	0.00 ± 0.02	2.81 ± 0.03	22.45 ± 0.38	6.68 ± 0.27	1.79 ± 1.35
Mean	0.19 ± 0.36	2.68 ± 0.37	22.31 ± 1.73	12.84 ± 4.54	3.37 ± 1.82
November – NB2 - Subtidal					
Depth Int. (cm)	**Lab-P** (μmol/g)	**Fe-P**	**Ca-P**	**Detr-P**	**Org-P**
0-1					
1-2	1.66 ± 0.05	3.72 ± 0.14	21.70 ± 0.05	7.00 ± 1.37	0.47 ± 0.41
2-3	2.41 ± 0.12	3.89 ± 0.06	24.09 ± 0.04	5.43 ± 0.07	0.00 ± 0.78
3-4	2.88 ± 0.14	3.68 ± 0.04	28.57 ± 0.56	5.73 ± 1.07	2.41 ± 0.83
4-5	0.05 ± 0.02	2.75 ± 0.14	27.52 ± 0.56	4.93 ± 1.06	0.15 ± 0.07
5-6	0.00 ± 0.06	2.56 ± 0.02	29.04 ± 1.06	5.20 ± 0.46	0.00 ± 0.16
Mean	1.75 ± 1.33	3.32 ± 0.62	26.19 ± 3.17	5.66 ± 0.81	1.01 ± 1.03

Table 8. November phosphorus concentrations determined at site NB2 using SEDEX.

November – NB2 - Intertidal					
Depth Int. (cm)	**Lab-P** (μmol/g)	**Fe-P**	**Ca-P**	**Detr-P**	**Org-P**
0-1	2.30 ± 0.01	3.06 ± 0.39	13.96 ± 0.01	28.37 ± 1.03	10.84 ± 0.16
1-2	0.58 ± 0.01	3.04 ± 0.34	14.37 ± 0.12	25.06 ± 1.14	8.72 ± 0.19
2-3	0.40 ± 0.04	3.14 ± 0.03	14.60 ± 0.36	21.44 ± 1.87	6.37 ± 0.01
3-4	0.45 ± 0.00	3.35 ± 0.18	15.20 ± 0.01	20.04 ± 0.26	6.43 ± 0.10
4-5	0.53 ± 0.03	2.98 ± 0.00	15.32 ± 0.28	20.13 ± 0.67	8.92 ± 0.45
5-6	0.60 ± 0.02	2.93 ± 0.12	15.79 ± 0.27	18.29 ± 1.07	7.37 ± 0.09
Mean	0.81 ± 0.73	3.09 ± 0.15	14.87 ± 0.68	22.22 ± 3.77	8.11 ± 1.73
November – NB2 - Subtidal					
Depth Int. (cm)	**Lab-P** (μmol/g)	**Fe-P**	**Ca-P**	**Detr-P**	**Org-P**
0-1	8.42 ± 0.78	6.95 ± 0.46	15.80 ± 0.27	17.93 ± 0.95	11.99 ± 1.13
1-2	8.03 ± 1.28	5.95 ± 0.14	16.05 ± 0.24	20.18 ± 0.21	12.23 ± 0.95
2-3	2.11 ± 0.02	3.45 ± 0.34	13.53 ± 0.35	25.22 ± 0.77	13.43 ± 0.03
3-4	1.64 ± 0.17	3.22 ± 0.60	14.31 ± 0.74	33.37 ± 2.55	11.87 ± 2.00
4-5	0.25 ± 0.08	2.10 ± 0.27	13.35 ± 0.50	34.55 ± 1.12	12.93 ± 4.08
5-6	0.07 ± 0.00	1.98 ± 0.06	13.25 ± 0.14	29.00 ± 0.37	9.68 ± 1.74
Mean	3.42 ± 3.80	3.94 ± 2.05	14.38 ± 1.26	26.71 ± 6.83	12.02 ± 1.29

Table 9. November phosphorus concentrations determined at site NB3 using SEDEX.

November – NB3 - Intertidal					
Depth Int. (cm)	**Lab-P** (μmol/g)	**Fe-P**	**Ca-P**	**Detr-P**	**Org-P**
0-1	1.27 ± 0.06	4.04 ± 0.14	14.75 ± 0.16	35.67 ± 0.90	13.48 ± 1.62
1-2	0.00 ± 0.04	3.71 ± 0.12	18.22 ± 0.34	29.18 ± 2.02	18.52 ± 1.49
2-3	0.00 ± 0.06	3.97 ± 0.13	16.31 ± 0.78	17.40 ± 0.22	29.18 ± 3.29
3-4	0.00 ± 0.00	3.45 ± 0.14	17.15 ± 0.04	20.86 ± 1.08	31.6 ± 0.15
4-5	0.00 ± 0.01	4.01 ± 0.08	17.40 ± 0.14	17.47 ± 0.18	31.96 ± 0.53
5-6	0.00 ± 0.16	2.60 ± 0.01	15.25 ± 0.27	28.87 ± 2.09	29.12 ± 0.00
Mean	1.27 ± 0.52	3.63 ± 0.55	16.76 ± 1.33	24.91 ± 7.45	25.66 ± 7.74
November – NB3 - Subtidal					
Depth Int. (cm)	**Lab-P** (μmol/g)	**Fe-P**	**Ca-P**	**Detr-P**	**Org-P**
0-1	0.18 ± 0.00		11.26 ± 1.18		
1-2	0.84 ± 0.01		13.24 ± 0.37		
2-3	0.39 ± 0.04		14.73 ± 0.05		
3-4	0.00 ± 0.07		12.57 ± 0.13		
4-5	0.00 ± 0.03		14.19 ± 0.06		
5-6	0.00 ± 0.01		15.41 ± 0.09		
Mean	0.47 ± 0.34		13.57 ± 1.52		

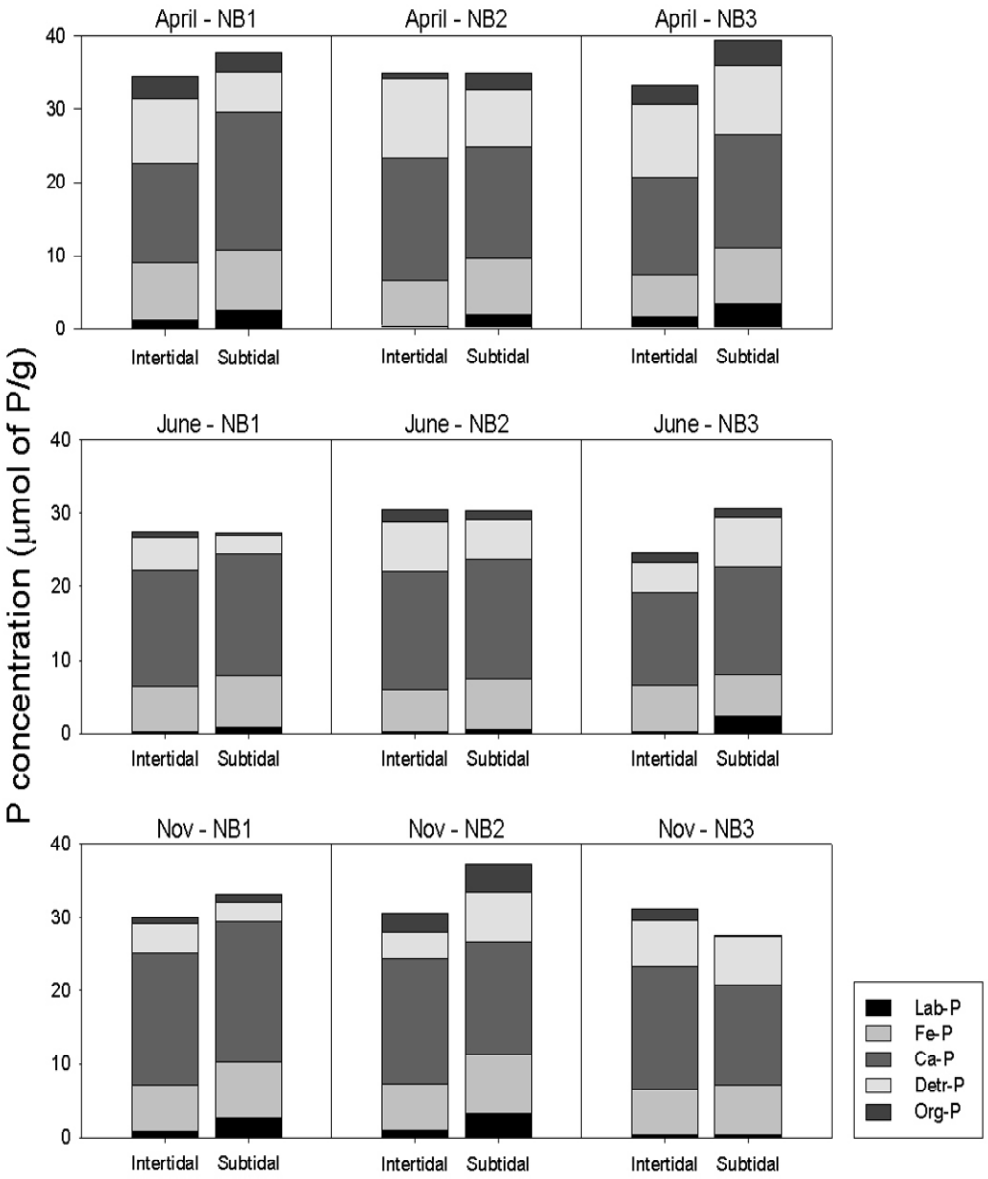

Figure 1. Mean P concentrations obtained using the SEDEX extraction procedure for each site and month. The sum of each fraction determines the total P concentration for each site.

VITA

Hilary Amanda Collis was born on September 1, 1979, in Caldwell, Idaho. She is the daughter of Anthony and Kim Collis and the older sister of Taryn. She graduated from Caldwell Senior High School in 1997. Hilary attended Eastern Oregon University in LaGrande, Oregon, during the 1997-98 school year, and then transferred to Pacific University in Forest Grove, Oregon, in September, 1998. There she received a Bachelor of Science degree in biology and a Bachelor of Science degree in philosophy. During a summer internship with the National Science Foundation's Research Experience for Undergraduates program at Michigan State University, Hilary became interested biogeochemistry and mitigating environmental impacts of increased nutrients on soils and watersheds. Following graduation, Hilary spent two years working as a fisheries technician for both the Idaho Fish and Game, and the U.S. Fish and Wildlife Service in Washington.

In August 2003, Hilary began her graduate studies in the Department of Oceanography and Coastal Studies at Louisiana State University under the guidance of Dr.'s William Patrick and Ron DeLaune, and in July, 2004 began working under Dr. Jaye Cable. The degree of Master of Science will be awarded in December of 2006.